Extraction, Encapsulation and In-vitro Stomach Digestion of Mamaku Extract

A thesis presented in partial fulfilment of the requirements

for the degree of

Master of Food Technology

at Massey University, Palmerston North, New Zealand

Rebecca Emily Tresidder

2018

Abstract

Process development aimed to scale up the extraction of Mamaku, with a resulting yield of 56%wt/wt (mass of liquid extract/100kg of fronds) and 2.8%wt/wt (mass of freeze-dried material/100kg of fronds); this being higher than the yield previously obtained at a small scale (~1% freeze-dried mamaku). The concentration of the liquid extract followed by freezing, as opposed to freeze-drying it, improved the shear-thickening properties of the Mamaku solutions. The critical temperature for processing was identified to be 63°C, whereby mamaku can be treated for 60 minutes without degradation. Higher temperatures were detrimental for the rheological properties of this polysaccharide, exhibiting a complete loss of shear-thickening when heated to 110°C. The shear-thickening properties of Mamaku solutions were also reduced when exposed to body temperature (37°C) and at the acidic pH found in the human stomach (pH 2-4).

Encapsulation experiments aimed to allow mamaku to be swallowed safely, targeting release in the stomach in a hydrated form, and without incorporating calories if used as an ingredient in functional foods aiming to target weight loss. Gelatin was chosen as the encapsulating agent and 7.5%wt/v concentration was selected, being this quantity able to successfully trap concentrated mamaku (4.5%wt/wt), but also exhibiting a melting point high enough (~31°C) to avoid melting in the mouth when consumed. A number of different encapsulation techniques were trialled. The most promising technique was the fluid gel system. The nozzle techniques proved not be suitable for the properties of mamaku. The emulsion templating system showed challenges around removing the oil. The micro-injector based system produced beads likely to be too large for practical use in a food product. Limitations in the encapsulation techniques included: (i) a low mamaku concentration was used (4.5%wt/v—obtained after concentration) and (ii) the gelatin gel appeared to be unstable when transferred to an aqueous environment.

The in-vitro stomach digestion results highlighted that encapsulated mamaku by gelatin will be released in the stomach, allowing the shear-thickening properties to re-form. Above 2.2%wt/v Mamaku, some shear thickening was observed (at high shear rates) after digestion of the Mamaku + gelatin mixtures. At least a 4.0%wt/v Mamaku concentration was needed in these mixtures, to obtain similar shear-thickening viscosity values after digestion, as those found by placing the mixture just under the acidic stomach conditions. Overall, a minimum of 10%wt/v of rehydrated mamaku should be delivered to the stomach to gain optimal shear-thickening properties at biological shear rates (1-10s^{-1}) similar to those found at native pH (~pH 5.3).

Overall, more research is needed to conclude about the viability of encapsulating Mamaku using gelatin as well as optimizing the encapsulation process based on fluid gel formation.

Acknowledgements

A massive thank you to Lara Matia-Merino, my main supervisor for scouting me for this project. I really appreciate all the time spent getting me up to date on the previous research and clarifying the original methods used, as well as the endless support given for my research and time spent fielding my ideas so I could use my limited time wisely. Your clear vision for future research on mamaku's properties is inspiring.

To my other co-supervisor Roger Lentle, thank you for the support and encouragement during my research. Your vision for the potential uses for mamaku is inspirational.

To my off-site co-supervisors, Kelvin Goh and Emilia Nowak, I have really enjoyed getting to know you this past year and would like to thank you both for the time spent during the numerous Zoom meetings about this project and the guidance offered whenever I had questions or needed help.

To Allan Hardacre my unofficial co-supervisor, thank you for the support throughout this entire project and the numerous ideas to all the difficulties faced. Thank you for all the time spent helping me with the extraction, for the numerous stops at my desk just to see how everything is going, and for your ability to drop everything and find time to help despite being busy. Thank you for the all the practical advice and the time spent building a spinning disc system from scratch.

To Matthew, my parents and wider family, and friends, thank you for the unconditional love, support and guidance and for encouraging me to do this project, even on the days when machines broke down or other difficulties were realised.

To Ngahere Extracts Limited, thank you for funding this project, through your own sources and a Callaghan Innovation grant.

To the Ngati Hine Forestry Trust, thank you for harvesting and shipping the 200kg of mamaku fronds extracted during this project.

To May Wee, thank you for doing a PhD on mamaku before me, including characterising mamaku and identifying the mechanism for thickening, and paving the way for my research.

To Marion Castle and Judy Barker, and the rest of the Animal Products team at Ministry for Primary Industries, thank you for encouraging and supporting me going back to University to complete a Master of Food Technology Degree.

To Steve Glasgow, thank you for helping with the mamaku extraction and building the custom in-vitro stirrer.

To Chris Hall, thank you for talking me through the original mamaku extractions you completed and offering advice on the scaled up process.

To Matthew Taylor, thank you for coming and helping cut fronds in half and also helping to mulch the fronds during the first extraction.

To Garry Radford, thank you for letting me use the pilot plant for the extraction of 200kg of fronds, despite the mess it made and the huge amount of space the dilute extract took up in the chillers before it was concentrated down to ~100kg.

To Michelle Tamehana, thank you for all the help, support and general chats whilst I was working in your lab. You brightened up the endless hours spent sitting at the rheometer measuring samples.

To Peter Jeffery, thank you for the photos you took during the mamaku extraction.

Table of contents

List of tables

List of figures

1 Introduction

1.1 Mamaku

New Zealand's native Black tree fern (Cyathea medullaris) is well known as Mamaku in Te Reo Māori. Mamaku is the tallest tree fern grown in the south pacific (Goh, Matia-Merino, Pinder, Saavedra & Singh, 2011). It typically grows to around 20m tall and is a common tree in NZ forests (Wee, Matia-Merino, Carnachan, Sims & Goh, 2014).

Traditionally the pith at the centre of the truck and within the fronds (stems) has been cooked and consumed as a food by the indigenous Māori people (Goh et al., 2011). Additionally, these same components were used to treat wounds, boils, eruption and gastrointestinal problems (Brooker, Cambie & Cooper, 1987; Matia-Merino, Goh & Singh, 2012). It also has been used to treat diarrhoea (Foster, 2008; Wee, Matia-Merino & Goh, 2015a, 2015b).

The wider research team here at Massey University have been working to characterise the properties of mamaku since 2007, and a summary of the key findings, including the proposed mechanism for the shear-thickening, can be found in the literature review (see Chapter 2).

As part of this work, mamaku has been placed in Rat ex-vivo and in-vivo stomachs to observe how the body reacts to its unique shear-thickening properties and whether delayed gastric emptying could be observed. The findings from these two studies in particular, is what prompted the work completed in this thesis and, therefore have been summarised in this introduction.

Findings of mamaku solution placed in an ex-vivo Rat stomach

This study looked at the visual changes in the stomach when different solutions were perfused into stomachs (maintained ex vivo) via the oesophageal cannula (Lentle, Janssen, Goh, Chambers & Hulls, 2010). The experiment involved 2 mL

being added over a time period of 4 minutes, allowing to rest for 8 minutes before repeating a total of five times, until 12 mLs had been added. The three solutions studied were physiological saline, 1.5% guar gum solution and 16.4% mamaku solution. The mamaku concentration was chosen to match the apparent viscosity of the guar solution at biological shear rates. The key results are shown in Table 1.1.

Table 1.1: Frequency, speed and amplitude findings in the ex-vivo stomach for each solution (Lentle et al., 2010)

	Saline	**1.5% Guar Gum**	**16.4% mamaku**	**Findings**
Frequency (cycles/minute)	5.03±0.08	5.06±0.06	5.70±0.19	mamaku was significantly higher
Speed (mm/s)	1.88±0.08	1.82±0.06	3.14±0.41	mamaku was significantly higher
Amplitude (mm)	1.91±0.19	1.62±0.13	1.62±0.16	No significant differences

Key observations include that the antrocorporal contractions changed with the addition of mamaku solution compared to the other solutions and were no longer consistently linear or bilinear. Additionally, other differences included variable site of initiation and direction of propagation and the failure of progression to antrum and out of the stomach. A proposed mechanism for these changes was the loss of antrocorporal coupling.

From this study, it is believed that the mamaku solution created the different response in the stomach because of residual stress in the stomach after each stomach contraction due to the unique elasticity of mamaku. It was specified further that the continuing action of this stress is causing the change in the antrocorporal contractions. This was linked to delayed gastric emptying (Lentle et al., 2010).

Findings of mamaku placed in an in-vivo Rat stomach

This study looked at the difference in rats when they were gavaged with either 15%wt/wt mamaku or deionised water five times on alternate days over a period of two weeks (Wee, Lentle, Goh & Matia-Merino, 2017). The daily body mass, daily food intake and weight of stomach contents upon euthanasia was recorded.

Key findings include that all rats ate less on days when gavaged than when they were not. This was supported by the weight gain analysis on days gavages occurred and days they did not. Additionally rats gavaged with mamaku, consumed less food in the next 24-hour period than the rats gavaged with deionised water. The fact that this only lasted 12-24 hours indicates any satiety effect of the mamaku is short-lived. Furthermore, there was no significant weight gain difference between the rats given mamaku versus the rats given deionised water. Lastly, the weight of the stomach contents of the rats gavaged with mamaku solution were significantly higher than the rats gavaged with deionised water indicating the mamaku provided a satiety effect through delayed gastric emptying.

Overall, the rats did not lose body weight during the study and this was thought to be because of the limited number of doses of the mamaku solution and the short duration of the study. It is also reasoned that the rats had time and the ability to over-eat in compensation on the days no gavage occurred (Wee et al., 2017).

1.2 Objective

The project aimed to develop a functional food system, which would include encapsulated mamaku. The need for encapsulation arose from the choking hazard the native concentrated mamaku created due to its shear-thickening properties. This is likely to create a choking hazard because the solution would thicken as it was swallowed forming an almost solid clump in the oesophagus, that would likely travel backwards up the oesophagus rather than down.

This food would be able to deliver the mamaku to the stomach where the encapsulating agent would break down and allow the mamaku to clump together and reform the shear-thickening properties. These shear-thickening properties would disrupt the normal gastric emptying processes of the stomach due to disrupted antrocorporal contractions. This causes the stomach to retain its contents for longer and thus creates a satiety effect. This should allow for weight loss, as people would feel fuller for longer delaying their desire to consume more food.

This project was divided into three key stages:

1. Extraction
2. Encapsulation
3. In-vitro digestion

The first stage, extraction, aimed to develop a scalable process for extraction of mamaku from the Black Tree Fern fronds. The objectives included the process design, mass and energy balance, and yield data. In addition, it included the rheological properties of the extract, studies of freeze thaw cycles, heat treatments and concentration among others; as well as the nutritional and microbial analysis of the extracted mamaku.

The second stage and third stage were concurrent. They aimed to firstly, encapsulate the mamaku and secondly, develop the delivery system and encapsulation process in such a way that the encapsulating agent was digested in the stomach to allow the mamaku to be released at a sufficient concentration, and to ensure that the process used could be scaled up appropriately.

Supplementary foods, such as what this work aims to develop, aim to help individuals to achieve weight loss and potentially reduce the prevalence of obesity in New Zealand and the world. This unique product could be hugely beneficial to the New Zealand economy, particularly because the functional mamaku is extracted from our native Black Tree Fern.

2 Literature Review

2.1 Introduction

This literature review covers all aspects to the project. Firstly, giving an overview of the previous research on mamaku completed over the last ten years. Secondly, an overview of digestion to give the required background to explain why the in-vitro digestion system was developed to ensure it is similar to the complex nature of digestion in the body. Lastly, an overview of encapsulation including release mechanisms and details on appropriate techniques for the situation.

2.2 Mamaku

2.2.1 Introduction

Within the fronds of the Mamaku tree, there is a slimy, brownish-red, mucus-like mucilage, which can be extracted by hot water extraction and is consequently called mamaku solution (Goh, Matia-Merino, Hall, Moughan & Singh, 2007; Goh et al., 2011; Matia-Merino et al., 2012; Wee et al., 2014, 2015a, 2015b). Mamaku solution has complex rheological properties shown in Figure 2.1.

Figure 2.1: Images showing the unique properties of mamaku including its elasticity (left) and rod climbing properties (right) (Goh et al., 2007)

In a later study, Goh et al. (2011) found that the rod climbing properties of mamaku solution could be partially explained by “stretching of long linear chains

occurring in the entangled state." Goh et al. (2007) found the rheological properties were created by the large non-starch polysaccharide fraction present (~10% of the freeze-dried mamaku). The full nutritional and elemental analysis is summarised in Table 2.1.

Table 2.1: Nutritional and elemental analysis (Goh et al., 2007)

Composition of freeze dried mamaku	**Percentage (%) (w/w)**
Moisture	9.25
Ash	16.07
Crude Protein	2.02
Fat	0.17
Crude Fibre	0.24
Tannins	0.09
Sugars	44.3
Non starch Polysaccharides	9.80 – uronic acid (72.5%), galactose (14.3%), xylose (7.1%), and arabinose (3.1%)
Unknown	18.06
Minerals	~16 – rich in potassium, sodium, calcium, magnesium and aluminum
Elemental analysis	32.78% C, 5.53% H, 0.37% N, and 52% O ~ $C_6H_{12}O_7$

Nutritional and elemental analysis were completed again after the purification and the key results are shown in Table 2.2.

Table 2.2: Nutrition and elemental analysis on purified mamaku (Goh et al., 2011)

Composition of freeze dried mamaku	**Percentage (%) (w/w)**
Carbohydrate	79%
Crude protein	4.49%
Ash	6.02%
Elemental analysis	33.50% C, 5.16% H, 2.45% N and 48% O ~ $C_6H_{12}O_6$ aka mainly hexose sugars

Multiple different methods were used to analyse the structure of purified mamaku (Wee et al., 2014). The results indicated that the mamaku polysaccharide consists

of a glucuronomannan backbone and this backbone comprises of the following (Wee et al., 2014):

- 4-linked methylesterified glucopyranosyl uronic acid residues, and
- 2, 3 and 2,3,4-linked mannopyranosyl residues

The backbone branches at O-3 and O-4 of the mannose residues. The branches consist of sugar side chains including (Wee et al., 2014):

- galactose,
- arabinose,
- nonmethylesterified glucuronic acid, and
- other simple sugars.

The key molecular characteristics found are summarised in Table 2.3.

Table 2.3: Molecular characteristics of mamaku (Goh et al., 2011)

Parameter	Value
Intrinsic viscosity, η	2020 ± 23 ml/g (in milliQ water)
Weight-average molar mass, M_w	3.20 ± 0.11 x 106 Da (in 0.1M NaCl)
Differential refractive index, d_n/d_c	0.178 ± 0.006 ml/g
Root-mean square radius, $(R^2_g)_z^{1/2}$	144 ± 1 nm (in 0.1M NaCl)
Z-average diameter	~ 75 nm
Polydispersity index	1.08 ± 0.05
Molecular conformation	Semi-flexible (extended) random coil (in 0.1M NaCl)

2.2.2 Rheological analysis

The rheological data when conducting a viscosity profile showed that the mamaku solutions displayed an area of Newtonian flow behaviour at low shear rates, followed by an area of shear-thickening behaviour at intermediate shear rates, followed by an area of shear thinning behaviour at high shear rates (Goh et al., 2007). This is shown in Figure 2.2.

Figure 2.2: Apparent viscosity and first normal stress difference of mamaku solutions as a function of shear rate at 20°C measured using cone and plate geometry (Goh et al., 2007)

Additionally, there were different effects seen with changing concentration. In particular, with the decreasing concentration of mamaku, the shear-thickening peak was shifted to higher shear rates (Goh et al., 2007).

Furthermore, analysis on the first normal stress difference (N_1) was also completed showing positive values for the mamaku solutions. “The first normal stress difference is traditionally used to measure the viscoelastic quantities often defined by processes like rod climbing or the Weissenberg effect.” (Goh et al., 2007)

Goh et al. (2007) believed that in this case, the difference describes the elasticity of the mamaku solution and the results indicate that the shear-thickening behaviour is the result of an increased elastic property in the solution during shear.

Figure 2.3: Elastic modulus (G') and viscous modulus (G'') of mamaku solutions plotted as a function of frequency obtained by oscillatory measurement using double gap geometry (Goh et al., 2007)

The oscillatory tests, shown in Figure 2.3 above, show G' and G'' crossing over, with G'' above G' at low frequencies. The crossover point gives an understanding of the relaxation time of the polymer. Goh et al. (2007) showed that when increasing the concentration of mamaku there is an increase in relaxation time. This indicates more cross-linking points between the polymer chains, either larger in size or in a greater number (Goh et al., 2007).

Figure 2.4: Up-down viscosity curves of mamaku as a function of shear rate at 20^{o}C measured with double gap geometry (Goh et al., 2007)

Viscosity profiles where the shear rate was increased then immediately decreased again are shown in Figure 2.4 above. It was clearly shown in the time dependent rheological behaviour (Goh et al., 2007, 2011). The results show that depending on the shear conditions mamaku can show the following behaviours (Goh et al., 2007, 2011):

- Newtonian – constant viscosity with increasing shear rates
- Shear-thickening – increase in viscosity with increasing shear rates
- Shear thinning – decrease in viscosity with increasing shear rates
- Thixotropy – suggesting network disruptions are occurring
  Defined as "decrease in viscosity with time under a constant shear" (Wee et al., 2015b)
- Antithixotropy – suggesting network formation are occurring
  Defined as "increase in viscosity with time under a constant shear" (Wee et al., 2015b)

A different paper examined the time dependence of the shear-thickening (Wee et al., 2015b). This paper showed that the large positive normal stress difference observed at these shear rates (both shear-thickening and with constant shear over time in that shear range) is causing an increase in the elasticity of the solution showing the shear-thickening to be a real phenomenon (Wee et al., 2015b).

Additionally Wee et al. (2015b) found that different measurement time intervals influenced the shear rate at the start of the shear-thickening, without affecting the maximum viscosity reached. Short measurement time intervals did not achieve steady state viscosity (1, 10 or 30-2s). The results are shown in Figure 2.5.

Figure 2.5: Viscosity curves of 5% w/w mamaku obtained with various data collection time settings at 20°C measured with cone and plate geometry (Wee, 2015)

These results led to the time dependency being further investigated at the shear rates where shear-thickening was observed (Wee et al., 2015b). The key results are shown in Table 2.4:

Table 2.4: Time until shear state was achieved for various shear rates (Wee et al., 2015b)

Shear rate	Time until steady state was achieved
1 s^{-1} or below	No time dependency
4 s^{-1}	8 minutes
6 s^{-1}	1.2 minutes
8 s^{-1}	0.5 minutes
10 s^{-1}	0.3 minutes

These results show antithixotropy at the shear-thickening shear rates (4-10s^{-1}). Wee et al. (2015b) summarise this to be because of a net increase in the formation of intermolecular interactions at these shear rates, most likely hydrogen bonds, leading to an increase in viscosity.

Lastly, the researchers looked at whether hysteresis effects were shown (Wee et al., 2015b). The hysteresis effect was shown clearly when sheared to 10s^{-1}, with all viscosities measured on the down curve being higher than those of the up curve.

No hysteresis effect was shown below $1s^{-1}$ or above $10s^{-1}$. Wee et al. (2015b) believe the hysteresis effect is the result of the interactions between molecules at these intermediate shear rates and the fact that these interactions cannot be disrupted by the lower shear rates very easily.

2.2.3 Mechanism for the Shear-thickening

The mechanism for mamaku's shear-thickening can be explained by energetically cross-linked transient network (ECTN) model (Lele & Mashelkar, 1998). The basis of the model is that the associations between the polymers are thermodynamically driven transient crosslinks (Wee et al., 2015b).

When the shear-thickening occurs, a number of things have happened (Wee et al., 2015b):

- Firstly, the shear induces the polymer chains to moved and untangled
- This exposes groups previously hidden before the shear occurred
- Secondly, they have orientated in a way in which interactions between these groups on one polymer molecule and a neighbouring one can occur (zipping of the ladder)

Wee et al. (2015b) believe that when shear thinning occurs the shear rate is sufficiently high enough to overcome these interactions and the chains separate but remain untangled, causing the decrease in viscosity (shear thinning).

2.2.3.1 Electrostatic interactions

Results of 7% (w/w) mamaku viscosity profiles obtained at different sodium chloride concentrations show shear-thickening at $10s^{-1}$ and shear thinning behaviour at 30 s^{-1} in all cases (Matia-Merino et al., 2012). At low shear rates 0.1-0.25M NaCl exhibited Newtonian flow, whereas 0.5M NaCl or higher produced shear thinning behaviour. Additionally salt concentrations above 0.5M NaCl produced an increase in the maximum viscosity during the shear-thickening phase. Matia-Merino et al. (2012) believed this showed mamaku has good salt resistance.

Figure 2.6: Apparent viscosity of 7% w/w mamaku at different sodium chloride concentrations at 20°C measured using double gap geometry. Inset shows an amplitude sweep oscillatory test obtained at 1Hz for 0.1M NaCl 7% mamaku solution at 20°C measured with double gap geometry (Matia-Merino et al., 2012)

The inset graph in Figure 2.6 shows strain hardening was not occurring when increasing strain was applied (Matia-Merino et al., 2012).

When studying the zeta potential and z average diameter of mamaku under different sodium chloride levels, dilute samples had to be analysed. Matia-Merino et al. (2012) explain that the negative charge of the mamaku is caused by the high uronic acid content. Increasing the salt caused the negative charge to be reduced. The z diameter was only reduced above 0.1M NaCl and a further increase in ionic strength did not have much of an effect.

Matia-Merino et al. (2012) found that the increase in shear-thickening seen with addition of salt could be linked to a partial screening of electrostatic forces, which means the shear-thickening is not the result of electrostatic interactions and actually is based on hydrogen bonding or hydrophobic interactions.

Additional tests on using salts were completed. Matia-Merino et al. (2012) found when testing potassium chloride, calcium chloride, magnesium chloride and sodium chloride all at 0.5M concentrations, only $MgCl_2$ increased the peak viscosity obtained in the shear-thickening profile. The others showed no apparent differences.

Matia-Merino et al. (2012) found that native mamaku has a pH of ~5 and that varying the pH from 1.0 to 12 showed a large variety of shades of brown. When studying the zeta potential and z average diameter of mamaku at different pH levels, dilute samples had to be analysed. Key findings regarding the zeta potential were that at pH 5.0 mamaku has a negative charge. In addition, increasing the pH from 5 to 12 did not show a large charge in the negative charge. Lastly, decreasing the pH form 5 to 1 showed a large reduction in negative charge (Matia-Merino et al., 2012).

Contrasting this, the z average diameter decreased when pH was increased from pH 1 to 12. Interestingly, this reduction in size happened from pH 3 when the molecule is less charged to pH 5 when the molecule is more charged (Matia-Merino et al., 2012). These authors believe this may be because of disaggregation. The pK_a of mamaku was found to be ~2.0 (May, 2015).

The overall conclusion is that mamaku has a high pH tolerance in the range of pH 3-9.

2.2.3.2 Hydrophobic interactions

Results show that increasing temperature decreased the viscosity and delayed the shear-thickening behaviour, as shown in Figure 2.7. At temperatures of 50^{o}C or higher no shear-thickening was observed. Increasing the temperature increases

the mobility of the polymer chains. Matia-Merino et al. (2012) believe this mobility prevents the interactions between the polymer chains occurring, which supresses the shear-thickening. Furthermore, if the shear-thickening interactions got stronger with an increase in temperature, this would imply hydrophobic interactions are responsible for the thickening behaviour. This does not seem to be the case according to the authors.

Figure 2.7: Apparent viscosity of 7% w/w mamaku versus shear rate measured at various temperatures using double gap geometry (Matia-Merino et al., 2012)

The shear rate at the start of shear-thickening and the apparent viscosity was found to vary with temperature according to Arrhenius behaviour. Furthermore, the shear-thickening, shear thinning, thixotropy, and antithixotropy effects were still present after heating 7% w/w mamaku solution to 80^{o}C for 30 minutes, with the solution retaining nearly the same viscosity profile. This showed no degradation of the polymer structure with the heat treatment (Matia-Merino et al., 2012).

This reversible loss of shear-thickening behaviour with temperature leads to the belief that hydrogen bonds are involved in the shear-thickening behaviour of mamaku (Matia-Merino et al., 2012; Wee et al., 2015b).

2.2.3.3 Testing hydrogen bond theory with urea

Urea is known to be a strong disruptor of macromolecular hydrogen bonds (Mirsky & Pauling, 1936). The results of different urea concentrations are shown in Figure 2.8.

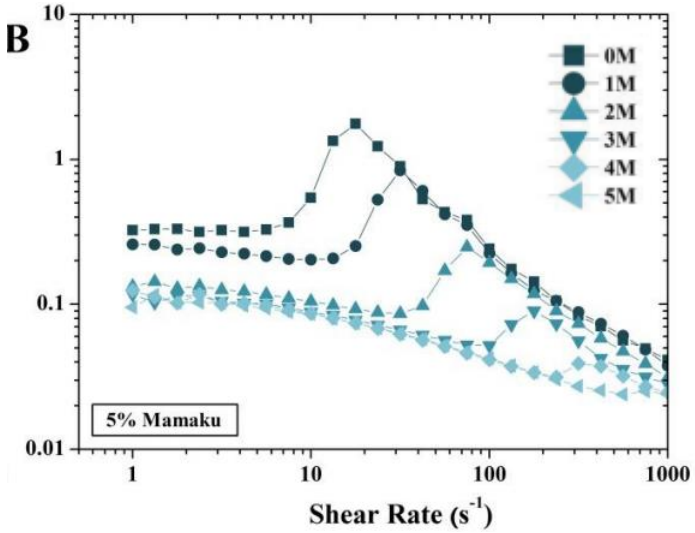

Figure 2.8: Effect of the addition of urea on the viscosity of a 5% w/w mamaku solution at 20°C measured with cone and plate geometry (Wee, 2015)

The key observations from this graph are that increasing the urea concentration reduces the peak viscosity, shifts the onset of shear-thickening to higher shear rates and reduces the viscosity at low shear (Wee, 2015). These results show that the shear-thickening of the mamaku solution is indeed caused by intermolecular hydrogen bonding.

2.2.3.4 Testing effect of ionic strength

Dialysis to remove minerals and low molecular weight sugars has been tested in the mamaku solution (Wee et al., 2015a). These authors found that this caused a loss of shear-thickening and a loss of hysteresis as shown in Figure 2.9.

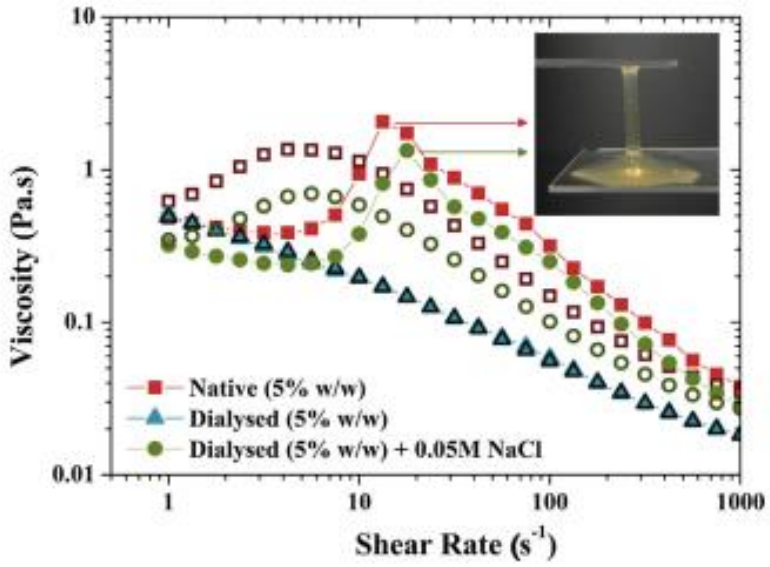

Figure 2.9: Viscosity curves of 5% mamaku before and after dialysis, and addition of 0.05M NaCl for increasing (filled symbols) and decreasing shear rates (unfilled symbols) at 20°C measured using double gap geometry (Wee et al., 2015a)

This figure also shows the recovery of shear-thickening properties and hysteresis upon re-addition of salts. It was found that "mono- (Na^+, K^+, $N(CH_3)_4^+$), di- (Ca^{2+}, Mg^{2+}) and trivalent (Al^{3+}, La^{3+}) cations were able to reinstate shear-thickening in the dialysed extract" (Wee et al., 2015a).

Monovalent Salts

The results of different monovalent salt concentrations are shown in Figure 2.10.

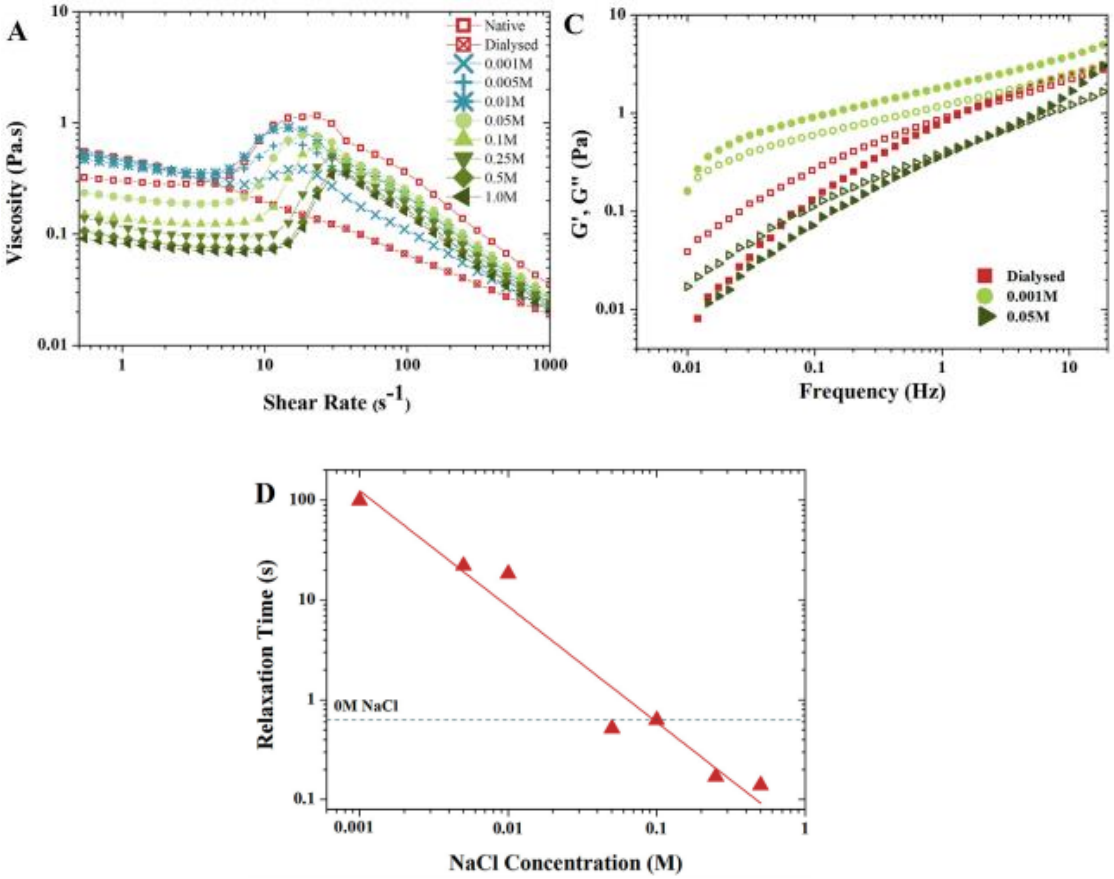

Figure 2.10: Left: Effect of NaCl concentration on shear-thickening properties of 5% dialysed mamaku at 20°C measured with double gap geometry. Right: Mechanical spectra G' (filled) and G'' (unfilled) of 5% w/w dialysed mamaku at different NaCl concentrations at 1% strain and 20°C measured using double gap geometry. Bottom: Relaxation time of dialysed mamaku with different NaCl concentrations (Wee et al., 2015a)

When adding monovalent salts to the dialysed sample, two trends are apparent (Wee et al., 2015a):

- From 0.001M to 0.01M a gradual increase in shear-thickening peak viscosity is seen and a shift in the shear rate at the onset of thickening to lower shear rates, meaning that the curve approaches the native mamaku viscosity profile.

- From 0.01M to 1.0M the low shear viscosity decreases (progressively up to 10 fold), the peak viscosity decreases and the sear rate at the onset of thickening increases.

This decrease of shear-thickening was expected, as the higher concentrations of ions would screen the negatively charged carboxylic acid groups on the polymer backbone, promoting a less extended structure and lowering viscosity (Wee et al., 2015a).

The results also show a reduction in G' with increasing salt concentration (Wee et al., 2015a). The relationship between relaxation time and salt concentration showed that network entanglements were strongly dependent on ionic strength (Wee et al., 2015a).

Divalent salts

The overall trend in the results for divalent salts was the same as for monovalent salts as shown in Figure 2.11.

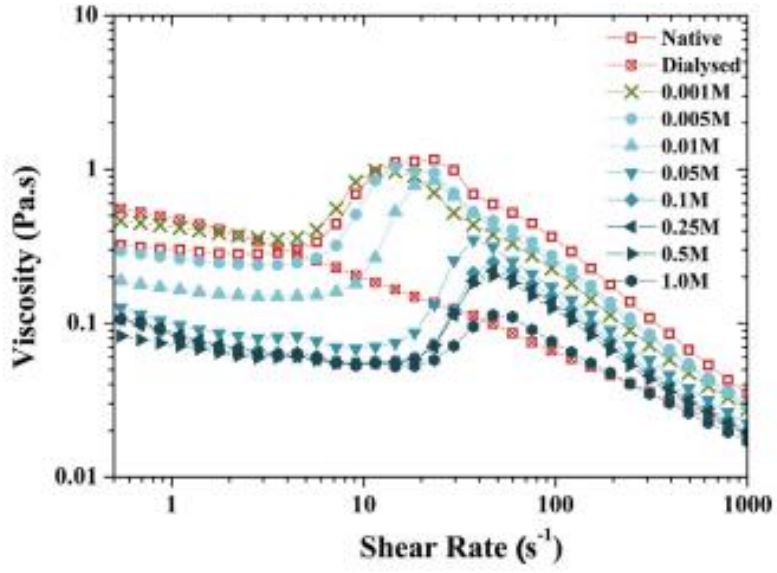

Figure 2.11: Effect of $CaCl_2$ concentration of shear-thickening of 5% dialysed mamaku at 20°C measured using double gap geometry (Wee et al., 2015a)

The only noticeable difference is that as concentration increased above 0.05M the shear-thickening peak viscosity reduced further than with monovalent salts (Wee

et al., 2015a). The authors believed that this is because the total ionic strength of the divalent cations was higher. Furthermore, based on these results they hypothesised that the shear-thickening effect is dependent on ionic strength not specific cations.

Trivalent salts

The trivalent cations had different effects than the other ions, as shown in Figure 2.12.

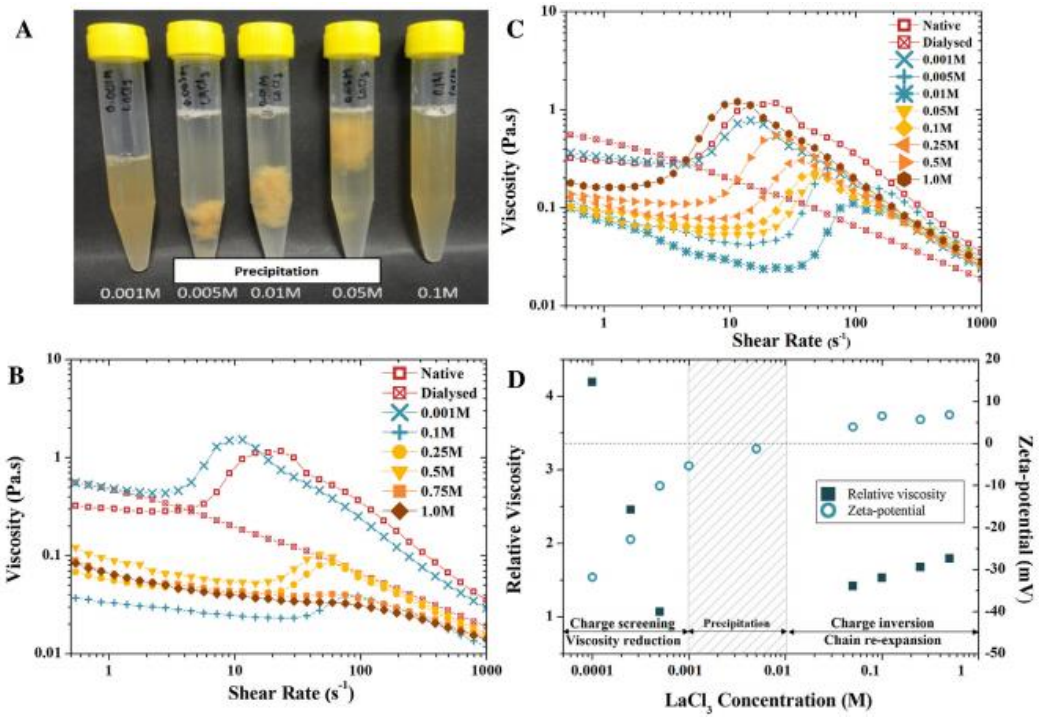

Figure 2.12: A. Dialysed mamaku in various concentrations of $LaCl_3.7H_2O$. B. Effect of $LaCl_3.7H_2O$ concentration on shear-thickening of 5% w/w dialysed mamaku at 20°C measured with double gap geometry. C. Effect of $AlCl_3.6H_2O$ concentration on shear-thickening of 5% w/w dialysed mamaku at 20°C measured with double gap geometry. D. Effect of $LaCl_3.7H_2O$ concentration of relative viscosity of 1% w/w dialysed mamaku and zeta-potential of 5% dialysed mamaku at 20°C (Wee et al., 2015a)

The key difference is the precipitation of the mamaku at concentrations of 0.005-0.05M lanthanum chloride, $LaCl_3$ (and anhydrous aluminium chloride, $AlCl_3$) (Wee et al., 2015a). Above 0.1M concentrations, the precipitates re-dissolved and the

shear-thickening was regained to a small extent. As concentration was increased to 0.75M, the shear-thickening was lost.

Hydrated $AlCl_3$ was also tested and revealed different behaviour to all other cations tested. There was no precipitation at all and interestingly increasing the concentration of salts increased the shear-thickening peak viscosity, the shear rate at onset of thickening and the initial viscosity (Wee et al., 2015a).

2.2.3.5 Final definition of the mechanism

The shear-thickening behaviour is "hypothesised to be a result of a shear-induced transition from intra- to intermolecular hydrogen bond formation promoted by the screening effect of cations" which allows the charged groups to approach each other, as shown in Figure 2.13 (Wee et al., 2015a).

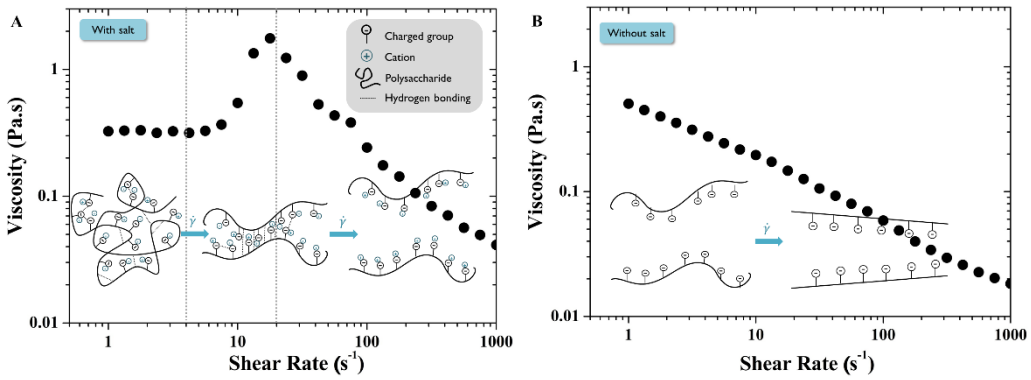

Figure 2.13: Schematic illustration of the shear-thickening of mamaku (left) and dialysed mamaku with no salts (left) (Wee et al., 2015a)

One key point being that shear is required to untangle and stretch the chains to allow the interactions to occur. In addition, the degree of shear-thickening can be related to the number of hydrogen bonds formed, which in turn is related to the ionic strength of the solution.

There are several possible groups, which could be involved in the hydrogen bonding as shown in Figure 2.14 (Wee et al., 2015a).

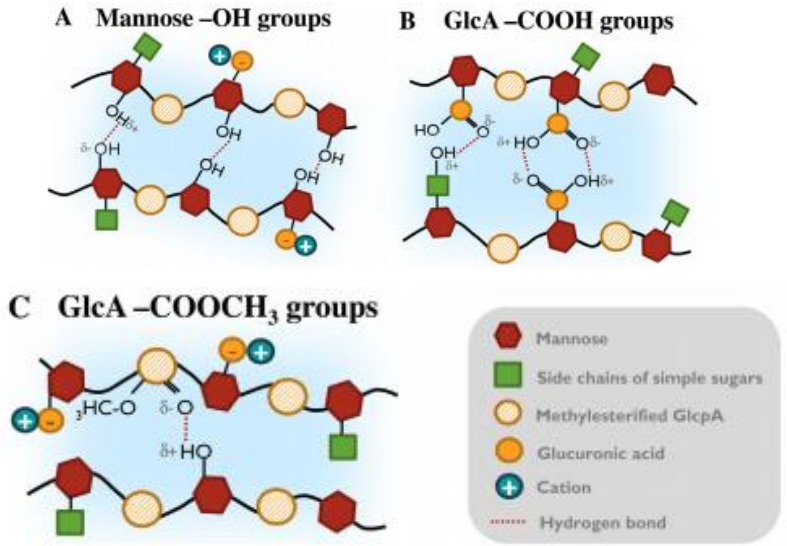

Figure 2.14: Schematic illustration of possible groups which could be responsible for the hydrogen bonding during shear-thickening (Wee et al., 2015a)

2.3 Overview of digestion

The human digestive track digests foods through a sequence of events, which occur in a linear order (Katouzian & Jafari, 2016). This review looks at the mouth and stomach because the mamaku acts in the stomach, thus reducing the need for intestinal processes to be looked at in detail.

2.3.1 Mouth

First, the food is introduced to the mouth where chewing/mastication occurs where food is mixed with saliva (Moughan, 2009). This turns the food into bolus through the addition salivary amylase, which begins to digest starches into simple sugars (Katouzian & Jafari, 2016). Next, the bolus is swallowed and travels to the stomach (Katouzian & Jafari, 2016; McClements & Decker, 2009; Moughan, 2009).

2.3.2 Stomach

2.3.2.1 Contents

When empty the adult healthy human stomach is well known to have an effective volume of about 75mL. When food or drink is consumed, the stomach expands to hold about one litre of food/liquid.

In the stomach, the food is mixed with gastric enzymes, minerals and surface-active compounds (McClements & Decker, 2009). Furthermore, on top of these other compounds, the stomach also exposes the food to an acid solution, which further digests it (Katouzian & Jafari, 2016).

One of the gastric enzymes present in the stomach is pepsin. The chief cells produce pepsinogens that are activated by the hydrochloric acid in the stomach creating pepsin. Pepsin is the enzyme responsible for gastric digestion of protein in the stomach. This yields a mixture of proteins and large polypeptides that are later absorbed into the blood stream when further digested into amino acids in the small intestine (Moughan, 2009).

The other gastric enzyme present in the stomach is gastric lipase. This enzyme acts to begin the digestion of fats within the food. Meaning that the fats are partially digested resulting in some free fatty acids being released into the food mixture (Lairon, 2009).

2.3.2.2 Environmental conditions and movement

The pH of the human stomach is usually in the range of one to three and its ionic strength is around 100mM (McClements & Decker, 2009). After food is ingested, there is usually an increase in the pH of the stomach contents. Furthermore, McClements and Decker (2009) explain that the pH gradually reduces back to a pH of two over the next hour.

The stomach creates complex flow and force profiles through its contractions and peristaltic waves to mix the contents inside (Lairon, 2009; McClements & Decker,

2009). These contractions mix the food components with the digestive enzymes to break down large food particles (McClements & Decker, 2009). These contractions and peristaltic waves usually occur at a frequency of three cycles a minute (Lairon, 2009).

The stomach can retain food for a time-period ranging from a few minutes to a few hours. Factors influencing the time-period include the following (McClements & Decker, 2009):

- Food quantity
- Physical state (solid/liquid)
- Structure
- Location within the stomach

McClements and Decker (2009) explain that often the stomach contents decreases by fifty percent within thirty to ninety minutes.

2.3.3 Intestine

The stomach contractions also function to move digested food out of the stomach and into the small intestine (McClements & Decker, 2009). Upon leaving the stomach, the digested food moves through the small and large intestine in turn. Throughout this process, the food is gradually absorbed into the bloodstream (Katouzian & Jafari, 2016).

2.4 Introduction to encapsulation

Encapsulation is the process of entrapping one substance within another (Zuidam & Shimoni, 2012). This carrier material needs to be able to form a barrier between the active ingredient and its surroundings (Roos & Livney, 2017; Zuidam & Shimoni, 2010). McClements (2012) and Thies (2001) summarise that suitable materials include a variety of proteins, biopolymers, carbohydrates and fats.

Encapsulation processes can be characterised by the particle size of encapsulates that they produce. The two main types include, nano-particles – where the encapsulated product is within the nm size range, and microcapsules –µn size range (Zuidam & Shimoni, 2010).

Thies (2001) explains that the encapsulation process chosen can create a range of mass distributions of core material in the encapsulated product. Typically giving a payload of 10-90 percent (Thies, 2001). Payload is the percentage of active ingredient entrapped within the encapsulating agent. The equation for payload is shown in equation 2 (Lakkis, 2007):

$$Payload\ (\%) = \frac{core}{core + encapsulating\ material} * 100 \qquad (2)$$

2.4.1 Structure of encapsulated products

Encapsulated products can have a variety of geometries including irregularly shaped, oval or spherical (Zuidam & Shimoni, 2010), though they are often drawn spherical for simplicity. There are three main configurations of encapsulated products, reservoir type, matrix type and combination type (Lakkis, 2007; McClements, 2014; Thies, 2001; Zuidam & Shimoni, 2010).

These structures are shown visually in Figure 2.15.

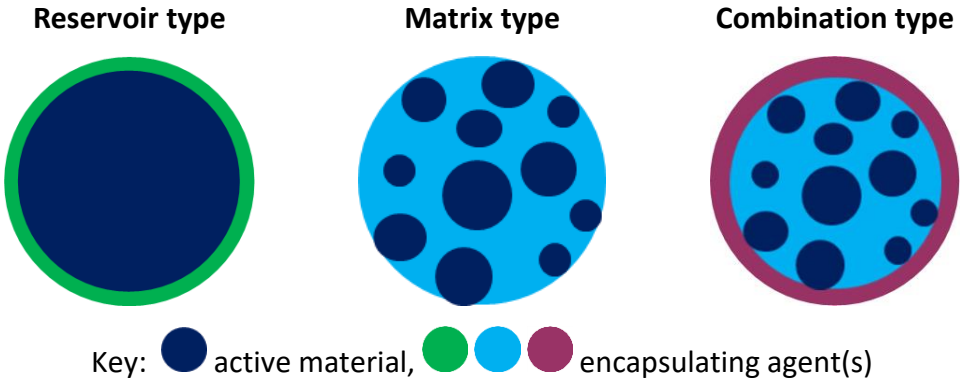

Figure 2.15: Possible structures of encapsulated products using a spherical shape for simplicity (adapted from Lakkis, 2007).

The disadvantage of the reservoir type is that they are sensitive to pressure and will burst and release their contents if too much force is applied (Lakkis, 2007; Zuidam & Shimoni, 2010). The main advantage is the high loading that is possible – the ratio of core to encapsulating material is high (Oxley, 2012; Zuidam & Shimoni, 2010). Oxley (2012) further explains that this type is ideal for creating encapsulated products with a continuous liquid core.

Zuidam and Shimoni (2010) clarify that the matrix type of encapsulates is also known as poly-core, multiple core type. The main disadvantages include lower loading capacity and that the active agents can be present on the surface of the encapsulate (Zuidam & Shimoni, 2010). Matrix systems created with a hydrogel, can swell without bursting (Lakkis, 2007; Zuidam & Shimoni 2010). This offers an advantage over the reservoir type. Additionally, the active agent is more dispersed throughout the carrier material meaning if bursting did occur not all active would be released at once (Zuidam & Shimoni, 2010). Lakkis (2007) points out that this type of system needs less quality control checks to ensure the active is thoroughly coated. Lakkis (2007) further establishes that this naturally leads to lower manufacturing costs.

The combination option overcomes the major weaknesses in each of the individual types (Lakkis, 2007; McClements, 2012; Zuidam & Shimoni, 2010). Zuidam and Shimoni (2010) establish that the combination type involves coating a matrix type

capsule in another encapsulating agent. They further reason that this reduces the likelihood that active agent is present on the outside of the encapsulated product.

2.4.2 Common food uses

Food applications could require the encapsulated product to be released immediately as soon as it is consumed (Thies, 2001). Thies (2001) further explains that other food uses could require the release of the encapsulated product to be delayed until it has reached the small intestine. Controlling mass transport and diffusion phenomena are critical in adjusting how the encapsulated product functions in its environment.

Zuidam & Shimoni (2010) outline numerous well-known uses for encapsulated food ingredients in the food industry including optimising the active ingredient in terms of its ability to be processed, food safety, stability/shelf life, limiting undesirable characteristics or improving desirable ones and controlled release.

2.5 Release mechanisms for the contents of an encapsulated product

The objective of encapsulation can be to provide controlled release of the active product (Jafari, 2017; Zuidam & Shimoni, 2010). Controlled release technologies are used in both the food industry and pharmaceutical/drug industry (Jafari, 2017).

The release of an active involves both mass transport and diffusion from a high concentration to the surrounding low concentration environment (Lakkis, 2007). Controlled release occurs when the barrier properties of the encapsulating agent chosen can be manipulated to release the active ingredient. Lakkis (2007) explains that the triggers for controlled release could be one or a combination of temperature, moisture, pH, enzymes, and shear.

Two key determinations are important in designing the encapsulation process to achieve the desired release profile. Firstly, the mechanism by which the

encapsulated product releases its contents when it is in the environment that favours release of the active. Secondly, the rate by which the active component is released when the favoured environment is reached.

2.5.1 Mechanisms for release

When the encapsulated product is in an optimal environment for it to release its active component a number of physical and chemical mechanisms could influence how the protective coating is overcome. McClements (2012) explains the various mechanisms and they are visually shown in Table 2.5.

Table 2.5: Diagrams showing visually the different mechanisms of release (adapted from McClements, 2012)

Original	Release Mechanism			
	Diffusion	Fragmentation	Swelling	Erosion
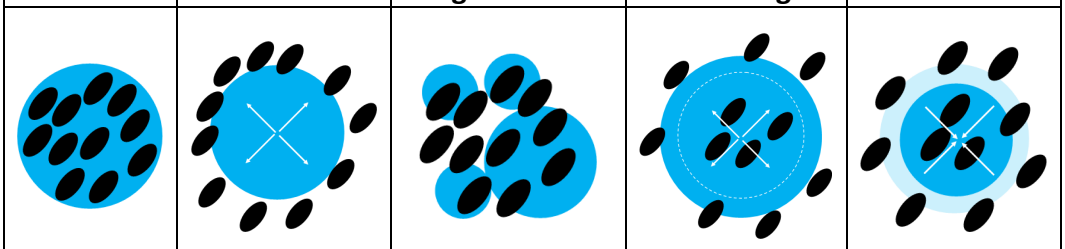				
Key: Encapsulating material Active material				

2.5.1.1 Diffusion

McClements (2012) explains that depending on the characteristics of the encapsulating agent chosen the active ingredient may be able to move out of the matrix by simple diffusion driven by a concentration gradient.

2.5.1.2 Fragmentation

McClements (2012) explains that fragmentation occurs when the encapsulating material's structure is fractured/disrupted. This increases the surface area of the encapsulated product meaning that diffusion of the active ingredient would occur faster and additionally active ingredient might be fully released upon the fracture of the matrix.

2.5.1.3 Swelling

This release mechanism is the result of the encapsulating agent absorbing a solvent and swelling. This then changes the properties of the encapsulating material (the pore size) and allows diffusion of the active ingredient to occur (McClements, 2012).

2.5.1.4 Erosion

This release mechanism is the result of erosion of the outer layer of the encapsulating agent thereby releasing the active material entrapped in that space (McClements, 2012).

2.5.2 Rate of release

Encapsulated products have such a wide variety of food applications due to their ability to be designed to allow for the release of the active component in a range of circumstances including burst release, sustained release or targeted release (McClements, 2012, 2014):

Lakkis (2007) states there are two main mechanisms, which contribute to the rate of release during controlled release of an active component from an encapsulated product:

i. Delayed release aims to hinder release of the active ingredient until the desirable circumstances at which point release is sudden.
ii. Sustained release aims to promote slow release of the active component until the concentration is optimal then aims to maintain that concentration over time.

The profiles are shown visually in Figure 2.16.

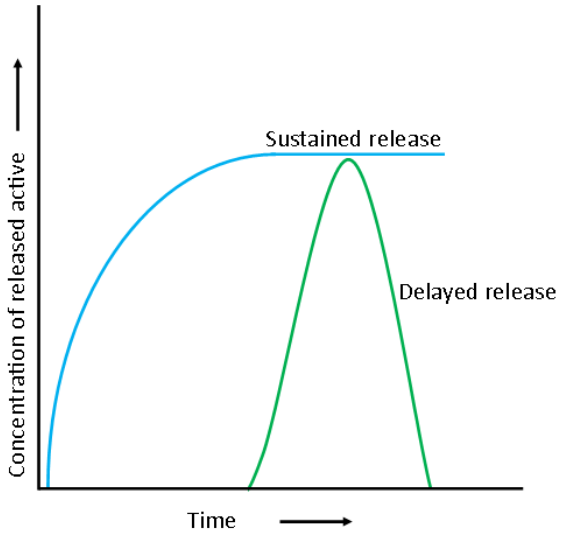

Figure 2.16: Difference between sustained release and delayed release concentration curves with time (adapted from Lakkis, 2007)

The release of an active component can usually be kinetically modelled by zero-order and first-order equations. Other rates are possible, for example, "Burst release". The visual representation of these rates are shown in Figure 2.17.

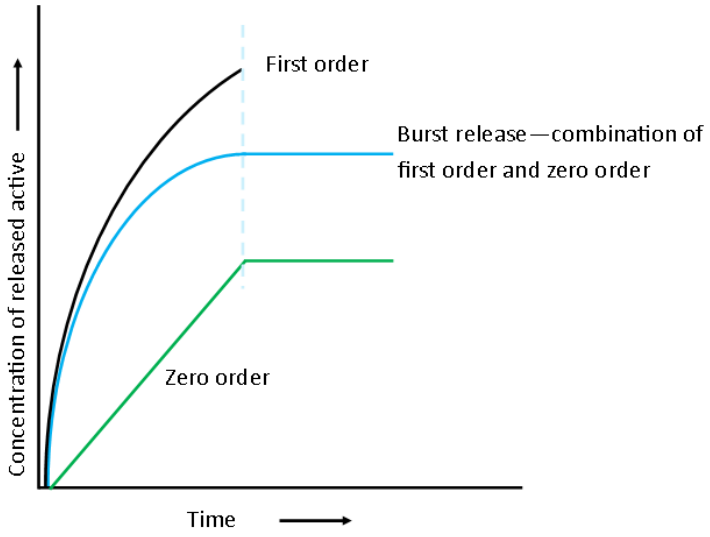

Figure 2.17: visual representation of possible release rates (adapted from Lakkis, 2007)

The equations for each rate are shown in equation 3 and 4 (Lakkis, 2007):

Zero-order release equation	-dA/dt=k	(3)
First-order release equation	-dA/dt=k [A]	(4)

where -dA/dt is the change in active concentration over time,

k is the rate constant, and

[A] is the active's concentration.

2.6 Encapsulation techniques

Because of the huge range of applications for encapsulated products, there is numerous technologies available to produce them. Each technique has its own capabilities and suitability for different situations.

Aiming to encapsulate mamaku provides multiple constraints to the techniques available. Firstly, mamaku is water-soluble, secondly, the mamaku needs to be in an aqueous form within the encapsulated product (it takes ~24 hours to rehydrate so we do not want a dried product) and thirdly, the technique cannot involve high temperatures since that damages the properties of mamaku. Additionally, there is the need to limit the overall calories in the final product since it will be targeted as a weight loss product. Lastly, there is the risk when adopting a reservoir structure that the encapsulated product would burst in the mouth or throat and release the mamaku creating a choking hazard, so a matrix or combination structure is preferred.

Table 2.6 lists some common encapsulation techniques and gives an overview of the products they produce (Zuidam & Shimoni, 2010), it also illustrates whether each technique could be suitable for encapsulating mamaku.

Table 2.6: Overview of common microencapsulation processes (adapted from Zuidam & Shimoni, 2010)

Technology	Morphology	Load (%)	Particle size (µm)	Applicable method for encapsulating mamaku (Y/N)
Spray drying	Matrix	5-50	10-400	No – need mamaku in a liquid form
Fluid bed coating	Reservoir	5-50	5-5000	No – need mamaku in a liquid form and don't want it encapsulated by fat/calories (aiming for low calorie product)
Spray-chilling/cooling	Matrix	10-20	20-200	No – can't have the mamaku encapsulated by fat (aiming for low calorie product)
Melt injection	Matrix	5-20	200-2000	No – require temperatures higher than what the mamaku can withstand
Melt extrusion	Matrix	5-40	300-5000	No – require temperatures higher than what the mamaku can withstand
Emulsification	Matrix	1-100	0.2-5000	Yes – requires a w/o emulsion but food product cannot be too high in fat/calories
Preparation of emulsions with multilayers	Reservoir	1-90	0.2-5000	No – reservoir structure would create a bursting if native liquid mamaku was added
Coacervation	Reservoir	40-90	10-800	Maybe – finding two immiscible phases where mamaku associates with one of them is difficult

Technology	Morphology	Load (%)	Particle size (µm)	Applicable method for encapsulating mamaku (Y/N)
Preparation of microspheres via extrusion or dropping	Matrix	20-50	200-5000	Yes – the design of the machinery is complicated
Preparation of microspheres via emulsification	Matrix	20-50	10-1000	Yes – the microspheres can lack uniformity in their shape and size
Co-extrusion	Reservoir	70-90	150-8000	Yes – the design of the machinery is complicated
Inclusion complexation	Molecular inclusion	5-15	0.001-0.01	No – only applies in specific circumstances
Liposome entrapment	Various	5-50	10-1000	No – only applies in specific circumstances
Encapsulation by rapid expansion of supercritical fluid (RESS)	Matrix	20-50	10-400	No – need mamaku in a liquid form
Freeze- or vacuum drying	Matrix	Various	20-5000	No – need mamaku in a liquid form

Each of these technologies that appear to be suitable for encapsulating mamaku, are looked at in more detail below.

2.6.2 Encapsulation into hydrogel matrices

A hydrogel matrix is created using polymers which are known to form a three-dimensional gelled network and absorb more water than their own weight. A hydrogel matrix consists of the following (Lakkis, 2007):

- Polymers
- Molecular linkers or spacers
- Aqueous solution.

Hydrogels are often created using physical cross-linking principles. Depending on the polymers chosen this could involve any of the following (Wang, Bamdad, Chen & Song, 2012):

- hydrogen bonds
- electrostatic interactions
- crystallized domains
- hydrophobic interactions, and/or
- temperature-induced sol-gel transitions.

Hydrogels can be used to create an encapsulated product due to their ability to entrap the active component within its structure. The environment of the gel can then be manipulated to allow the active component to be released via diffusion due to gel-phase changes (Lakkis, 2007; Wang, Bamdad, Chen & Song, 2012). The properties of the active component can affect the diffusion process including (Lakkis, 2007):

- Hydrogen bonds
- Ionic bonds
- Electrostatic interactions
- Hydrophobic interactions
- Molecular size and conformation
- Molecular weight

The diffusion of the active component out of the hydrogel matrix can be predicted from the lower critical solution temperature (LCT). This is because the hydrogel matrix shrinks as the LCT is reached resulting in its dehydration (Lakkis, 2007).

Encapsulated products need the hydrogel to show a sharp phase transition upon swelling. The swelling occurs due to environmental conditions such as temperature, pH, electric field etc. (Lakkis, 2007; Wang, Bamdad, Chen & Song, 2012).

2.6.3 Coacervates

Thies (2001) explains that coacervation is based upon the ability of cationic and anionic polymers to interact in aqueous solutions creating different phases. This principle results in liquid-liquid phase separation into polymer-rich and polymer-poor phases (Zuidam & Shimoni, 2010).

Usually core materials that are water insoluble whether in solid or liquid form are used in this process. This is due to their ability to stay undissolved in the aqueous phase (Lakkis, 2007). The encapsulated product formed usually have a reservoir type structure, however the shell is uneven in thickness (Thies, 2001), often with an oval shape (Zuidam & Shimoni, 2010).

There are two types of coacervation processes: simple and complex (Zuidam & Shimoni, 2010). Simple only involves one polymer whereas complex involves two polymers (Roos & Livney, 2017; Zuidam & Shimoni, 2010). Lakkis (2007) explains simple coacervation is based on a solution of water and one polymer, where the polymer is 'salted out' by the addition of salts or alcohols, which have more affinity to water than the polymer did. This forces a separation of the liquid phase, which can be utilised to encapsulate active ingredients.

Complex Coacervation is usually the type used to create encapsulated products (Zuidam & Shimoni, 2010) with both polymers forming part of the final encapsulating shell (Roos & Livney, 2017; Thies, 2001). The mixing of the second polymer into the system containing the first polymer and core material creates the complex coacervate (Zuidam & Shimoni, 2010).

Thies (2001) explains further, an equilibrium system forms between the concentrated phase and the dilute phase. Essentially forming a continuous (dilute phase) and dispersed phase (concentrated phase). This creates a solution of three immiscible phases; oil (containing an active ingredient), polymer-rich (coacervate), and polymer-poor phase (Zuidam & Shimoni, 2010). Zuidam and Shimoni (2010) further explains that this occurs because of interfacial sorption where the

concentrated polymer phase will deposit on the oil droplets. Then a solidification step or hardening process will occur which creates the final encapsulated product (Thies, 2001).

When encapsulating products, a common polymer used as the cationic polymer is gelatin (Thies, 2001). There are various anionic water-soluble polymers, which can be used to form complex coacervates with gelatin, including gum Arabic (Thies, 2001; Zuidam & Shimoni, 2010).

This process usually produces encapsulated product with a diameter of 30-800 microns and a loading of 80-90 weight percentage (Thies, 2001). The type of polymers chosen to form the coacervate affects the formation and integrity of the encapsulated product formed. This is due to the following characteristics of the polymers chosen and other processing conditions:

- Molecular weight (Lakkis, 2007)
- W/W ratios (Lakkis, 2007)
- Temperature (Lakkis, 2007)
- Processing time (Lakkis, 2007)
- Polymer strength (Zuidam & Shimoni, 2010)
- Polymer quantity (Zuidam & Shimoni, 2010)
- Charge density of the polymer (Zuidam & Shimoni, 2010)
- pH (Zuidam & Shimoni, 2010)
- turbulent flow of the system (Zuidam & Shimoni, 2010)
- emulsion size (Zuidam & Shimoni, 2010)
- ionic strength (Zuidam & Shimoni, 2010)
- Cooling rate of the system (Zuidam & Shimoni, 2010)

2.6.4 Polymer-polymer incompatibility

Encapsulation through polymer-polymer incompatibility occurs when two immiscible polymers are both mixed and dissolved in the same solvent. Their incompatibility results in the formation of two distinct liquid phases due to the repulsion between the molecules (Thies, 2001).

Thies (2001) explains further that an equilibrium system forms where each phase contains a high concentration of one of the polymers and a very low concentration of the other.

The encapsulation process utilizes one of these polymers and not the other, with one polymer becoming the capsule shell. In practice, small amounts of the other polymer might end up entrapped in the final encapsulated product as an impurity. They often are made using ethyl cellulose shells and are irregularly shaped 200-800 micron particles. The active ingredient is usually a solid particle (Thies, 2001).

2.6.5 Emulsification

Zuidam and Shimoni (2010) explain emulsions are two-phase systems, which are kinetically not thermodynamically stable. Emulsions are commonly made under high shear (Roos & Livney, 2017; Zuidam & Shimoni, 2010). Stabilising the interface with surfactants might prevent or delay phase separation (Roos & Livney, 2017; Thies, 2012; Zuidam & Shimoni, 2010).

Emulsion droplets can be used to form encapsulated products in two distinct situations (Zuidam & Shimoni, 2010):

i. In extrusion processes – an emulsion may be one of the fluid(s) being extruded, or
ii. In fluid based systems e.g. coacervates – where the emulsion creates a template for further processing.

The fluid based systems are looked at below. Extrusion processes have their own section (section 2.6.6).

Calcium Chloride might be added to a pre-formed emulsion (Thies, 2012; Zuidam & Shimoni, 2010). This emulsion would contain suspended droplets of alginate solution and the active material with the continuous phase being vegetable oil. Zuidam and Shimoni (2010) explain that when the Calcium Chloride is added it results in the emulsion breaking down while simultaneously the active is encapsulated due to the alginate gelling.

Zuidam and Shimoni (2010) also explain an alternative process involving adding both alginate and an insoluble form of calcium into the water phase of the emulsion. Next, an oil soluble acid is added which causes the pH to decrease. This, in turn, initiates the gelling of alginate because of the calcium ions released due to the lower pH.

An alternative process is making the water and oil emulsion hot with gelatin added to the water phase, then once the emulsion is formed rapidly chilling it to gel the water droplets (Tepsongkroh, Harnsilawat, Maisuthisakul & Chantrapornchai 2015).

The final encapsulated product in all situations would likely have to be washed to remove residual oil on their surfaces (Tepsongkroh et al., 2015; Zuidam & Shimoni, 2010).

2.6.6 Extrusion Processes

This is a very large category of encapsulation technologies and includes a variety of nozzle types and extrusion methods. It can also accommodate more than multiple fluid systems using co-extrusion techniques (Thies, 2001; Zuidam & Shimoni, 2010). Thies (2001) explains the process could involve a disk or a nozzle. The most well documented systems have nozzles, which are rotating, stationary, or vibrating (Thies, 2001; Zuidam & Shimoni, 2010). However, other options are available, as shown in Table 2.7 and Table 2.8.

Table 2.7: visual representation of possible nozzle systems (adapted from Zuidam & Shimoni, 2010)

Vibrating nozzle	Coaxial air flow	Electrostatic potential
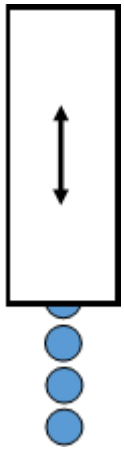	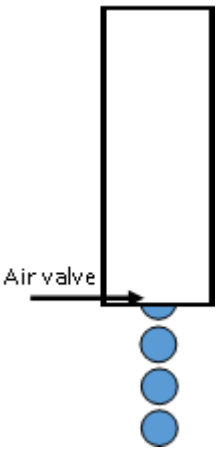	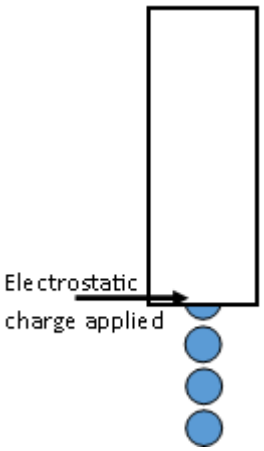

Table 2.8: visual representation of possible disk based systems (adapted from Zuidam & Shimoni, 2010)

Atomised jet cutter	Spinning disk
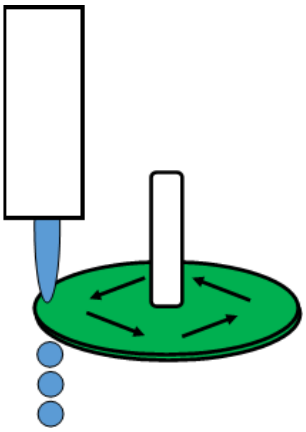	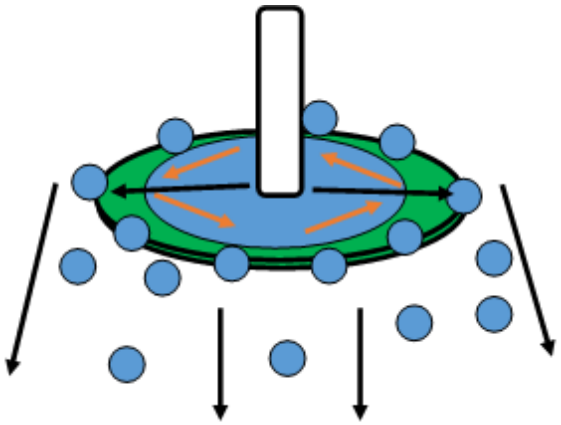

2.6.6.1 Difference between co-extrusion and simple extrusion:

In this situation, co-extrusion involves two fluids leaving the nozzle at once with one fluid encompassing the other to create a coating (Oxley, 2012). Extrusion, on the other hand, involves only one fluid leaving the nozzle (Oxley, 2012). This author further explains that both processes could involve an emulsion.

The shell material used in a co-extrusion process is often a gelling water-soluble polymer. This gelation usually occurs by one of two means (Bleiel, Kent & Brodkorb, 2017; McClements, 2014; Thies, 2012; Zuidam & Shimoni, 2010):

- interfacial gelling (gelling via ions) or
- gelation by cooling.

2.6.6.2 Difference between submerged and suspended nozzle processes:

Submerged nozzle processes are identified by the fact that the nozzle(s) are always immersed in another fluid to act as the carrier (Thies, 2001). Zuidam and Shimoni (2010) explain that this provides the benefit that the shell of the encapsulated product cannot be disrupted upon contact with the cooling liquid. Oxley (2012) explains further that the use of a carrier fluid aids encapsulation due to the following:

- capsule flattening during hardening and collection
- avoids inter-capsule collisions
- improves temperature control, and
- improves capsule size regulation.

Thies (2001) explains that suspended nozzle processes are identified by the fact that the nozzles are suspended in air. This means that fluid droplets, possibly containing more than one phase, are ejected from these nozzles into air. These droplets are then solidified, either, in the air by cooling, in a cool oil bath, or in an ion based gelling bath.

2.6.6.3 Stationary nozzle systems

Oxley (2012) believes stationary nozzle extrusion is the simplest technique. In this system, gravity is used to break the liquid stream into droplets (Oxley, 2012; Thies, 2001)). Alternatively, an applied external pressure may be used to form the droplets (Thies, 2001).

However, in this type of nozzle system there are instabilities in the breakup of the liquid stream into droplets and this leads to a range of sized capsules being produced, typically a bimodal size distribution (Oxley, 2012).

2.6.6.4 Vibrating systems

Vibrating systems have been developed to overcome the limitations with a stationary nozzle. Zuidam and Shimoni (2010) explain that the stream of liquid is broken up through the constant vibration making equal sized droplets. This results in a decrease in the particle size distribution observed (Oxley, 2012; Thies, 2001). This is achieved by vibrating the nozzle at a frequency that matches droplet formation.

The difference between the two systems is outlined in Figure 2.18.

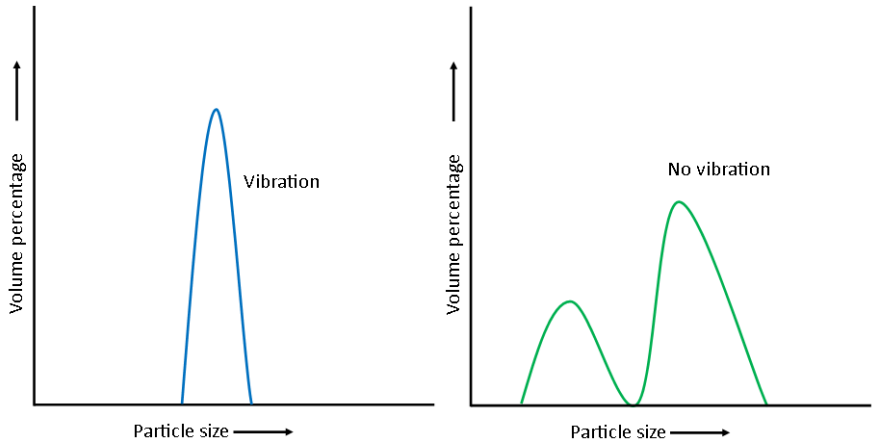

Figure 2.18: Graph showing the difference in particle consistency of encapsulated products made with either a stationary (left) or vibrating nozzle (right) (adapted from Oxley, 2012)

2.6.6.5 Rotating/spinning systems

In order to create large-scale systems with large number of capsules being produced, spinning/rotating systems were developed. The production capacity can be increased by either increasing the flow rate of solution fed into the nozzle or by increasing the number of nozzles or by creating nozzles/discs with more than one orifice (Oxley, 2012; Thies, 2001).

Zuidam and Shimoni (2010) explain that in a spinning or rotating system, the nozzle or disc is rotated very fast. This creates centrifugal forces on the extruded liquid and droplets are formed due to Raleigh instabilities.

An example of the set-up for a centrifugal nozzle is shown in Figure 2.19.

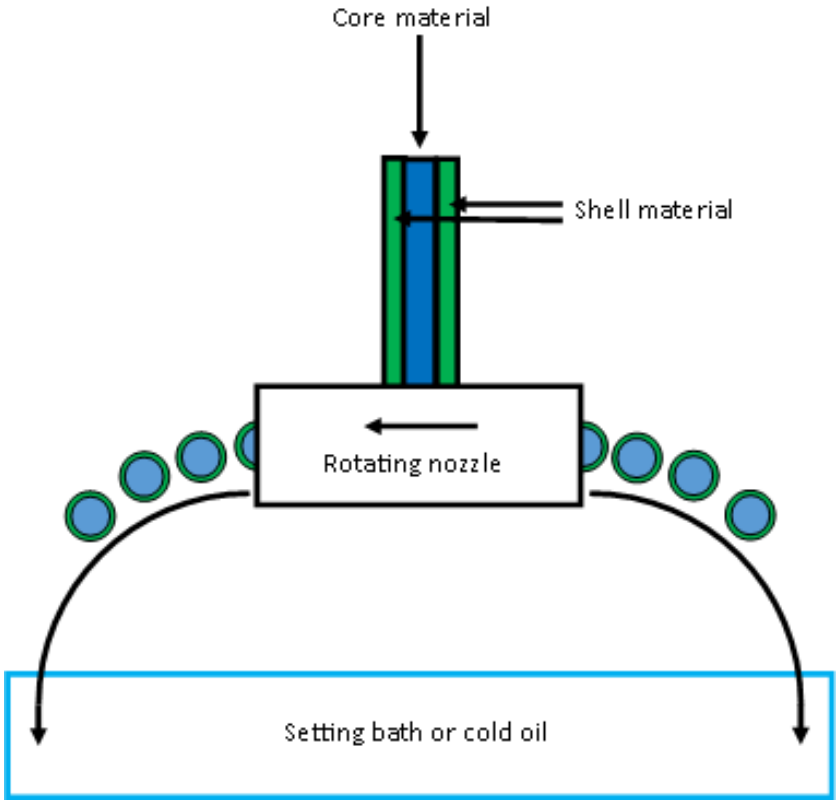

Figure 2.19: Image showing a centrifugal co-extrusion nozzle (adapted from Oxley, 2012)

2.6.6.6 Example Systems

Example – Suspended Centrifugal nozzle:

This technology involves two mutually immiscible liquids being pumped through a spinning two-fluid nozzle, which forms a stream of liquid, which breaks up into droplets upon leaving the nozzle (Thies, 2001). Each droplet contains a continuous core with a shell around the circumference (McClements, 2014).

Two types of shell materials can be used in this process; hot melt waxes or gelling aqueous polymers. Thies (2001) explains that hot melt waxes need to be relatively

low viscosity, which crystallise rapidly upon cooling. Gelling aqueous polymers can either gel upon cooling (gelatin) or upon falling into a gelling bath (sodium alginate into a calcium chloride bath) (McClements, 2014; Thies, 2001, 2012; Zuidam & Shimoni, 2010). Furthermore, Thies (2001) outlines that some encapsulation systems might need pre-hardening via a spray to minimise breakage upon contact with the gelling bath.

Example – Suspended Spinning or rotating disk:

In this process, core material and shell material are coextruded onto the rotating disc (Roos & Livney, 2017; Thies 2001). Thies (2001) elaborates that the disc may be bowl-shaped rather than flat. The disk is spun to create centrifugal force (Roos & Livney, 2017; Thies 2001). This forces the dispersed core material and liquid coating across the surface of the disc to the outer edge (McClements, 2012; Roos & Livney, 2017; Thies 2001). Thies (2001) explains that next the solution is spun off the disk into the air as discrete droplets.

The core material can be either particles or an emulsion/dispersion (Thies, 2001). This creates discrete particles covered with a thin film (Roos & Livney, 2017; Thies, 2001), and droplets filled with dispersed core material respectively (Thies, 2001).

Thies (2001) explains that the shell material can be a hot melt wax. Alternatively, the shell material could also be an aqueous polymer that gels (McClements, 2012; Thies, 2001). This can be by ions, cooling or a combination of the two (Thies, 2001; Zuidam & Shimoni, 2010).

The size of the encapsulated product produced is affected by (Thies, 2001):

- Disc geometry
- Diameter of disc
- Speed of rotation
- Volume flow rate across the disc
- Surface tension of the aqueous phase as it falls into the gelling bath (in the case of gelling by ions).

3 Extraction process development

3.1 Introduction

This stage involved developing the existing benchtop process to a small commercial scale. This chapter presents the results of the two extractions completed for the project including the trials done on microbial loading, concentration effects and heat treatments as well as a final nutritional analysis. Finally, it also looks at a detailed mass and energy balance for the second extraction.

3.2 Existing process

Previous work at Massey had been conducted using the benchtop process below (Wee, 2015):

1. The fronds were cut into logs ~50cm long (Figure 3.1a)
2. The fronds were washed and cut into slices of ~6mm thick using a benchtop slicing machine (Figure 3.1b)
3. ~50^{o}C warm water was added at a ratio 2:1 ratio (water to frond ratio) (Figure 3.1c)
4. The mixture was put through a wet disintegrator for 2 minutes to extract the mamaku into the water phase (Figure 3.1d)
5. The pulp was separated from the extract using cheese cloth and applying pressure by hand squeezing (Figure 3.1e)
6. The extract was centrifuged at 13600 g for 30 minutes at 20^{o}C to remove insoluble materials.
7. The supernatant was filtered through a sieve of aperture size 345 µm to remove any further impurities (Figure 3.1f)
8. The extract was then freeze-dried.

The figure presented in May's thesis (Wee, 2015) is reproduced on the next page in Figure 3.1, visually showing some of the process explained in the steps above.

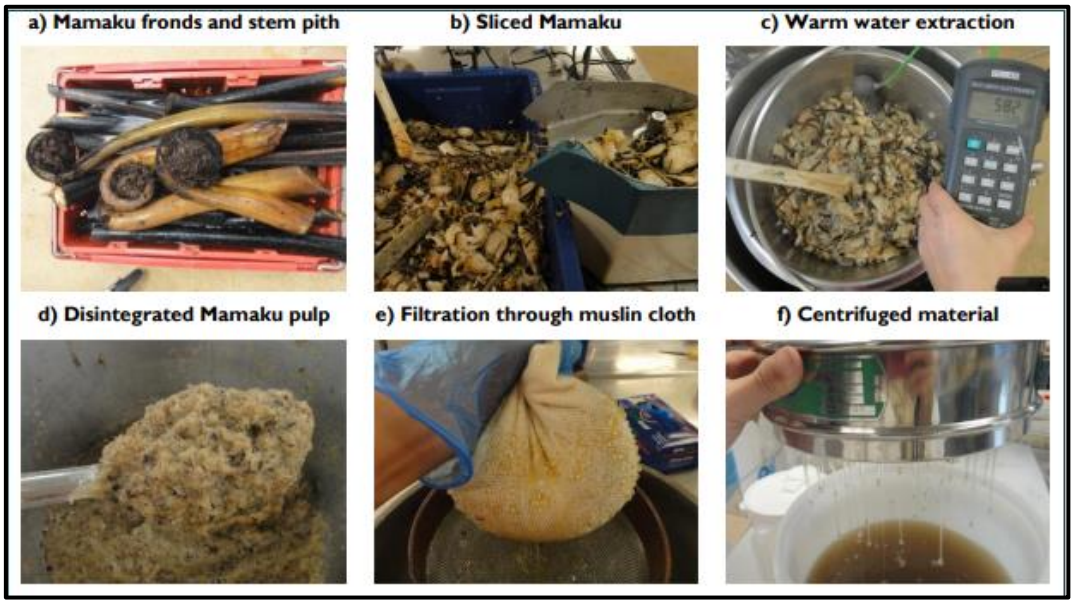

Figure 3.1: Pictorial representation of original mamaku extraction process (Wee, 2015)

This process was developed with the aim of producing the purest mamaku polysaccharide possible. Because of this, the process was time consuming and was based on a total batch extraction of 12kg. This process achieved a yield of 1%wt/wt mamaku from the original weight of fronds and the final mamaku still had a moisture content of ~10%.

This current project required handling greater quantities of mamaku (>100kg). Furthermore, the mamaku obtained was not being used to study fundamental science but to develop a food ingredient, so any slight impurities were not detrimental to the research findings.

This lead to the process being redesigned to enable the extraction of mamaku from 200kg of fronds, at small industrial scale.

3.3 Scaled up process

For this project, there was the need to create an optimum commercially viable process. The main purpose was to up-scale to allow large quantities of mamaku to be extracted at once.

This aimed to provide the client with an idea of the yield that could be achieved in a factory when using this mamaku for food use, not strictly for research purposes, as well as an idea of the type of equipment, which could be used.

The process developed to extract mamaku from 200kg of fronds is outlined below:

1. Fronds were mulched in commercial mulcher with some water being added to help eject the pulp from the machine instead of sticking to the blade.
2. Mulched fronds were added to a 300L steam jacketed pan with warm water at ~50^{o}C at a 2:1 ratio (two parts water to one part mulched fronds) and heated to 55^{o}C while continuously mixing and then held there for 15 minutes.
3. The solution was scooped/poured into mesh bags within the wine press collecting all liquid, which ran out. The bags were folded down to seal and pressure was applied until the wine press was pressed down at least half the height of the original full bags. The extract was collected as it was pressed out. The press was unloaded saving the pulp in a container for the second extraction. The bags were filled and the steps repeated until the whole batch was processed.
4. Steps two and three were repeated until all mulched fronds were extracted. At this point, the first extraction is complete.
5. Steps two and three were repeated with the left over pulp from the first extraction to obtain the second extraction.
6. The raising film evaporator was used to evaporate the dilute mamaku extract to obtain concentrated mamaku extract. The processing

parameters used for the evaporator are detailed in Table 3.1. The dilute solution had a concentration of ~1%wt/v mamaku and was concentrated to ~5.5-6.6%wt/v mamaku.

Table 3.1: Processing parameters used in the raising film evaporator

	Steam Side	**Product Side**
Temperature	70°C	50°C
Pressure	-14.9 inches mercury gauge 50% vacuum 50.8 kPa absolute	-30 inches mercury gauge 100% vacuum 0 kPa absolute

7. The concentrated mamaku was chilled overnight and then placed in a large steam jacketed pan and heated gently to 63°C. It was then held at 63°C for 30 minutes to pasteurize it. This ensured that the mamaku is safe to consume from a microbiological perspective.
8. The mamaku solution was bagged while it is still warm and sealed. It was then frozen when cool.

In this process, there is the potential to target a more concentrated mamaku solution. However, the more concentrated the solution the greater the shear-thickening properties are, and the harder the solution is to work with. This could cause processing difficulties.

The ideal concentration to target is established in future work (Chapter 6) taking into account the concentration needed to provide the effect in the stomach and the need to keep the mamaku solution at a concentration that can be processed easily.

3.3.2 Batch 1

This extraction started with ~80kg of fronds. There was 30kg of mamaku solution obtained at the end with a total solids content of 6.6%wt/v. Some photos of the process are shown in Table 3.2.

Table 3.2: Photos showing the extraction process

Mulched fronds	Extraction process in steam jacketed pan	Wine press extracting mamaku extract	Final mamaku extract (before concentrating)
			

This extraction was done with a small mulcher, which required a time consuming step where the fronds to be cut down lengthwise and a lot of water to be added to actually get the mulcher to expel the fronds. After extracting, the dilute extract was frozen.

Microbial testing

Microbial testing was conducted on the dilute extract to establish the microbial loading. One sample was left for the weekend in the refrigerator and the other sample was frozen. The test results are shown in Table 3.3 and the full report can be found in Appendix A.

Table 3.3: Results for standard plate count testing of dilute mamaku extract when left refrigerated for the weekend and when left frozen for the weekend

Sample number	Sample name	APC (30°C)
1	mamaku extract (Frozen for weekend)	4.0×10^2CFU/ml
2	mamaku extract (Chilled for weekend)	4.5×10^2CFU/ml

These results show that the microbial loading of the mamaku extract is low and keeping it chilled for three days does not show much of an increase.

Evaporation trial

Due to the freeze-drier not being installed in the Pilot Plant on campus at Massey during the extraction time period, it was decided to evaporate the excess water using a raising film evaporator under 100% vacuum instead of freeze-drying it.

The first step in developing the process involved a trial of ~60L of dilute mamaku being evaporated over 3 hours until the volume was below the capacity of the evaporator. This trial established, firstly, what temperatures the mamaku would be exposed to and for how long; and secondly, if the mamaku still displayed shear-thickening behaviour after being concentrated.

This trial showed that the temperature of the mamaku solution could be kept well below 60^{o}C and that running the evaporator for three hours would result in an excessively viscous solution difficult to measure, pour and work with. Somewhere between two and three hours per batch was decided to be more of an ideal timeframe for maintaining the consistency of the mamaku solution for handling.

In order to see if the shear-thickening behaviour of the mamaku obtained during this trial was still suitable, flow behaviour properties were measured. This was completed using the rheometer, geometries and peltier plate outlined below:

- Anton Paar Physica MCR 302
- C-DG26.7/T200, part number 79017, diameter internal 23.826mm, diameter external 27.589mm
  DG26.7, part number 79017, diameter 26.660mm, diameter internal 24.650mm, length 40.000mm
- C-CC27/T200, part number 79025, diameter 28.923mm
  CC27, part number 78234, diameter 26.659mm, length 40.000mm
- C-PTD200-SN82242374

The settings used to programme the rheometer are detailed in Table 3.4.

Table 3.4: Interval settings for the viscosity profile

Parameter	Interval	Temperature	Shear Rate
Profile chosen	Variable measurement point duration	Constant	Ramp log
Value	/	20°C	/
Initial	30s	/	0.01 s^{-1}
Final	2s	/	1000 s^{-1}
Meas. Points	41		

The results of this trial are shown in Figure 3.2.

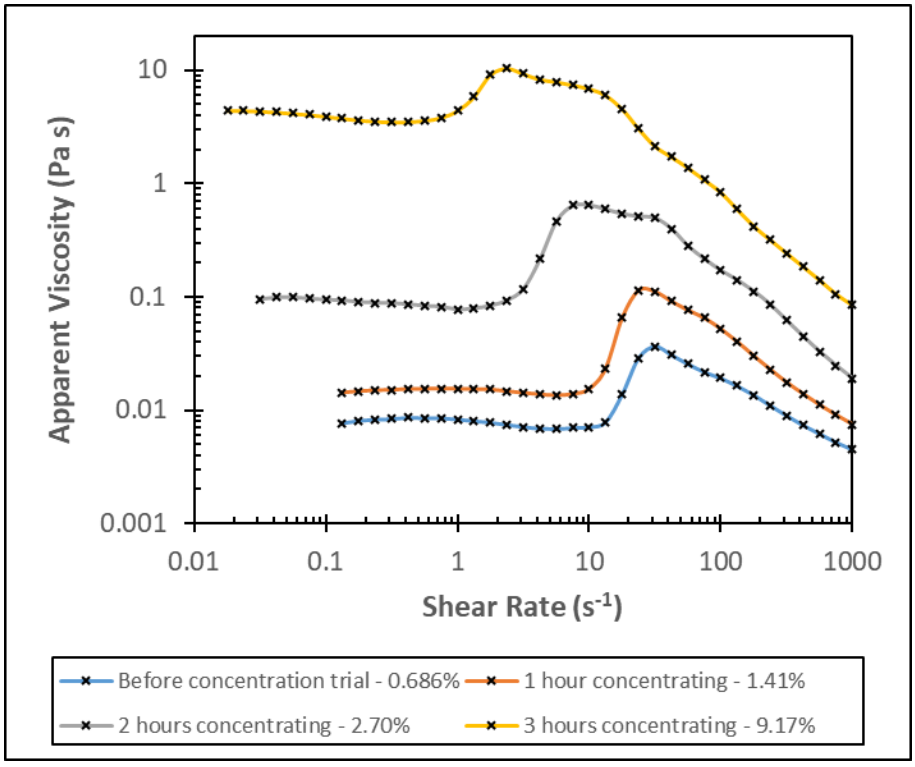

Figure 3.2: Effects of mamaku concentration on the shear-thickening peak measured

This graph clearly showed that over time, the viscosity of the mamaku solution increases, as did the shear-thickening peak viscosity. Additionally, the shear rates of the shear-thickening peak viscosity decreased, as the mamaku got more concentrated.

After the trial was deemed a success, the rest of the extract was concentrated in batches until the remaining extract was concentrated leaving ~30kg. At which

point the concentrated extract was pasteurised using a heat treatment of 63°C for 30 minutes. This heat treatment was chosen based on the results of heating regimes in Chapter 4, because it was shown not to damage the shear-thickening properties of the mamaku.

Microbial testing was conducted on the concentrated extract to establish the microbial loading after the heat treatment. The test results are shown in Table 3.5 and the full report is in Appendix B.

Table 3.5: Results for standard plate count testing of concentrated mamaku extract after heat treatment of 63°C for 30 minutes

Sample number	Sample name	APC (30°C)
1	mamaku	2.1×10^2CFU/ml

This result shows that the microbial loading of the mamaku solution is low and the heat treatment was successful at creating an extract, which is safe to eat. The intention was to create a product, which is safe to eat, not completely sterilised.

3.3.3 Batch 2

This extraction started with 130kg of fronds. There was 72kg of mamaku solution obtained at the end with a total solids content of 4.51%wt/v. Photos detailing the process are shown in the following tables, Table 3.6 to Table 3.9.

Table 3.6: Photos showing the mulching step of the extraction[1]

Raw fronds	**Large mulcher**	**Mulching the fronds with water from the hose**
		

[1] Pictures taken by Peter Jeffery or Rebecca Tresidder, Massey University.

Final mulched fronds	Final mulched fronds
	

Table 3.7: Photos showing the warm water extraction and pressing steps of the extraction[2]

Warm water extraction	Wine press
	
Extracting mamaku through the wine press	**Sieving the extracted mamaku before concentration step**
	

[2] Some pictures taken by Peter Jeffery or Rebecca Tresidder, Massey University.

Table 3.8: Photos showing the evaporation step of the extraction[3]

Running the evaporator	Running the evaporator
	

Table 3.9: Photos showing the pasteurisation and packaging steps of the extraction

Pasteurisation in steam jacketed pan	Final end product
	

[3] Pictures taken by Peter Jeffery, Massey University. Reproduced with permission.

At the end of the pasteurisation step, the 72 kg was bagged and measured into a variety of containers. In addition, microbial testing was conducted on the concentrated extract to establish the microbial loading after the heat treatment. The test results are shown in Table 3.10 the full report is in Appendix C.

Table 3.10: Results for standard plate count testing of concentrated mamaku extract after heat treatment of 63°C for 30 minutes

Sample number	Sample name	APC (30°C)
1	mamaku	6.0×10^2CFU/ml

This result shows that the microbial loading of the mamaku solution is low and the heat treatment was successful at creating an extract, which is safe to eat.

3.4 Final extract analysis

Upon the completion of the two extractions, a number of tests were conducted to identify any key differences in the two batches of mamaku. Firstly, a proximate analysis was conducted on both batches. Secondly, the rheology was investigated to see if either batch showed a different shear-thickening profile.

3.4.1 Proximate analysis

The proximate analysis was conducted by the Nutrition Laboratory, Riddet Innovation, Massey University. The nutrition report can be found in Appendix D. The methods used to measure each value provided for the wet basis include:

- Ash: Furnace 550°C AOAC 942.05 (Feed, meat)
- Crude protein: AOAC 968.06 (Dumas method). N-P = 6.25
- Fat: (Mojonnier) Acid, (Baked, extruded products) AOAC 922.06
- Total Dietary fibre: Megazyme, AOAC 991.43
- Avail Carbohydrate (Carb): By difference
- Starch: α-amylase Megazyme kit, AOAC 996.11
- Sugars: Phenol sulphuric, Sub-contracted

- Moisture: Vacuum oven, AOAC 990.19, 990.21

Equation 5 shows how the dry basis percentage values were obtained.

$$Dry\ basis\ \% = \frac{Wet\ basis\ \%}{Total\ solids\ \%} * 100 \quad (5)$$

The results from the nutritional analysis have been summarised in Table 3.11.

Table 3.11: Wet basis and dry basis nutritional information for mamaku extract obtained from batch 1 and batch 2

	Wet basis		Dry basis	
	Batch 1	**Batch 2**	**Batch 1**	**Batch 2**
Moisture %wt/wt	92.5	95.1	0	0
Total solids %wt/wt [4]	7.5	4.9	100	100
Ash %wt/wt	1.45	1.09	19.4	22.2
Protein %wt/wt	0.14	0.08	1.9	1.6
Fat %wt/wt	0.05	0.03	0.6	0.6
Total Carbohydrates %wt/wt	5.25	3.34	70.2	67.9
Soluble Sugars g/100g	4.5	2.7	60	55
Starch %wt/wt	0.16	0.06	2.2	1.1
Total Dietary Fiber %wt/wt	0.58	0.38	7.8	7.8

These results show reasonably good agreement across the two batches in terms of the nutritional profile of the mamaku extract. This showed that despite the two batches occurring about a month apart, there had not been much seasonal variation in the nutritional composition of the fronds of the mamaku within that timeframe.

The total solids values shown for batch one are higher than what was previously measured (6.6%wt/v - see section 3.3.2 above). This can be explained by the fact that this batch was not mixed together in one large steam jacketed pan, so it is likely that there is some variation across the final packages of batch one.

[4] Total solids % is calculated from 100 minus moisture %

Again the total solids for batch two is higher than what was previously measured (4.51%wt/v- see section 3.3.3 above). However, the variation in the values is much smaller than what is shown for batch one, likely as a result of the thorough mixing of the entire batch while undergoing the pasteurisation step.

3.4.2 Rheology of final product

In order to see if the shear-thickening behaviour of the mamaku obtained in the two extraction batches was similar in rheological terms, viscosity profiles were produced. This was completed using the rheometer, geometries and peltier plate outlined below:

- Anton Paar Physica MCR 301
- Concentric cylinder: C-CC27/T200, part number 79025, diameter 28.923mm
  CC27, part number 78234, diameter 26.659mm, length 40.000mm
- C-PTD200-SN870436

The settings used to programme the rheometer are detailed in Table 3.12.

Table 3.12: Settings for the viscosity profile

Parameter	Interval	Temperature	Shear Rate
Profile chosen	Variable measurement point duration	Constant	Ramp log
Initial	30s	20°C	0.01 s^{-1}
Final	2s		1000 s^{-1}
Meas. Points	41		

The results can be seen in Figure 3.3. This graph showed that firstly, the final samples are showing shear-thickening behaviour between shear rates of 2-10s^{-1}. Secondly, that the curves obtained from the samples from each extraction batch agree with each other. Thirdly, that the trend in the curves between the two extraction batches agree. Lastly, the shear rates at which peak viscosity occurs

shows a small difference between the two extraction, with extraction two having its shear thickening occurring at a slightly lower shear rate than extraction one.

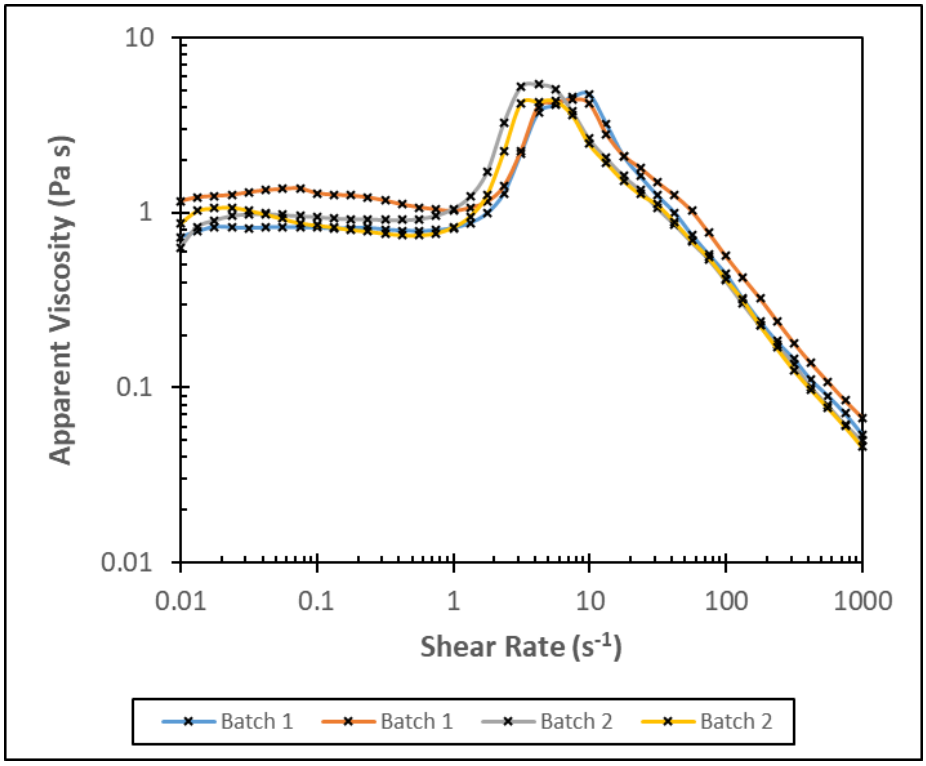

Figure 3.3: Viscosity profile showing the differences in the shear-thickening peak viscosity of mamaku at 20°C between the two extraction batches (6.6%wt/vol and 4.5%wt/v mamaku solutions) after pasteurisation, measured in duplicate.

These results follow the same flow pattern as seen in the past research (Goh et al., 2007, 2011, Wee, 2015). Showing an area of Newtonian flow, followed by shear-thickening at intermediate shear rates and as the shear rate increases further shear-thinning is observed.

Additionally the results obtained show higher viscosities at all points and a reduced shear rate at onset of thickening than those observed at similar concentrations during the most recent research (Wee, 2015). This can be seen in section 4.3.4 where the concentration of mamaku is compared with May's results.

The differences show that there is some improvement to the shear-thickening properties of the mamaku extracted using this method. However, there could be

differences in the age of the fronds, the freeze-drying or seasonal variation in the quantity of mamaku within a frond, which could also account for this increase in shear-thickening properties at similar concentrations.

3.5 Mass and energy balance

A mass and energy balance was completed during the second extraction to provide insight into the quantity of water required to extract the mamaku and the yield at each step. The calculations involved are detailed in Appendix E and Appendix F. The raw data for the weights involved is detailed in Appendix G, Appendix H, Appendix I and Appendix J. The following tables, Table 3.13 - Table 3.20, detail the mass and energy balance for each step in the process flow and Table 3.21 provides a summary of the key results obtained.

Table 3.13: Process flow in and out during the mulching step

Step 1: Mulching Fronds		
In		
Fronds	129.65	kg/batch
Water	41.92	kg/batch
Estimated Yield of Fronds	100	%
Temperature	18	°C
Out		
Mulched Fronds	171.57	kg/batch
Temperature	18	°C

Table 3.14: Process flow in and out during the chilling the mulched fronds step

Step 2: Chilling Mulched Fronds		
In		
Mulched Fronds	171.57	kg/batch
Temperature	18	°C
Specific heat	**unknown**[5]	kJ/kg/K
Enthalpy	Need specific heat to calculate	kJ/kg
Out		
Mulched Fronds	171.57	kg/batch
Temperature	4	°C
Cooling energy required	Need specific heat to calculate	kJ/batch

[5] unknown heat capacity for the mulched fronds due to unknown nutritional profile of the mulched fronds

Table 3.15: Process flow in and out during extraction round 1 of mamaku

Step 3: Extracting mamaku - extraction 1		
In		
Mulched Fronds	171.24	kg/batch
Water	340.00	kg/batch
Total	511.24	kg/batch
Temperature fronds	4	°C
Temperature water	50	°C
Temperature final	34.6	°C
15 minute Holding period - Environment Conditions		
Temperature of air	18	°C
Specific heat of air	1.005	kJ/kg/K
Enthalpy	18.1	kJ/kg
Heated mixing - Process steam in		
Heating steam	17.68	kg/batch
Holding period steam	5.96	kg/batch
Total steam	23.64	kg/batch
Temperature	100	°C
Vaporisation enthalpy	2202	kJ/kg
Specific heat of water at 100°C	4.219	kJ/kg/K
Total enthalpy	2392	kJ/kg
Heated Mixing - Process condensate out		
Water	17.68	kg/batch
Holding period water	5.96	kg/batch
Total water	23.64	kg/batch
Temperature	55	°C
Out		
Extract	342.19	kg/batch
Pulp	154.24	kg/batch
Yield of Extract (Dry)	200	%
Yield of Extract (Wet)	67	%
Yield of Pulp (Dry)	90	%
Yield of Pulp (Wet)	30	%
Temperature	55	°C
Specific heat	4.052[6]	kJ/kg/K
Enthalpy	222.9	kJ/kg
Heating energy required to heat to 55°C	42281[7]	kJ/batch
Heating energy required to maintain 55°C for 15 minutes	14258[8]	kJ/batch

[6] estimated based on the nutritional profile of final concentrated mamaku
[7] assuming that the loss of heat to the metal of the heat jacketed pan is negligible
[8] assuming that only 5% of the mass is losing heat to the environment and that the batch time unit is minutes already

Table 3.16: Process flow in and out during extraction round 2 of mamaku

Step 4: Extracting mamaku - extraction 2		
In		
Mulched Fronds	154.24	kg/batch
Water	310.51	kg/batch
Total	464.75	kg/batch
Temperature fronds	18	°C
Temperature water	50	°C
Temperature final	39.4	°C
15 minute Holding period - Environment Conditions		
temperature of air	18	°C
specific heat of air	1.005	kJ/kg/K
Enthalpy	18.1	kJ/kg
Heated mixing - Process steam in		
Heating steam	12.30	kg/batch
Holding period steam	5.42	kg/batch
Total steam	17.72	kg/batch
Temperature	100	°C
Vaporisation enthalpy	2202	kJ/kg
Specific heat of water at 100°C	4.219	kJ/kg/K
Total enthalpy	2392	kJ/kg
Heated Mixing - Process condensate out		
Water	12.30	kg/batch
Holding period water	5.42	kg/batch
Total water	17.72	kg/batch
Temperature	55	°C
Out		
Extract	343.53	kg/batch
Pulp (estimated)	107	kg/batch
Yield of Extract (Dry)	223	%
Yield of Extract (Wet)	74	%
Yield of Pulp (Dry)	70	%
Yield of Pulp (Wet)	23	%
Temperature	55	°C
Specific heat	4.052[9]	kJ/kg/K
Enthalpy	222.9	kJ/kg
Heating energy required to heat to 55°C	29419[10]	kJ/batch
Heating energy required to maintain 55°C for 15 minutes	12961[11]	kJ/batch

[9] estimated based on the nutritional profile of final concentrated mamaku
[10] assuming that the loss of heat to the metal of the heat jacketed pan is negligible
[11] assuming that only 5% of the mass is losing heat to the environment and that the batch time unit is minutes already

Table 3.17: Process flow in and out during the evaporation step

Step 5: Evaporation[12]		
In		
Extract from extraction 1	342.19	kg/batch
Extract from extraction 2	343.53	kg/batch
Total Extract	685.72	kg/batch
Temperature	ranging from 4-55	°C
Out		
Concentrated Extract	76.20	kg/batch
Water lost	609.52	kg/batch
Temperature	50	°C
Total solids	4.51	%wt/v

Table 3.18: Process flow in and out during the chilling step

Step 6: Chilling Concentrated Extract		
In		
Concentrated Extract	76.2	kg/batch
Temperature	50	°C
Specific heat	4.052	kJ/kg/K
Enthalpy	16.21	kJ/kg
Out		
Concentrated Extract	76.2	kg/batch
Temperature	4	°C
Cooling energy required	14205	kJ/batch

[12] there is a quantity of steam and water required to run the evaporator However it was not practical to measure since it changed was continuously tweaked to get the machine to run optimally for each small batch and there were instances when the steam available dropped lowering the efficiency of the evaporation

Table 3.19: Process flow in and out during the pasteurisation step

Step 7: Pasteurising mamaku		
In		
Concentrated extract	76.20	kg/batch
Temperature extract	4	°C
15 minute Holding period - Environment Conditions		
Temperature of air	18	°C
specific heat of air	1.005	kJ/kg/K
Enthalpy	18.1	kJ/kg
Heated mixing - Process steam in		
Heating steam	7.74	kg/batch
Holding period steam	2.19	kg/batch
Total steam	9.93	kg/batch
Temperature	100	°C
Vaporisation enthalpy	2202	kJ/kg
Specific heat of water at 100°C	4.219	kJ/kg/K
Total enthalpy	2358	kJ/kg
Heated Mixing - Process condensate out		
Water	7.74	kg/batch
Holding period water	2.19	kg/batch
Total water	9.93	kg/batch
Temperature	63	°C
Out		
Extract	72.66[13]	kg/batch
Temperature	63	°C
Specific heat	4.06[14]	kJ/kg/K
Enthalpy	255.6	kJ/kg
Heating energy required to heat to 63°C	18240[15]	kJ/batch
Heating energy required to maintain 63°C for 30 minutes	5169[16]	kJ/batch

[13] the difference in weight here is mainly due to a split bag which happened while I was sealing it meaning about a third of large bag of product ~2-3kg was lost. There would be some evaporative losses but not likely to be more than 1 kg

[14] estimated based on nutritional profile of final concentrated mamaku

[15] assuming that the loss of heat to the metal of the heat jacketed pan is negligible

[16] assuming that only 5% of the mass is losing heat to the environment and that the batch time unit is minutes already

Table 3.20: Process flow in and out during the cooling then freezing step

Step 8: Cooling then Freezing mamaku Solution		
In		
mamaku solution	72.66	kg/batch
Temperature	63	°C
Specific heat	4.06[17]	kJ/kg/K
Latent heat of fusion[18]	334	kJ/kg
Enthalpy	-73.03	kJ/kg
Out		
Mass flow rate	72.66	kg/batch
Temperature	-18	°C
Cooling energy required[19]	48149	kJ/batch

Table 3.21: Summary of results from mass and energy balance[20]

Raw materials needed to obtain the dilute mamaku solution		
Materials In		
Fronds	129.65	kg/batch
Water for mulching step, and hot water extraction	692.43	kg/batch
Materials Out		
Dilute mamaku extract	685.72	kg/batch
Pulp	154.24	kg/batch
Raw materials needed to concentrate the mamaku extract and heat treat		
Materials In		
Total Extract	685.72	kg/batch
Materials Out		
Concentrated Extract (after heat treatment)	72.7	kg/batch
Total solids	4.5	%wt/v
Water lost	609.52	kg/batch
Overall yield	56.1	%wt/wt
Estimation to the quantity obtained if the mamaku extract was freeze-dried		
Materials In		
Concentrated Extract (after heat treatment)	72.7	kg/batch
Total solids	4.5	%wt/v
Materials Out		
Concentrated Extract (after heat treatment)	3.64	kg/batch
Total solids	90	%wt/v
Overall yield	2.8	%wt/wt

[17] estimated based on nutritional profile of final concentrated mamaku
[18] estimated to be similar to water/ice
[19] assuming the heat capacity of frozen mamaku is the same as liquid mamaku
[20] the summary only accounts for the water needed to extract the mamaku not to run the evaporator and the moisture content of freeze-dried mamaku was assumed to be 10%

The overall yield when the extract was frozen was 56%wt/wt, based on 72.7 kg of final concentrated extract and 129.65 kg of fronds.

The overall yield if the extract was freeze-dried was calculated based on the assumption that drying will lower the moisture to 10% and that 4.5% is a true estimation of the total solids of the full 72.7kg of concentrated extract. This estimates the freeze-dried mass to be 3.64kg, giving an overall yield of 2.8%wt/wt.

The previous extraction obtained a yield of ~1%wt/wt (Wee, 2015). This lower value is partially explained by the additional purification steps that were done for that extraction to obtain more pure mamaku. Additionally, the pressing of the pulp was done manually by Wee (2015), which would have provided significantly less force than what the wine press did. These two factors account for the higher yield obtained by this up-scaled process.

3.6 Conclusions

This chapter details the work completed to develop a commercially viable extraction process and the results obtained when extracting each of the two batches of mamaku.

It also showed the brief analysis done on the final mamaku solution obtained including the microbial loading, nutritional analysis and its shear-thickening properties. Findings from this include that the two extractions produced solutions with similar properties.

Lastly, a mass and energy balance was completed on extraction two to provide some insight into the yield obtained, finding that 56%wt/wt yield was obtained based on the frozen solution and 2.8%wt/wt yield was obtained based on an estimate of the final weight of material if it was freeze-dried.

4 Mamaku analysis

4.1 Introduction

During the extraction of the mamaku, it was important to test the rheological properties to ensure that the new processing techniques did not damage the material affecting its functionality. Additionally, since it was extracted from the fronds taken from the plant, seasonal variation could affect the properties as well as the age of the fronds. Thus, it was necessary to identify the properties inherent to the actual raw material used, rather than relying on data previously measured with a different batch of mamaku, extracted a different way and at a specific time of the year.

Furthermore, there were conditions that the mamaku solution would be exposed to, which had not been tested previously in the past research on mamaku (Goh et al., 2007; 2011; Jaishankar et al., 2015; Lentle et al., 2010; Matia-Merino et al., 2012; Wee, 2015; Wee et al., 2014; 2015a; 2015b; 2017). Consequently, it was necessary to identify how each of these conditions may or may not have influenced the shear-thickening properties of mamaku. All the analysis aimed at measuring the viscosity properties of mamaku exposed to different conditions to gain a comparison of the viscosity at different shear rates. The following six factors were analysed:

- Freeze thaw cycles;
- Freeze-drying versus concentrating and freezing;
- Heating regimes;
- Mamaku concentration;
- Combined concentration and temperature effects on viscosity, and
- Combined pH and temperature effects on viscosity.

4.2 Methods

4.2.1 Viscosity profile set up

The following rheometer, geometries and peltier plate were used:

- Anton Paar Physica MCR 301
- C-DG26.7/T200, part number 79017, diameter internal 23.826mm, diameter external 27.589mm
  DG26.7, part number 79017, diameter 26.660mm, diameter internal 24.650mm, length 40.000mm
- C-CC27/T200, part number 79025, diameter 28.923mm
  CC27, part number 78234, diameter 26.659mm, length 40.000mm
- C-PTD200-SN870436

The settings used to programme the rheometer are detailed in Table 4.1.

Table 4.1: Interval settings for the viscosity profile

Parameter	Interval	Temperature	Shear Rate
Profile chosen	Variable measurement point duration	Constant	Ramp log
Value	/	20°C or 37°C	/
Initial	30s	/	0.01 s^{-1} or 0.1 s^{-1} if dilute
Final	2s	/	1000 s^{-1}
Meas. Points	41		

4.2.2 Sample preparation

The age of the mamaku solution was monitored for all measurements, ensuring all samples were discarded if they had been defrosted for more than 72 hours. This also, applied for rehydrated freeze-dried samples. Samples were stored in the fridge before being used and were equilibrated at room temperature before measurements were taken.

Freeze-dried mamaku was kept in a desiccator (with the silica beads monitored and refreshed as needed) to limit moisture uptake, the moisture content of the freeze-dried mamaku was 10%wt/v. Freeze-dried samples were rehydrated at room temperature for 24 hours prior to use under continuous stirring.

Temperature treatments were completed in the rheometer at a constant shear rate of $1s^{-1}$. The temperature was increased and decreased at a rate of 5°C per minute. Samples were then allowed to recover for 15 minutes at 20°C before the viscosity profile was measured. Mineral oil was added on top of all samples to be heat treated to minimise the effects of evaporation.

Finally, when re-freezing for subsequent freeze thaw cycles each sample was frozen for 12 hours before defrosting again. In addition, when adjusting the pH using 1M HCl or adjusting the concentration of mamaku, adequate stirring was completed to ensure the samples were well mixed. Each sample was then allowed to equilibrate before the measurements were taken.

4.2.3 Sample loading technique

Depending on the concentration of mamaku, either a pipette or syringe was used to load into the geometry with the appropriate amount of sample (~1mL for cone and plate, ~5mL for double gap and ~15mL for concentric cylinder). As the probe was lowered, the geometry was checked each time to ensure enough sample had been added eliminating the excess.

As explained by Wee (2015), the unique rheological properties of mamaku led to sample expulsion (in the case of cone and plate) or climbing the rod (in the case of double gap and concentric cylinder) at high shear rates, particularly when excessive sample is added.

4.2.4 Optimisation of rheological measurements

4.2.4.1 Recovery from shear

Figure 4.1, shows the visual reduction in the shear-thickening peak of mamaku solution upon subsequent shearing of the same sample.

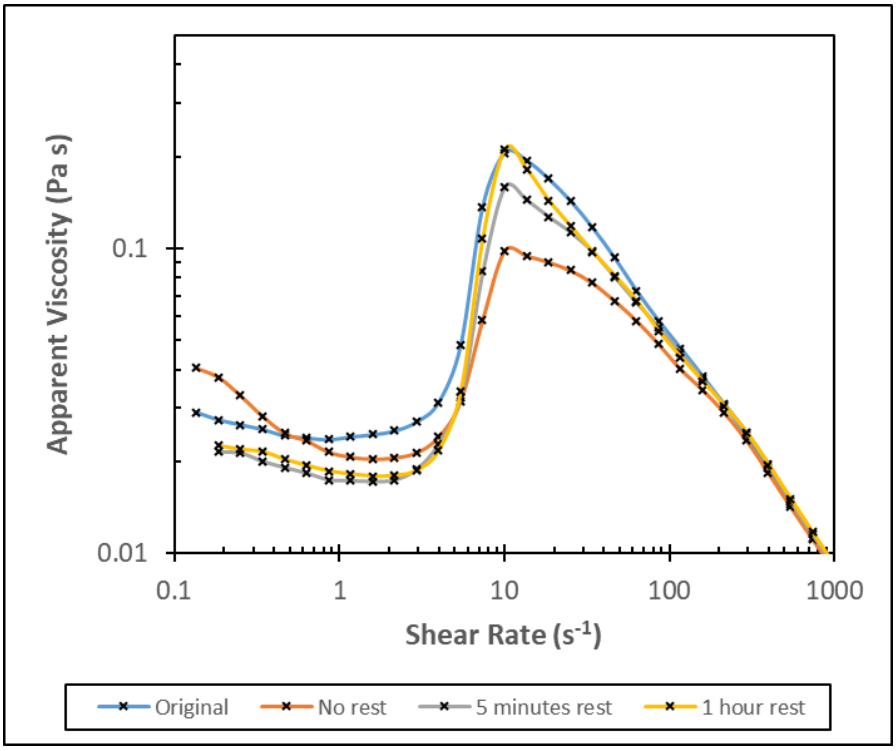

Figure 4.1: Viscosity profile showing the effect of high shear on the shear-thickening peak of 1.5%wt/v concentration mamaku solution measured after being exposed to a shear rate of 1000 s^{-1} at 20°C

The graph clearly showed that the shear-thickening profile was regained when the sample was given enough time to recover. These results clearly demonstrate the importance of allowing a sample time to recover after high shear is applied. It also showed that if given enough time the sample will fully recover. Wee (2015) explains that the high shear rates (above 20s^{-1} for 1.5%wt/v mamaku at 20°C) force the mamaku molecules to untangle and adopt stretched conformation. This in turn lowers the viscosity as shear increases further. After being sheared to 1000s^{-1} and the shear is stopped, there is a time delay for the mamaku chains to revert back

to their favoured conformation (semi-flexible extended random coil) and entanglement (Goh et al., 2007).

This forms the basis for allowing all measurements five minutes time to recover from being loaded into the rheometer (and any stirring that the sample might have undergone before loading into the rheometer).

4.2.4.2 Measuring geometries for concentrated sample

Cone and plate (CP), double gap (DG) and concentric cylinder (CC) geometries were compared to see if different viscosity profiles were obtained for concentrated mamaku solution. Figure 4.2, showed that each geometry led to a different viscosity profile for the concentrated mamaku solution (CP, DG and CC). This became a potential issue when the mamaku solution became so viscous that it could not easily be pipetted into the geometry. Furthermore, when using the double gap geometry, the measurement was not showing a shear-thickening peak.

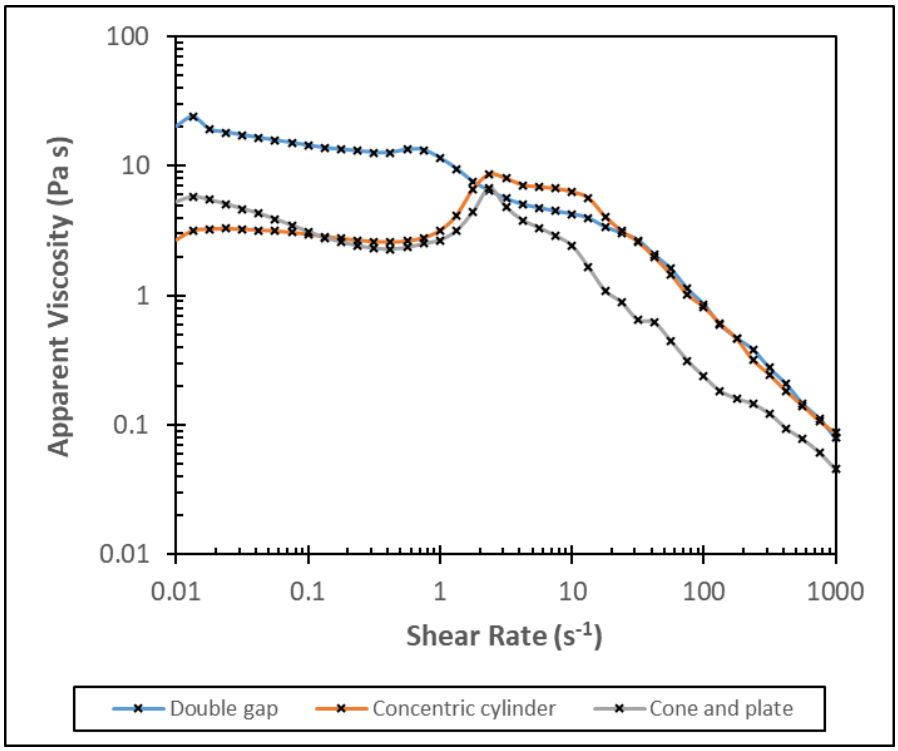

Figure 4.2: Viscosity profile of a 9.17%wt/v mamaku solution using DG, CC and CP geometries at 20°C.

This graph showed that the double gap geometry gives a completely different profile to that of the concentric cylinder and the cone and plate geometries. This showed that the measuring system chosen affects the results and clearly, in this situation the double gap is not an ideal measuring system for concentrated mamaku solution due to its inability to measure the shear-thickening peak viscosity accurately. This is supported with the physical evidence seen when measuring these samples in the rod climbing effect seen when using the double gap geometry.

The cone and plate, and concentric cylinder geometries align more closely, particularly at the shear-thickening peak. It is clear that the concentric cylinder is likely to be a better measuring geometry than the cone and plate. This is because the cone and plate measurement had already shown measurement issues in the past because of sample expulsion (May, 2015). This leads to the assurance that the concentric cylinder is the best, of those tested, for measuring concentrated mamaku. Concentric cylinder geometry was chosen as the geometry for measuring concentrated mamaku solution for the remainder of the experimental work.

4.3 Results and Discussion

4.3.1 Freeze thaw cycles

The freeze thaw stability of mamaku both at dilute and slightly higher concentrations was investigated. This had not been previously explored, because in the past research the mamaku was always freeze-dried (Goh et al., 2007; 2011; Matia-Merino et al., 2012; Wee, 2015; Wee et al., 2014; 2015a; 2015b).

The mechanism for the shear-thickening of mamaku relies on the polysaccharide chains firstly, becoming untangled and unfolder via shear, then orientating in such a way that hydrogen bonds can form between the mamaku chains, aided from charge screening effects provided by cations (Wee et al., 2015a). Then as shear is

further increased, these bonds are overcome and the solution shows shear thinning properties. This is shown visually in Figure 4.3.

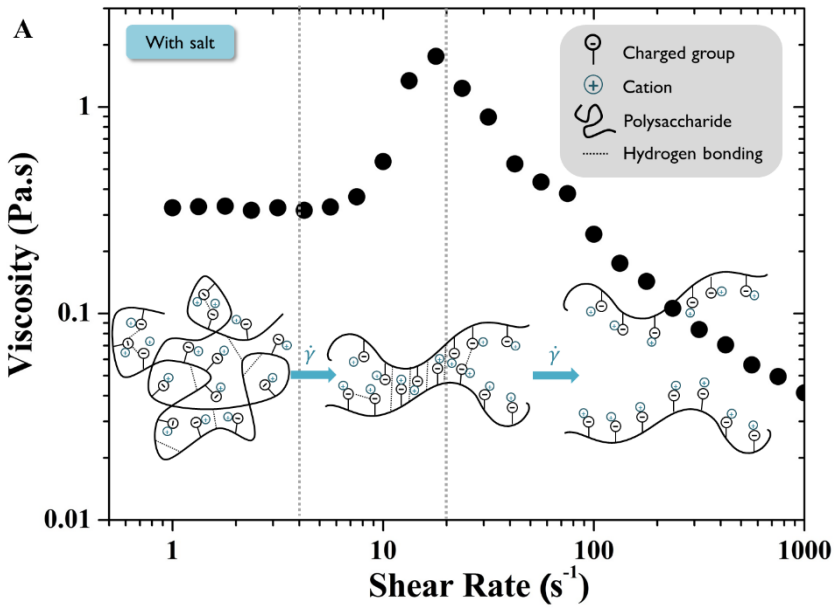

Figure 4.3: Illustration of the shear-thickening of mamaku (Wee et al., 2015a)

Although low concentrations of polysaccharides are often used as cyroprotectants in frozen foods (Goff, 1995), there was still the small possibility that an irreversible change to mamaku's conformation might occur meaning less mamaku chains would open up under shear to produce the thickening effect. Figure 4.4, showed that subsequent freeze thaw cycles do not have a large impact on the shear-thickening peak viscosity of the mamaku solutions. It showed there was a very small reduction by the time there had been three freeze thaw cycles in the dilute sample. The higher concentration also showed minimal impact of the cycles.

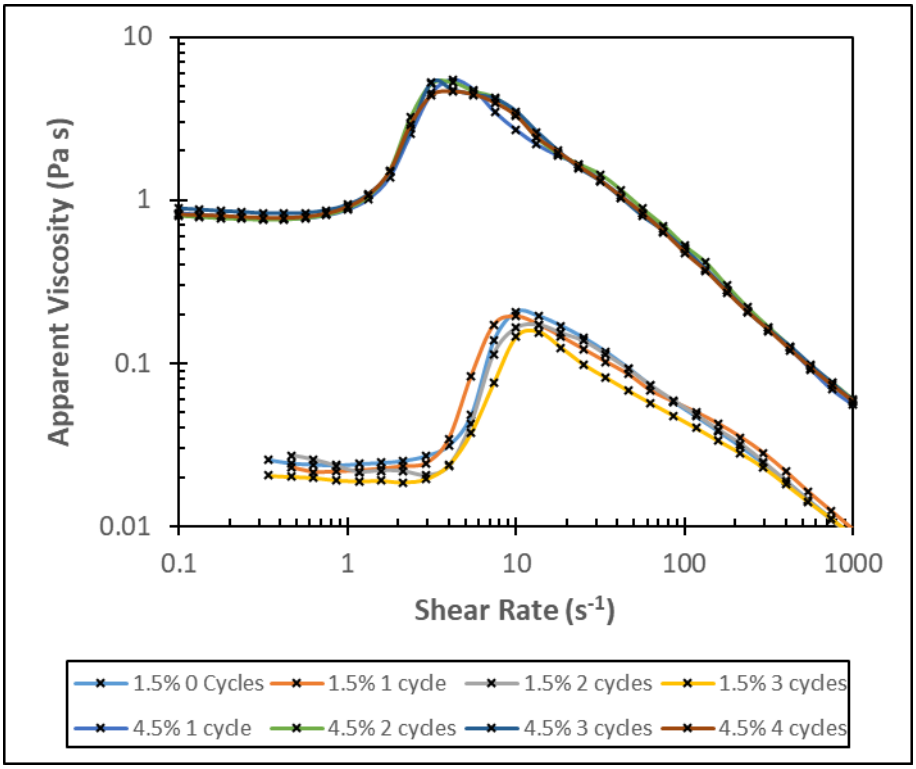

Figure 4.4: Viscosity profile showing the effect of freeze thaw cycles on the shear-thickening peak of 1.5%wt/v and 4.5%wt/v mamaku solution at 20°C

There was only a small difference between each freeze thaw cycle in the 1.5%wt/v mamaku solution. In particular, after three-freeze thaw cycles, the initial Newtonian viscosity had decreased slightly. The shear rate at onset of shear-thickening did not shift considerably. The peak viscosity decreased slightly from 0.21 Pa s in the original sample to 0.16 Pa s after three freeze thaw cycles. Additionally, the shear rate at peak viscosity show a slight increase from shear rates of 10 to 14 s^{-1} as the number of freeze thaw cycles increase.

Additionally, there was minimal changes in all parameters with subsequent freeze thaw cycles for the 4.5%wt/v mamaku solution. There was a small reduction in peak viscosity with each subsequent freeze thaw cycle. However, the shear rate at the peak viscosity did not change.

During a freezing process, the water phase in a polysaccharide solution can effectively be divided in two, free and bound water. The free water is not associated with the polysaccharide and therefore, will follow a simple freezing

process and expand when frozen. Whereas, the bound water is the water associated with the polysaccharide. Some of this bound water will freeze and the remainder will not freeze. When the free water and the freeze-able portion of the bound water freezes, the polysaccharide will be trapped in the conformation it was in at that point in time (Kocherbitov, 2016).

Upon thawing, the freeze-able portion of the bound water thaws and can interact with the polysaccharide again. In addition, the free water thaws and the polysaccharide molecules regain their ability to move and interact with each other. Furthermore, the polysaccharide can regain its ability to adopt an optimal conformation for its extended semi-flexible random coil structure (Goh et al., 2011).

As shown in the results, the freeze thaw cycles did not have a substantial impact on the viscosity profile of the mamaku, as it still displayed the same degree of shear-thickening. This means that the freezing and thawing process did not cause permanent changes to the conformation of the mamaku molecules, and the untangling, unfolding and orienting of molecules to form hydrogen bonds during thickening, was not affected.

4.3.2 Freeze-drying versus concentrating and freezing

Another factor investigated was the difference in properties of the same concentration mamaku solution when one sample was freeze-dried and rehydrated and the other was concentrated and frozen. This became a point of study because freeze-dried mamaku had been studied in the past but the majority of mamaku extracted for this project was concentrated and frozen.

Figure 4.5, showed that rehydrated freeze-dried mamaku did appear to have quite different properties than the frozen counterpart. The large difference appears to get somewhat smaller with higher concentrations.

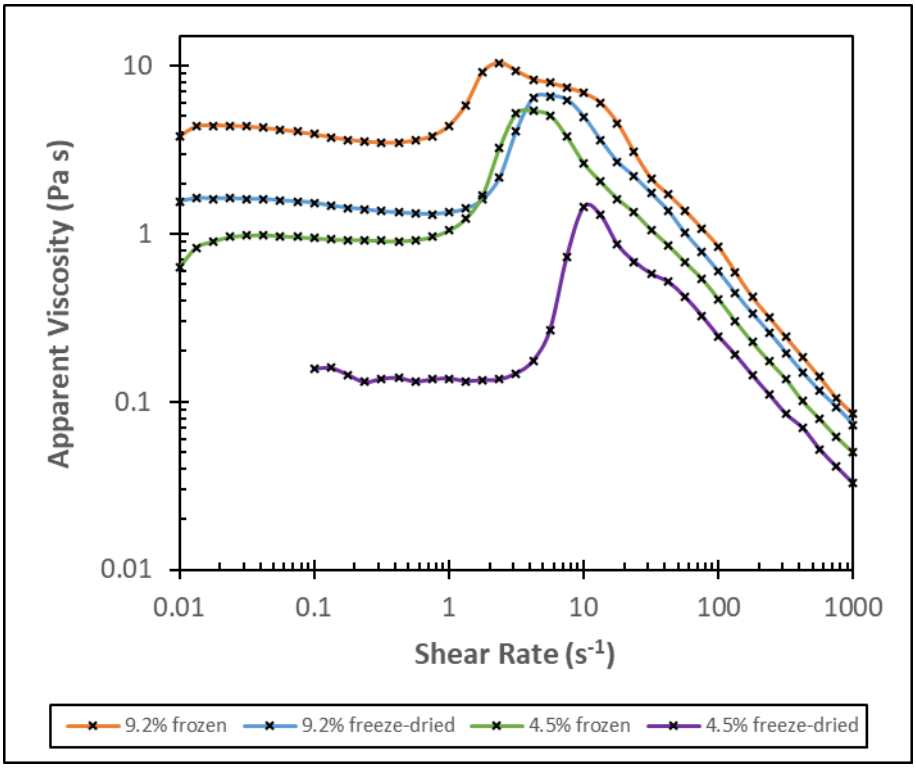

Figure 4.5: Viscosity profile showing the effect of freeze-drying on the shear-thickening peak of 9.2%wt/v and 4.5%wt/v mamaku solution at 20°C and 4.5%wt/v at 37°C

These results show not only does freeze-drying appear to reduce the initial Newtonian viscosity and the peak viscosity. It also appears to shift the shear rates at onset of shear-thickening, and shear rates at peak viscosity to higher shear rates. The differences in the peak viscosity are much smaller at the higher concentration, 9.2%wt/v, but the shear rate at the peak viscosity was still sifted when using the rehydrated mamaku.

Femenia, Selvendran, Ring and Robertson (1999) showed freeze-drying processes are less damaging to polysaccharide structure (and subsequently to the rehydration properties), than other drying methods involving heat. However, in their situation all solutions were dried. In the case of the two different mamaku solutions, one process did not involve a drying step at all, just concentration then freezing. Therefore, the effect of rehydrating versus not needing to rehydrate at all is actually the critical difference between the solutions.

Drying to 10%wt/wt moisture, or lower, can result in irreversible structural changes to a food, resulting in a reduction of a food's ability to absorb water upon rehydration (García-Segovia, Andrés-Bello & Martínez-Monzó 2011; Krokida & Marinos-Kouris, 2003). This was hypothesised to be because of a reduction in water absorption is proportional to the reduction in volume changes in the material (swelling) (Krokida & Marinos-Kouris, 2003). In the case of a polysaccharide, this would be linked with a reduction in the polysaccharide interacting with water.

This means upon rehydration each mamaku molecule adopts a less extended conformation, which leads to a reduction in viscosity of the solution at all shear rates. This change in conformation also increases the shear rates at onset of shear-thickening and of peak viscosity, because the mamaku chains are further away from each other meaning fewer interactions between the mamaku molecules can occur at any shear rate. This in turn, delays the onset of shear-thickening until higher shear rates occur. These changes to the shear-thickening profile occur as a result of the shear-thickening mechanism already explained in 4.3.1, which relies on the mamaku molecules untangling, unfolding and orienting in a way that the hydrogen bonds can form between molecules (Wee, 2015).

This explains the trends seen in the results, with the freeze-dried then rehydrated solutions showing considerable reduction in the viscosity profile than the concentrated + frozen counterparts. These findings have implications for the results obtained in Chapter 6 regarding the in-vitro digestion trials because freeze-dried mamaku was used for the higher concentration mamaku samples, rather than concentrated + frozen mamaku.

Overall, these results show that in order to obtain the highest degree of shear-thickening for the total solids concentration it is much more advantageous to extract and then concentrate before freezing, and not freeze-dry the mamaku at all.

4.3.3 Heating regimes

A key step in extracting the mamaku was ensuring it is safe to consume through a heat treatment step. It was already known that exposing the mamaku to high temperatures even for a short time irreversibly damaged its shear-thickening properties (Wee, 2015). Polysaccharide structure can be irreversibly changed by heat treatments and processing conditions (Femenia, García-Pascual, Simal & Rosselló, 2003). Thus, it was critical to test different heat treatments to ensure the one chosen would not damage the properties.

Figure 4.6, shows the effects of different heating regimes on the shear-thickening peak viscosity of 4.5%wt/v mamaku solution.

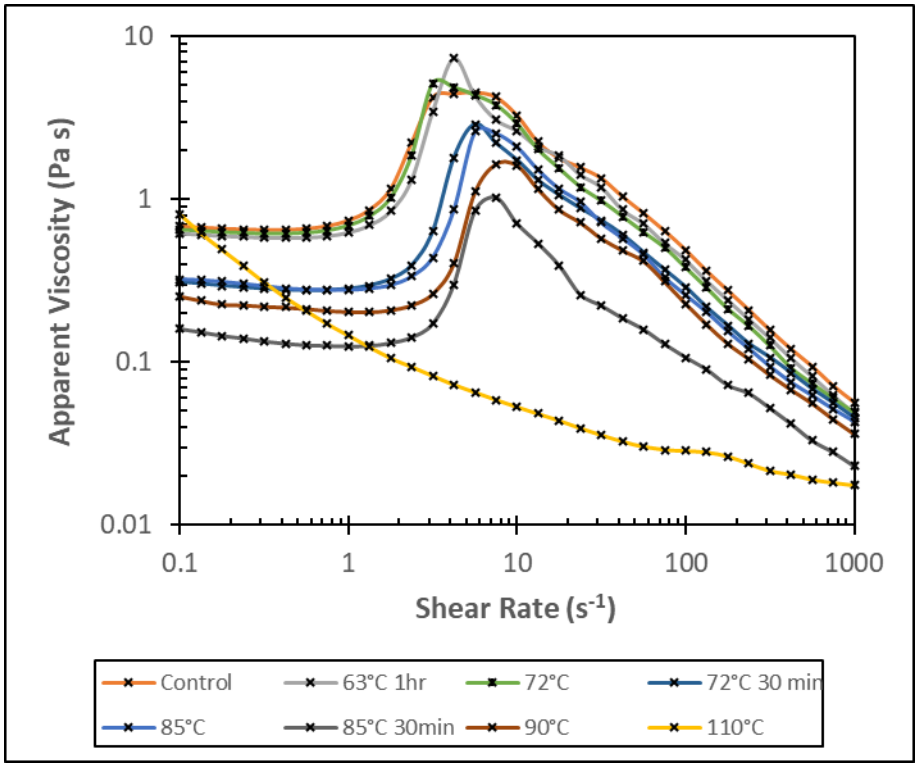

Figure 4.6: Viscosity profile showing the effect of various heat treatments on the shearing thickening peak of 4.5%wt/v mamaku solution. This was measured after being heated to the temperature at a rate of 5°C/minute, (and held there if appropriate) and cooled at a rate of 5°C/minute, then being left to recover for 15 minutes before conducting the viscosity profile at 20°C

This graph showed that both heating to 63°C for 60 minutes and to 72°C with no hold time had a very similar resulting shear-thickening peak viscosity as the control sample. This gave confidence that processing a standard heat treatment of 63°C for 30 minutes would not result in damage to the shear-thickening properties. The fact that mamaku can tolerate 60 minutes at 63°C provides a buffer to account for different heating and cooling rates, since depending on the scale of production heating and cooling at a rate of 5°C a minute might be too rapid.

The other heating regimes showed various degrees of irreversible degradation to the shear-thickening peak viscosity and the initial Newtonian viscosity. In addition, the shear rates at onset of shear-thickening was increased, as was the shear rates of the peak viscosity. Higher temperatures with and without a hold time showed higher degradation than lower temperatures with and without a hold time. Holding at any temperature above 63°C shows a further reduction in viscosity. There was a reduction in the viscosity at all shear rates as the temperature increased beyond 72°C. The shear-thickening properties were irreversibly lost when heated to 110°C.

There were clear trends in the results, including that the higher temperatures shifted the shear rates more than the longer times at the same temperatures, e.g. 85°C with no holding time and 90°C with no holding time, showed a large shift in the shear rates. However, increasing the time at the same temperature had a big impact on the initial Newtonian viscosity and peak viscosity but minimal change to the shear rates of each, e.g. 85°C with no holding time and 85°C for 30 minutes.

The secondary structure of a polysaccharide is dependent on the degree of branching and the tertiary structure is dependent on the presence of chain entanglements (May, 2015). It is well known that the flow behaviour is dependent on these secondary and tertiary structures of a polysaccharide and temperature and other environmental conditions can affect this reversibly or irreversibly. An irreversible change in conformation can be caused by depolymerisation of the polysaccharide caused by a proportion of the glyosidic bonds breaking, mostly

likely through β-elimination of uronic acid groups, as a result of high temperatures and low pH (BeMiller & Kumari, 1972; Bengtsson, Wikberg & Tornberg, 2011). This causes changes to the primary structure and therefore affects both the secondary and tertiary structure of the polysaccharide.

In this case, removing the uronic acid groups means a proportion of one of the three charged groups, proposed to be responsible for the intermolecular hydrogen bonds (Wee, 2015), is removed. This change reduces the repulsion within each molecule allowing the molecules to adopt a more favoured contracted conformation, resulting in increased volume within the solution because of the molecules being further apart. This causes an increase in the shear rates required for the onset of thickening (and thus shear rates at peak viscosity) due to stronger intramolecular bonds. It also causes a reduction in initial Newtonian viscosity because the molecules adopt a more contracted conformation, meaning they can flow past each other easier. Additionally, removing the uronic acid groups also means a reduction in peak viscosity because there are less sites available for hydrogen bonds to form between molecules reducing the shear-thickening occurring within the solution. This is supported by the trends in the results, with the higher temperatures and longer time periods showing greater degradation because more uronic groups would be removed.

Overall, these results show a heat treatment of 63^{o}C for 30 minutes does not degrade the shear-thickening properties. Higher temperatures did show degradation. The critical temperature for processing was 63^{o}C whereby the mamaku can be stored at that temperature for 60 minutes without any degradation. Heating the mamaku to 110^{o}C results in the complete loss of all shear-thickening properties.

4.3.4 Mamaku Concentration

The effects of concentration of mamaku had already been reported in the literature (Goh et al., 2007; May, 2015). However, it was important to check the mamaku that was extracted behaved similarly to the past. Figure 4.7, shows the viscosity profile of mamaku solutions at different concentrations.

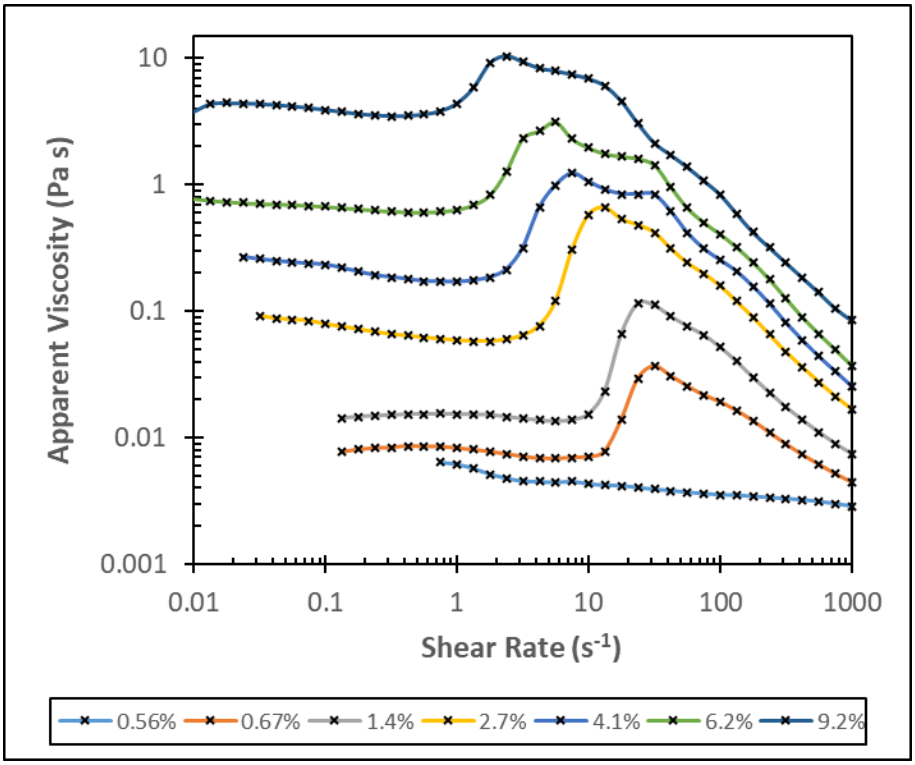

Figure 4.7: Viscosity profile showing the effect of concentration (%wt/v) of mamaku solution on the shear-thickening peak viscosity at 20°C

As can been seen in the graph and as reported in the literature (Goh et al., 2007), increasing the concentration changes the behaviour of the mamaku in the following ways:

- increased the viscosity of the solution at all points;
- decreased the shear rate at the onset of shear-thickening;
- increased the shear-thickening peak viscosity, and;
- decreased the shear rate at the peak viscosity.

The effect of concentration as quantified earlier (May, 2015) is reproduced in Figure 4.8. Some clear differences in both the initial Newtonian viscosity at various concentrations, and also the peak viscosity and shear rates involved in the shear-thickening are shown.

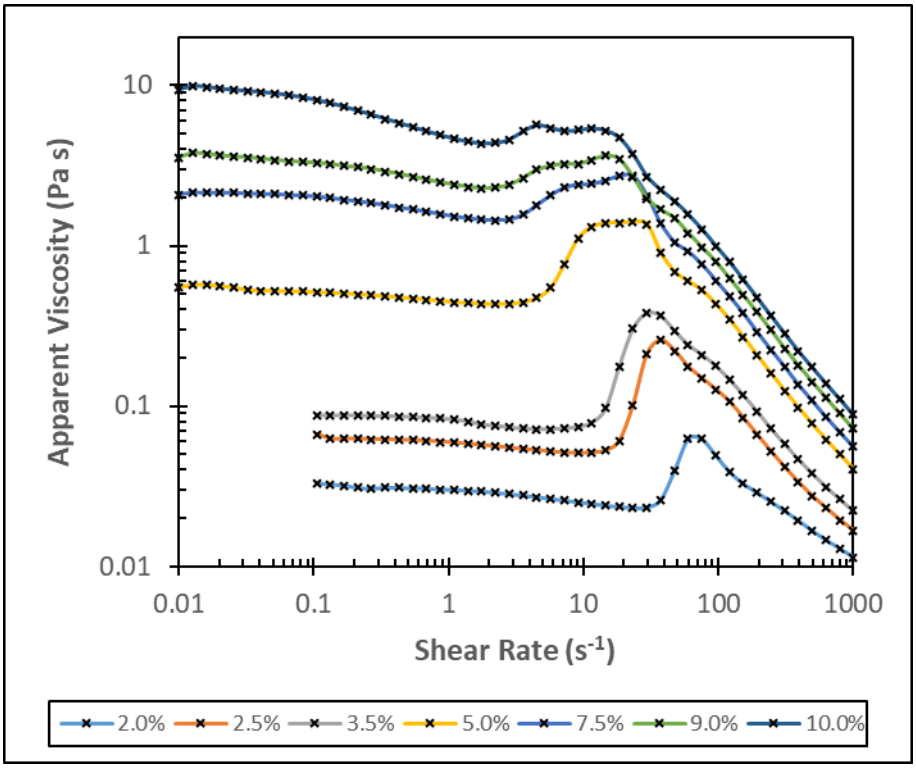

Figure 4.8: Viscosity profile showing the effect of concentration (%wt/v) of mamaku solution on the shear-thickening peak viscosity, measured at 20°C (May, 2015)

The improvement to the shear-thickening profile with this scaled up process compared to the original bench top process, is already outlined in section 3.4.2. A major contributor to these differences is likely to be the effect of freeze-drying already discussed in section 4.3.2. Additionally, the results were obtained using different rheometer settings and a less favourable geometry for high concentrations of mamaku (see section 4.2.4.2). Unfortunately, no comparison could be conducted at a similar time and with the same settings and geometry, to check if seasonal variation affects the shear-thickening properties.

The trends in the results can be explained by the shear-thickening mechanism already explained in 4.3.1, which relies on the mamaku molecules untangling, unfolding and orienting in a way that hydrogen bonds can be formed between molecules (Wee, 2015). When the mamaku concentration is increased, there is a greater number of molecules in the solution. This has two implications, firstly the free volume of the solution is decreased which reduces the average distance between mamaku molecules. Secondly, more molecules means more chances of the molecules orientating in a way favourable for the interactions between molecules to occur. This accounts for both the increased initial Newtonian viscosity and the decreased shear rate at onset of shear-thickening and peak viscosity shown in the results.

However, the higher the concentration of mamaku the greater the number of entanglements in the mamaku chains. This limits the total number of chains, which untangle, unfold and orientate allowing interactions to occur. This leads to a reduction in the extent of shear-thickening (the difference between initial Newtonian viscosity and peak viscosity) as concentration increases above a critical level. In the results, the flattening of the shear-thickening peak was pronounced above 6.2%wt/v (from this experimental work) or 5%wt/v concentration (May, 2015).

Overall, these results show that increasing the concentration can affect the shear rates at the onset of shear-thickening as well as the peak viscosity reached. The mamaku extracted for this project appears to have slightly better shear-thickening properties than that analysed in the past.

4.3.5 Combined concentration and temperature effects on viscosity

One gap in the previous research on mamaku was the combined effect of concentration and temperature. This was particularly relevant for the in-vitro studies in Chapter 6 where samples need to be analysed at body temperature (~37^{o}C) after dilution with gastric fluid. Therefore, various concentrations were

measured at 20°C and 37°C to gain an understanding of the combined effect. Figure 4.9, shows the viscosity profiles obtained at both 20°C and 37°C for various concentrations of mamaku.

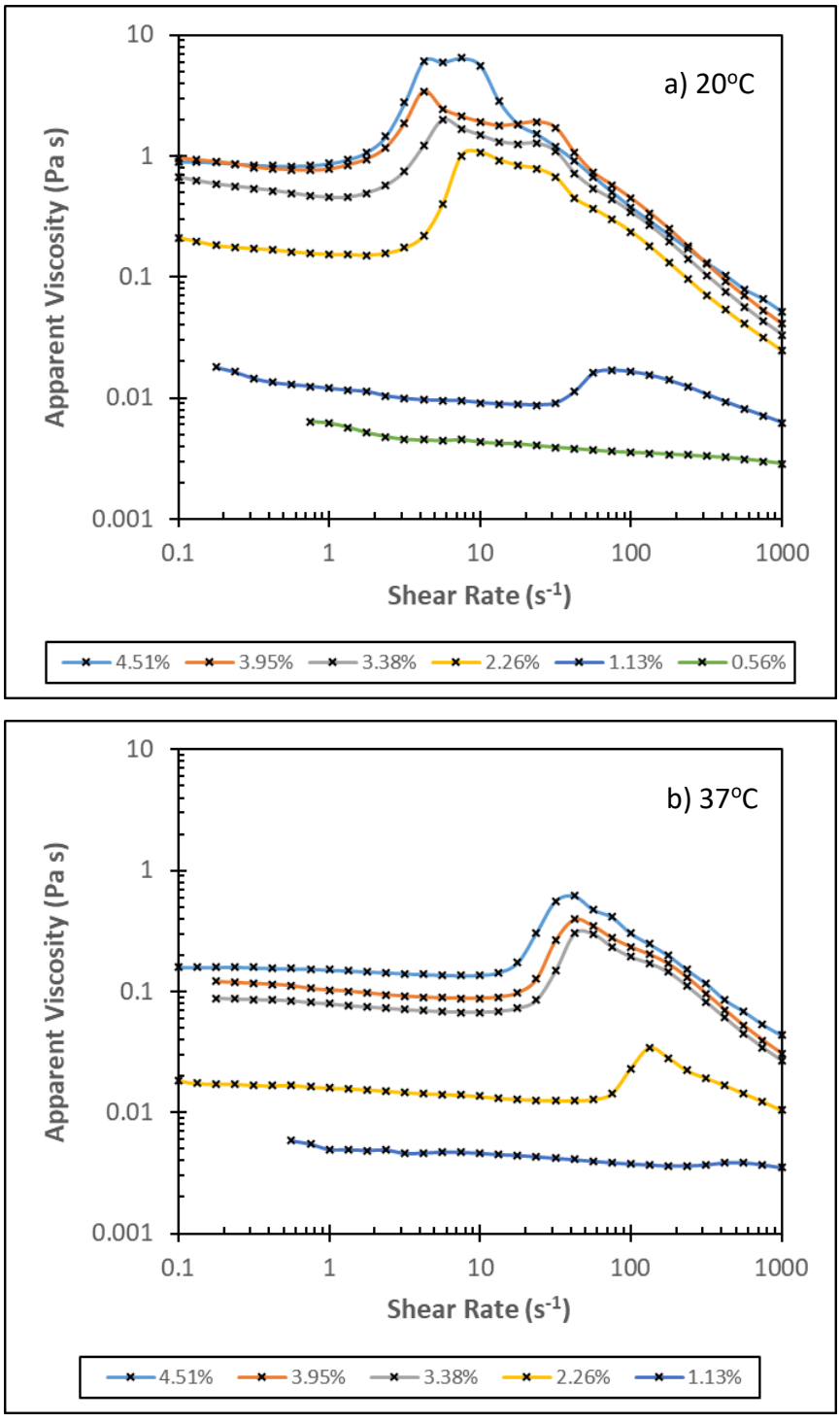

Figure 4.9: Viscosity profile showing the effect of mamaku concentration on the shear-thickening peak of mamaku at: (a) 20°C and (b) 37°C

The same trends are shown within each of the above graphs as those reported above in section 4.3.4. However, when comparing the two graphs you can see that increasing the temperature results in:

- A reduction in the viscosity of the solution at all points;
- Increased shear rate at the onset of shear-thickening;
- Decreased shear-thickening peak viscosity, and;
- Increased shear rate at the peak viscosity.

These trends are to be expected based upon the knowledge of the proposed shear-thickening mechanism detailed in 4.3.1 (Wee et al., 2015a). The concentration affects both the amount of polysaccharide present and the mineral content (and thus the ionic strength). Additionally, temperature increases the thermal mobility of the polysaccharide therefore reduces the number of hydrogen bonds forming, lowering the viscosity and the shear-thickening peak as well as the shear rates at the onset of thickening and of the peak viscosity (Matia-Merino et al., 2012).

These findings have implications for the results obtained in Chapter 6 regarding the pH of the in-vitro digestion trials because of the combined effects based on both concentration and pH at 37^{o}C (see section 4.3.6).

4.3.6 Combined effect of pH and temperature on viscosity

Another gap in the previous research on mamaku was the combined effect of pH and temperature when measuring the viscosity profiles. This was particularly relevant for the in-vitro studies in Chapter 6. Therefore, various pH-adjusted samples were measured at 20^{o}C and 37^{o}C to gain an understanding of the combined effect at body temperature. Figure 4.10, shows the viscosity profiles obtained at both 20^{o}C and 37^{o}C for various pH-adjusted solutions of mamaku.

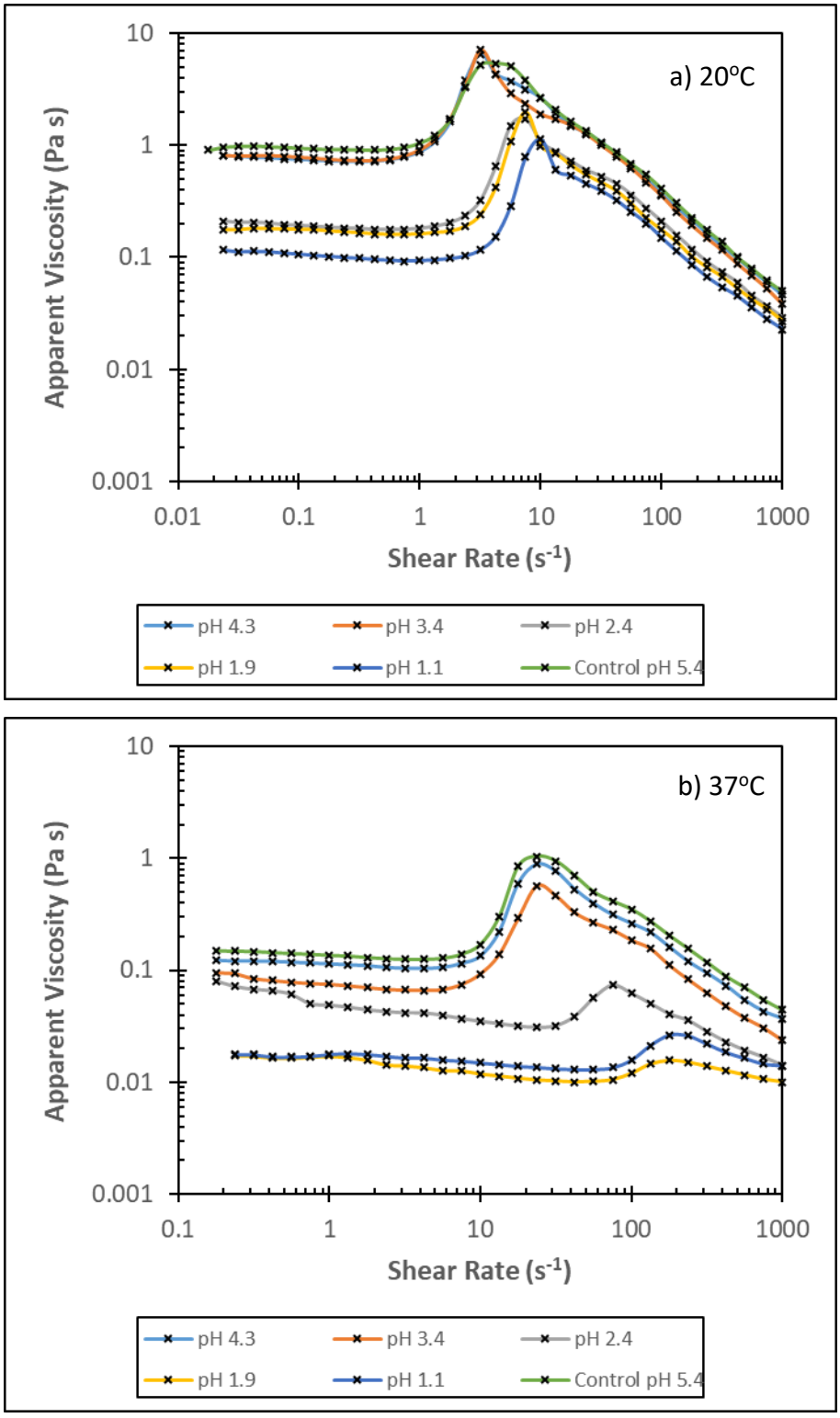

Figure 4.10: Viscosity profile showing the effect of pH on the shear-thickening peak of 4.5%wt/v mamaku at: (a) 20°C and (b) 37°C

The same trends are shown within each of the above graphs as those reported by Matia-Merino et al. (2012) with the characteristic sharp peaks observed with reducing pH. However, when comparing the two graphs, the higher temperature showed a flatter shear-thickening profile, which additionally appears to flatten as the pH was reduced along with the other trends outlined below:

- A reduction in the viscosity of the solution at all points;
- Increased shear rate at the onset of shear-thickening;
- Decreased shear-thickening peak viscosity, and;
- Increased shear rate at the peak viscosity.

These trends are to be expected based upon the knowledge of the proposed shear-thickening mechanism (Wee et al., 2015a). As mentioned in section 4.3.5, increasing the temperature causes a reduction in viscosity at all points and at the shear-thickening peak, additionally it increases the shear rates at the onset of thickening and of the peak viscosity (Wee et al., 2015a).

Additionally, decreasing the pH will reduce the negative charge of the polysaccharide (Matia-Merino et al., 2012). Since the pK_a of mamaku is ~2.0 (May, 2015), above this pH (pH 2-4) charges are still expected though reduced the closer the pH is to the pK_a. This means that there is less inter-molecular repulsion due to charge screening when the pH is decreased resulting in shrinkage of the molecular conformation (Wee et al., 2015a). When this charge screening is very strong (around the pK_a), higher shear rates are required to get the molecules to unfold because of the stronger intramolecular bonds. This delays the shear rate at onset of shear-thickening as shown in the results.

These findings have implications for the results obtained in Chapter 6 regarding the pH of the in-vitro digestion trials because of the combined effects based on both concentration (see section 4.3.5) and pH at 37^{o}C.

4.4 Conclusions

Overall, these results show there was minimal degradation of the mamaku via freeze thaw cycles. It would be sensible to reduce the number of times the dilute mamaku is frozen if possible, however, once the solution is concentrated it does not appear to substantially degrade with subsequent freeze thaw cycles.

In addition, these results show that not only does freeze-drying appear to reduce the initial Newtonian viscosity and the peak viscosity, but it also appears to shift the shear rates at the onset of shear-thickening and the shear rate at peak viscosity to higher shear rates. Therefore, wherever possible, the extraction of mamaku should involve concentration and freezing rather than dehydration via freeze-drying.

Furthermore, these results show a heat treatment of 63^{o}C for 30 minutes does not degrade the shear-thickening properties. Higher temperatures did show degradation. The critical temperature for processing was 63^{o}C, whereby the mamaku can be stored at that temperature for 60 minutes without any degradation. Heating the mamaku to 110^{o}C results in the complete loss of all shear-thickening properties.

Additionally, these findings show that increasing the concentration can manipulate the shear rates at the onset of shear-thickening as well as the peak viscosity reached. The mamaku extracted for this project appears to have slightly better shear-thickening properties than that analysed in the past.

Lastly, these findings show the reduction in shear-thickening viscosity and shear rates at onset of thickening and peak viscosity, at the pH and temperature of the stomach.

5 Encapsulation of mamaku

5.1 Introduction

This project aimed to encapsulate mamaku to make it safe to swallow, targeting release in the stomach. The encapsulating technology is limited by the following:

- mamaku is a water-soluble polysaccharide;
- the encapsulating agent must be digested in the stomach to release the mamaku and generate the satiety effect;
- the mamaku must be in a hydrated form as the dissolution time is longer than the 30-90 minutes that the food would stay in the stomach, and
- the final use of the food is for a diet product so the calorie content is an important consideration in the technique used.

Based on the literature review, the most promising encapsulating techniques for the situation included extrusion technologies using nozzles or spinning disks, emulsion based systems after removing the oil, and hydrogels using broken gel/fluid gel systems.

Gelatin was thought to be a promising polymer to use as an encapsulating agent, in this work, because:

- it is a protein meaning it will be digested in the stomach by pepsin, and
- gelatin is a thermo-reversible gel meaning that the gel will break down at around body temperature (dependent on the gelatin type and concentration) aiding release of the mamaku in the stomach.

Other potential options included proteins such as pea protein, casein or whey protein isolate. Such proteins are able to form networks, which might be able to entrap the mamaku. The network would be formed using heat to denature the proteins then inducing coagulation through of the addition of calcium. These proteins have a limitation in that they do not form a thermo-reversible network

that melts at body temperature. This means it is likely that there would be a greater delay in the release of mamaku in the stomach. There are complications around the fact that the heating step requires higher temperatures, which could have irreversibly damaged the shear-thickening properties of mamaku and the network formed might not trap the mamaku successfully.

For these reasons gelatin, was chosen as the encapsulating agent for all work done on the encapsulation of mamaku as part of this thesis.

5.2 Gelation Experiments

These experiments aimed to establish the required amount of gelatin to add to the mamaku for this use, with the aim of setting the melting point as high as possible to limit the chance of the gelatin melting in the mouth or before reaching the stomach.

5.2.1 Preliminary experiments

This set of experiments was designed to identify which of the two gelatin samples obtained would be more effective in gelling the mamaku. Additionally, it aimed to identify the starting point for the concentration of gelatin required to gel the mamaku.

The two gelatin samples tested were both Type B and 14 mesh. However, the bloom strength was different, one being 200 and the other 250. These samples were obtained from Gelita NZ Ltd. and the specifications located in Appendix K.

These experiments were based on 25 mL of 4.5%wt/v mamaku solution being mixed with 25 mL of gelatin. The overall concentration of gelatin was either 5%wt/v (2.5 g of gelatin in 50 mL overall) or 10%wt/v (5 g of gelatin in 50mL overall). The mamaku was heated to 50^{o}C in a water bath and held at that temperature.

The gelatin was dissolved in water under continuous stirring for 10 minutes. The 50°C mamaku solution was added to the gelatin solution at 65°C and stirred for 2 minutes. The timer was started and the mixture was left to gel at room temperature (21°C) for up to an hour undisturbed.

A visual representation of the results obtained is shown in Table 5.1.

Table 5.1: Pictures displaying the results visually for: 5%wt/v gelatin + 2.25%wt/v mamaku solution (a, b) and 10%wt/v gelatin + 2.25%wt/v mamaku solution (c,d), noting which solutions had set and which were still liquid like

a) 200 Bloom 5%wt/v gelatin not set after 1 hour		b) 250 Bloom 5%wt/v gelatin not fully set after 1 hour – i.e. a skin forms on the top but when pushed the inside was runny.	
			
c) 200 Bloom 10%wt/v gelatin fully set after 45mins		d) 250 Bloom 10%wt/v gelatin fully set after 30 minutes	
			

These results clearly show that the 250 Bloom gelatin produced stronger gels as both concentrations at least partially set. Additionally, the 10%wt/v gelatin + 2.25%wt/v mamaku set fully, while the 5%wt/v gelatin+ 2.25%wt/v mamaku had mixed results; where the solutions did not set at all, or they did not set completely. This indicated that 5%wt/v gelatin+ 2.25%wt/v mamaku is likely not enough gelatin, but 10%wt/v gelatin + 2.25%wt/v mamaku might have been providing an excess amount and that 250-bloom strength was the preferred sample to use.

Therefore, after establishing the appropriate range, 7.5% and 10%wt/v 250 bloom strength gelatin + 2.25%wt/v mamaku was tested in the rheometer.

5.2.2 Gelation under controlled shear

These experiments were based on 25mL of 4.51%wt/v mamaku solution (concentrated in the evaporator) being mixed with 25mL of gelatin with a bloom strength of 250. The overall concentration of gelatin was either 7.5%wt/v or 10%wt/v. The aim was to obtain data of the gelling profile through both the cooling phase, hour-long annealing stage (holding period for gel strength to develop) and heating phase. The rheometer was set up with cone and plate geometry for these experiments, see Figure 5.1.

Figure 5.1: Pictures showing the set-up of the rheometer, including the cone and plate geometry with a sample loaded in

This experiment was completed using a cone and plate geometry (CP40-4, Part Number 2629, Diameter 39.958mm, Concentricity ±9µm, Parallelity ±4µm, Angle 4.000^{o}, Truncation 49µm).

The methodology followed is shown in Figure 5.2.

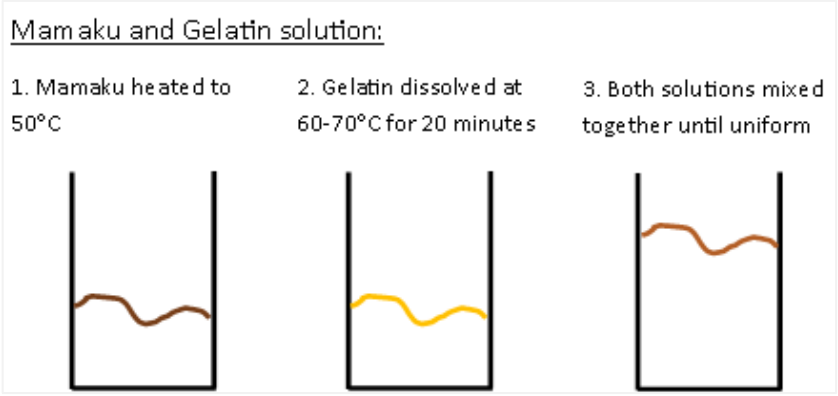

Figure 5.2: Flow diagram for making mamaku + gelatin solution

The methodology followed is explained below:

1. The mamaku was defrosted and equilibrated to 50°C in a water bath.
2. The gelatin was hydrated in 250 mL of water at 60-70°C for 20 minutes at about 400 rpm. In order to limit the chance of overheating the bottom of the beaker, a larger beaker of water was placed directly on the hot plate and the beaker for the gelatin was submerged inside, as shown in Figure 5.3.

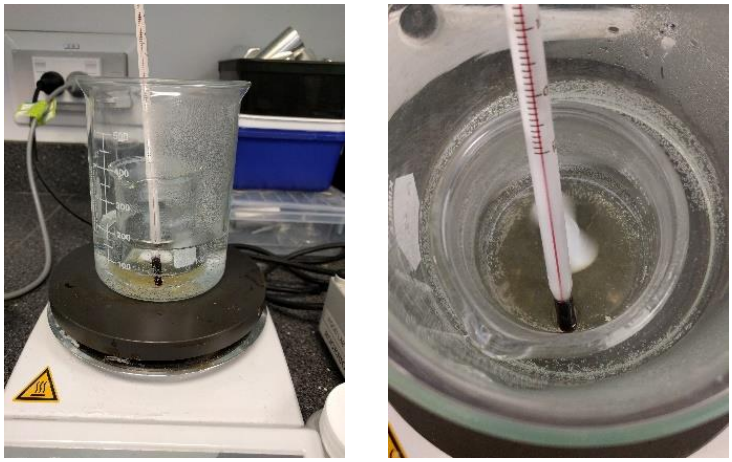

Figure 5.3: Pictures showing the set-up used to dissolve the gelatin. The large beaker contains only hot water; the smaller beaker contains the gelatin solution, a magnetic stirrer and the thermometer.

3. The mamaku was added and mixed at 600 rpm for about 1 minute until the solution appeared uniform.
4. The sample was loaded into the pre-heated rheometer plate (50°C), the cone lowered and the test started.

The settings used to programme the cooling, annealing and heating profile whilst in the rheometer are detailed in Table 5.2, Table 5.3 and Table 5.4. These were based off a similar gelation study of gelatin, with and without milk proteins added, by Pang, Deeth, Sopade, Sharma and Bansal (2014).

Table 5.2: Oscillation Settings for the gelation profile of the gelatin samples in the rheometer during all phases

Parameter	Amplitude settings	Frequency settings
Set variable	Strain	Frequency
Profile	Constant	Constant
Value	0.5%	1 Hz

Table 5.3: Interval settings for the gelation profile of the gelatin samples in the rheometer during the cooling, annealing and heating phases

Parameter	Phase		
	Cooling	Annealing	Heating
Profile	Fixed measuring point duration	Fixed measuring point duration	Fixed measuring point duration
Measuring point interval	0.5 min	0.5 min	0.5 min
Duration	46.5 min	60 min	46.5 min
Measuring points	93	120	93

Table 5.4: Peltier plate temperature settings for the gelation profile of gelatin samples in the rheometer during the cooling, annealing and heating phases

Parameter	Phase		
	Cooling	Annealing	Heating
Set variable	Temperature	Temperature	Temperature
Profile	Heating rate	Constant	Heating rate
Value	/	4°C	/
Initial	50°C	/	4°C
Final	4°C	/	50°C
Rate	1°C/minute	/	1°C/minute

The results obtained are shown in the in Figure 5.4 and Figure 5.5.

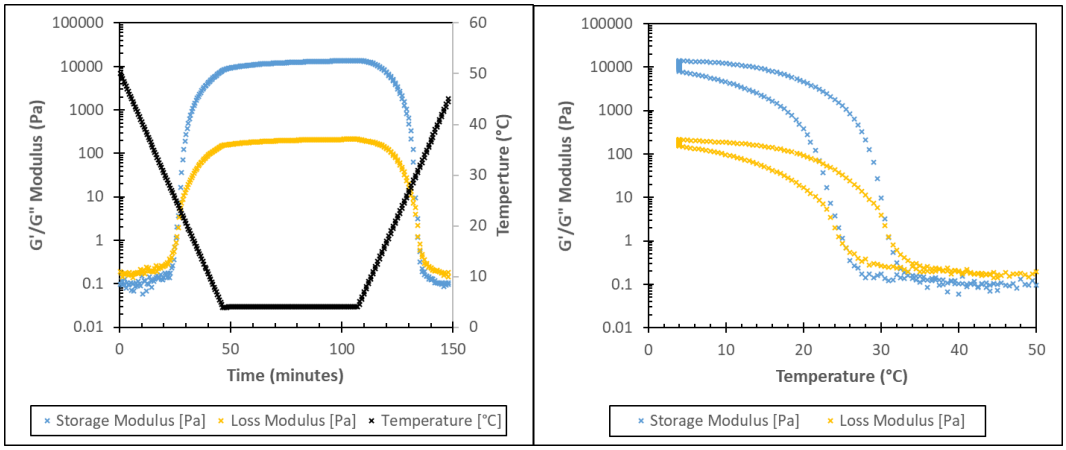

Figure 5.4: Graphs showing G' and G'' over time for the 10%wt/v gelatin + 2.25%wt/v mamaku solution also showing the temperature profile with time (left) and G' and G'' over temperature for the 10%wt/v gelatin + 2.25%wt/v mamaku solution (right)

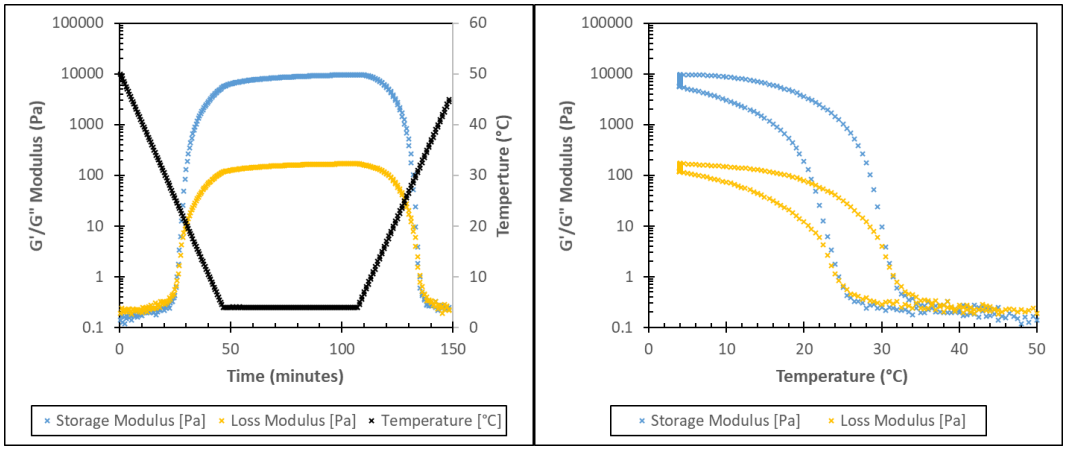

Figure 5.5: Graphs showing G' and G'' over time for the 7.5%wt/v gelatin + 2.25%wt/v mamaku solution also showing the temperature profile with time (left) and G' and G'' over temperature for the 7.5%wt/v gelatin + 2.25%wt/v mamaku solution (right)

The temperatures where the G' and G'' curves overlap can be analysed to find the gelation point and melting point of the gel. This is outlined in Table 5.5.

Table 5.5: Gelling and melting temperature for two gelatin gels containing 2.25%wt/v mamaku solution

	10%wt/v gelatin	**7.5%wt/v gelatin**
Melting Temperature	31.8°C	31.3°C
Gelling temperature	25.3°C	25.8°C

The results showed that 10%wt/v and 7.5%wt/v gelatin had similar melting, and gelling points. This indicated that the 7.5%wt/v gelatin solution should be selected, even if only for cost purposes. The melting and gelling temperature of gelatin is known to depend on the type of gelatin, the concentration, its bloom strength and the pH, with higher concentrations increasing the melting temperature (Osorio, Bilbao, Bustos & Alvarez, 2007).

5.2.3 Conclusions

These experiments showed that Type B gelatin was able to trap the mamaku within its gelled structure. This work determined 14%wt/v gelatin solution (250-bloom strength), prepared using the hot water dissociation method, added on a 1:1 basis with mamaku creating 7.5%wt/v gelatin overall, was sufficient to gel the whole solution trapping the 2.25%wt/v mamaku solution.

Additionally, this concentration of gelatin showed a melting point between 31°C and 32°C, low enough to promote melting in the stomach but likely to be high enough to be safe to consume while in the mouth. This concentration has been used for all further work on encapsulating the mamaku.

5.3 Emulsion templating

This technique refers to encapsulation using a water in oil emulsion, which is subsequently broken down and the oil removed. This can be referred to as emulsion templating. It typically involves creating a stable emulsion, gelling the water droplets containing an active ingredient, washing to remove the oil and subsequently transferring the gelled droplets into a water phase. This process thus creates encapsulated ‘beads’.

This experiment involved trying to make a stable water in oil emulsion, while the gelatin was melted, then rapidly cooling the emulsion to gel the gelatin in the droplets. The aim was to create a stable water in oil emulsion containing gelled

droplets, which trapped mamaku within. The next step aimed to remove the oil and obtained dispersed gelatin + mamaku particles in RO water.

5.3.1 Methodology

5.3.1.1 Ingredient specification and formulation

The details and specifications for each ingredient are outlined below:

- Gelatin was sourced from Gelita Ltd. Its specification was Beef skin edible gelatine 250-bloom 14 mesh.
- Extracted mamaku solution was defrosted in the water bath at 52°C.
- Oil used was bulk Soya bean oil from Gilmours.
- PGPR used was manufactured by Danisco Grindsted PGPR 90 (polyglycerol polyricinoleate).

Pervious work, in section 5.2, showed that 14%wt/v gelatin solution added at a 1:1 ratio with 4.5%wt/v mamaku solution was sufficient to gel the structure. This mixture created an overall gelatin concentration of 7.5%wt/v and mamaku concentration of 2.25%wt/v and these concentrations were used for the emulsion templating experiments. The formulations used are detailed in Table 5.6 and Table 5.7.

Table 5.6: mamaku + gelatin solution formulations

Ingredient	**Quantity (mL)**	
	50:50/original	**90:10**
mamaku	250	450
Gelatin (g)	37.5	37.5
RO Water	250	50
Total	500	500

Table 5.7: Ingredient Formulation of the emulsions

Ingredient	**Quantity (mL)**		
	8% v/v	**4% v/v**	**0% v/v**
mamaku + gelatin solution	100	100	100
Oil	360	380	400
PGPR	40	20	0
Total	**500**	**500**	**500**

5.3.1.2 Preparation of emulsion

The methodology followed is shown in Figure 5.6.

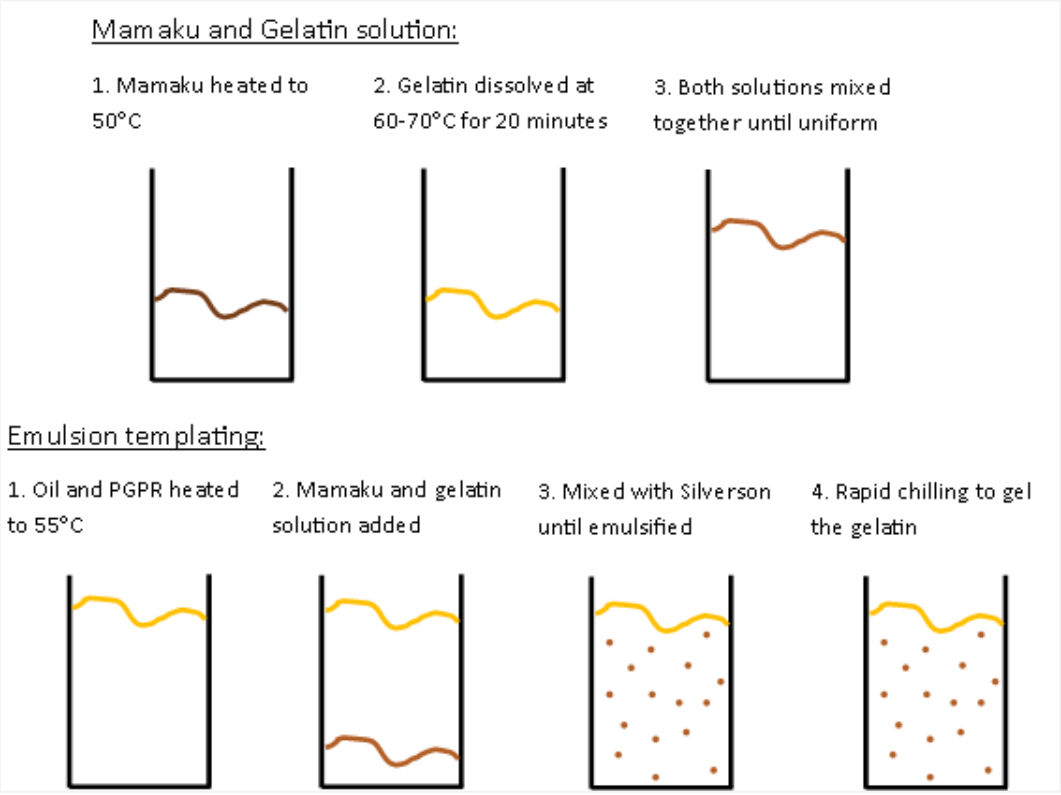

Figure 5.6: Flow diagram for emulsion templating methodology

The methodology followed is outlined below:

1. The 2.25%wt/v mamaku + 7.5%wt/v gelatin solution was prepared as outlined in section 5.2.2.
2. Each solution was prepared one at a time and allowed to equilibrate for 30 minutes before transferring to the pilot plant for emulsification in a Silverson mixer.
3. Oil and PGPR (if required) was measured and placed into a 1L plastic beaker in a water bath at 55°C.
4. The hot water-based solution was added once prepared.
5. Once the solution had equilibrated, each mixture was mixed with the Silverson mixer using the disc with the smallest diameter holes as shown in Figure 5.7.

Figure 5.7: Photo showing the Silverson mixer

5.3.1.3 Cooling steps

Upon the end of mixing, each formulation was quickly poured (or scooped in the case of the 0% v/v PGPR) into 50mL containers, sealed and dropped into an ice bath measuring 4°C. This cooled all mixtures to below 20°C within 5 minutes. Ice was added to the ice bath as needed to ensure the temperature did not raise above 4°C. Each formulation was left in the ice bath for one hour before transferring to the fridge.

5.3.2 Results

5.3.2.1 Levels of PGPR

As a starting point for these trials, a constant emulsion ratio was chosen and the impact of different levels of emulsifier was investigated. All these trials were done with mamaku + gelatin solution at a 50:50 ratio, with concentrations of 2.25%wt/v mamaku + 7.5%wt/v gelatin (see section 5.3.1.1, Table 5.6).

Research done by Tepsongkroh et al. (2015) suggested that a ratio of 80 oil to 20 water was likely to create a stable water in oil emulsion. Additionally this research suggested 8% PGPR was a common amount of PGPR added for this type of encapsulation system. In the interest of reducing cost if possible, a system with 4%

PGPR was also created, testing also a system with no PGPR to establish if it was needed in the first place.

This trial aimed to establish the appropriate PGPR (0%-8% v/v) level for emulsification. Each solution was prepared as per the methodology outlined in section 5.3.1. During mixing with the Silverson, the temperature was recorded to ensure it did not rise above 65^{o}C, to limit any damage to the mamaku's shear-thickening properties, as previously discussed in section 4.3.3. The difference in appearance of the solution before and after mixing is shown in Figure 5.8.

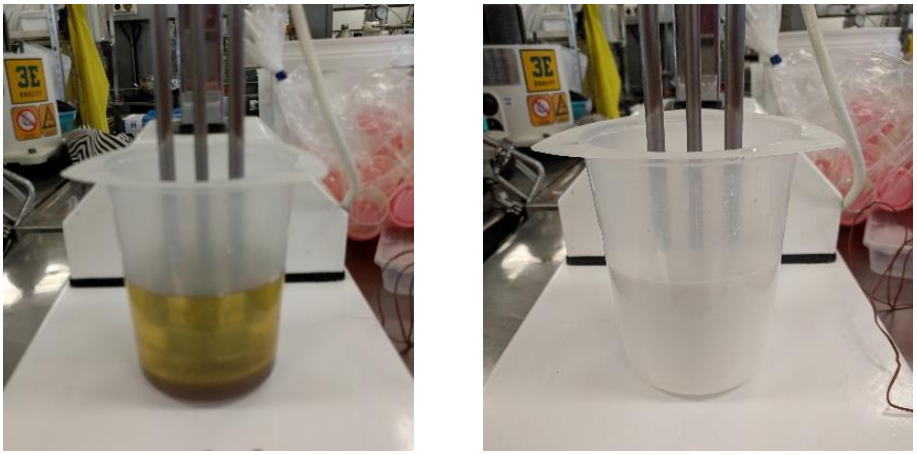

Figure 5.8: Images showing the difference in appearance of the 8% v/v PGPR solution before (left) and after (right) emulsification using the Silverson mixer

Each formulation had a slightly different mixing profile due to the PGPRs effects on the ease of mixing. Additionally, the higher shear rates required by the lower levels of PGPR generated more heat, increasing the temperature rapidly. This is outlined in Table 5.8.

Table 5.8: Mixing profile for each formulation

Formulation	Mixing Profile	End Temperature
8% v/v PGPR	5 minutes total mixing time. 1 minute to ramp up to 6500 rpm. Remaining 4 minutes at 6500 rpm.	49°C
4% v/v PGPR	5 minutes total mixing time. 1 minute to ramp up to 8500 rpm. 3 minutes at 8500 rpm at which point the temperature increased to 59°C. Remaining 1 minutes at 6500 rpm.	55°C
No PGPR	5 minutes total mixing time. 1 minute to ramp up to 8700 rpm. 1 minute at 8500 rpm at which point the temperature increased to 60°C. 1 minute at 6500 rpm at which point the temperature increased to 63°C. Remaining 2 minutes at 4500 rpm.	61°C

At the end of mixing both the 4% v/v and 8% v/v PGPR solutions remained liquid like. However, the 0% v/v PGPR solution was thick and behaved more like a solid.

Upon cooling the emulsions with 4% v/v and 8% v/v PGPR remained stable in a liquid form. However, the emulsion without PGPR actually gelled creating a continuous solid network with no obvious oil leakage. Although an interesting observation, this was not appropriate for the situation because it needs the encapsulated product to be in a liquid form and not high in calories.

Undiluted emulsion could not be focused under a light microscope; therefore, each sample was diluted 1-part emulsion to 9-parts mineral oil. One drop of the diluted sample was placed on a microscope slide and a coverslip was applied. A picture was taken with a phone (nexus 6P) camera. For the oil immersion, 100x objective magnification a drop of mineral oil was added to the coverslip. The results are shown in Table 5.9.

Table 5.9: Microscope images of 1 week old: (a) 20% w/o emulsion stabilised by 8% PGPR v/v (water phase 7.5%wt/v gelatin + 2.25% mamaku wt/v) and (b) 20% w/o emulsion stabilised by 4% PGPR v/v (water phase 7.5%wt/v gelatin + 2.25% mamaku wt/v) under various objective magnifications

	10x	40x	100x oil immersion
a)		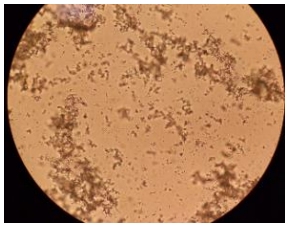	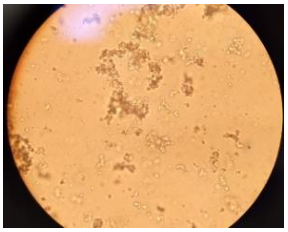
b)		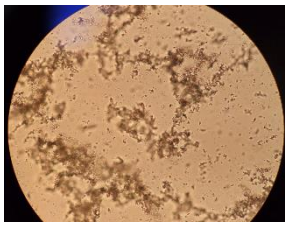	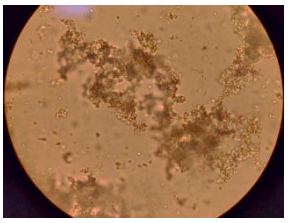

These results show that both emulsions appeared to be aggregated, with an almost network-like structure. This could be caused by the unique stickiness and elasticity of the mamaku meaning discrete droplets were not formed in the emulsion. Alternatively, the gelatin molecules might have gelled to form a network upon cooling, particularly if aggregation was promoted by the mamaku solution. Another alternative was that the emulsions underwent destabilization under storage and PGPR did not prevent the gelatin + mamaku droplets from linking together into a network. However, 8% v/v PGPR, within a 20% o/w emulsion, appears to be a common concentration for this sort of application (Tepsongkroh et al., 2015).

Overall, the results were inconclusive, 8% v/v PGPR was selected as the concentration used from this point forward, because the mixing process during the emulsification step was easier with the higher concentration and the temperature damage to mamaku was lower.

5.3.2.2 Ratio of mamaku to gelatin

Aiming to increase the concentration of mamaku within each droplet, an additional trial was done with 8% v/v PGPR with different mamaku + gelatin ratios, 50:50 and 90:10. This was the simplest way to increase mamaku concentration without freeze-drying or defrosting and concentrating a large quantity of extract. The key between this emulsion formulation and previous one is decreasing the amount of water used to dissolve the gelatin from 50% to 10% of the water phase, and increasing the mamaku volume. Overall, within the mamaku + gelatin solution, the gelatin concentration remained the same – 7.5%wt/v, but the mamaku concentration was increased from 2.25%wt/v to 4.05%wt/v. Therefore, within the emulsion, the overall concentration of gelatin was 1.5%wt/v and mamaku was 0.81%wt/v.

This experiment produced stable emulsions with no visual separation upon cooling indicating that the mamaku had not separated out from the oil. The microscope images for each of the samples are shown in Table 5.10. The procedure used was the same as outlined in section 5.3.2.1 but instead of a phone camera, a light microscope with a camera attached was used and the samples were only one day old, not one week old.

Table 5.10: Microscope images of 1 day old: (a) 20% w/o emulsion stabilised by 8% PGPR v/v (water phase 7.5%wt/v gelatin + 2.25% mamaku wt/v) and (b) 20% w/o emulsion stabilised by 8% PGPR v/v (water phase 7.5%wt/v gelatin + 4.05% mamaku wt/v) under various objective magnifications

	100x	400x	1000x oil immersion
a)	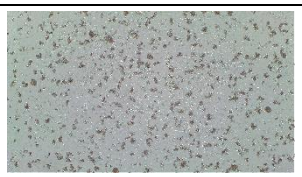		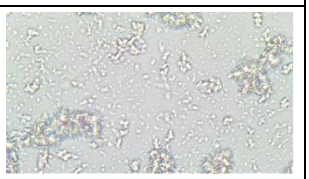
b)		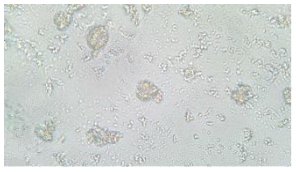	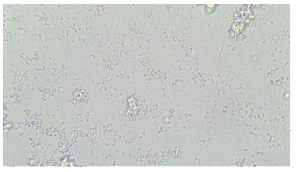

The emulsion systems with higher concentrations of mamaku did not show a huge difference. This experiment appears to show less aggregation than the previous one. This was most likely due to the difference in age of the emulsions. However, due to the challenges removing the oil (see section 5.3.3), this was not investigated further.

The experiment found that modifying the water phase to contain 7.5%wt/v gelatin + 4.05%wt/v mamaku, within the 20% w/o emulsion stabilised by 8% PGPR v/v, did not affect the ability of the water phase to form droplets that gelled upon cooling. Droplet size within these emulsions was d_{32} = ~100µm.

5.3.2.3 Rheological properties

Flow behaviour properties were examined to determine whether the emulsion displayed any shear-thickening behaviour. If the mamaku was encapsulated successfully, the sample should not show shear-thickening behaviour. The rheometer, geometries and peltier plate used to measure the viscosity profile are outlined in section 4.2.1, as are the settings used to programme the rheometer.

Figure 5.9, shows the viscosity profile of both the 4% v/v and 8% v/v PGPR emulsions measured using double gap geometry.

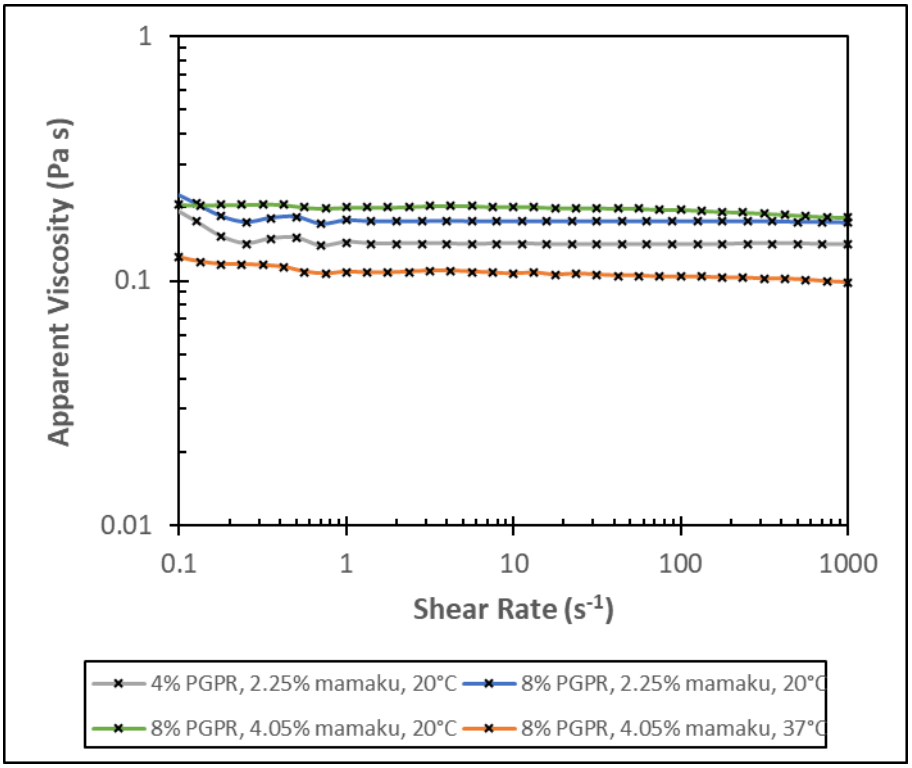

Figure 5.9: Viscosity profile comparison of 20% w/o emulsions (2.25%wt/v mamaku + 7.5%wt/v gelatin) with 4% v/v PGPR or 8% v/v PGPR at 20°C, and 20% w/o emulsions (4.05%wt/v mamaku + 7.5%wt/v gelatin) with 8% v/v PGPR at 20°C or 37°C

This graph showed that the flow behaviour of the 4% v/v PGPR emulsion containing 2.25%wt/v mamaku, and 8% v/v PGPR emulsion containing 2.25%wt/v mamaku, is Newtonian. The aim of making the emulsion was to encapsulate the mamaku successfully so no shear-thickening behaviour could be observed. However, the issue with these results was that the overall concentration of mamaku within the emulsion was very low 0.45%wt/v (50:50 ratio). There is a high chance that no thickening was detected due to the final concentration of mamaku being too low to show any effect, as shown in previous work in section 4.3.4. Therefore, subsequent samples showing a higher mamaku concentration (4.05%wt/v) were analysed (Figure 5.9), also showing Newtonian behaviour at 20°C and 37°C.

At 37°C, the gelatin should have melted and released the mamaku, however, no shear-thickening peak was observed. Again, the overall concentration of mamaku

within the emulsion was very low 0.81%wt/v (90:10 ratio). There is a high chance that no thickening was detected due to the final concentration of mamaku being too low to show any effect at 37°C, as shown in previous work in section 4.3.5, on the effect of mamaku concentration at higher temperatures. Therefore, despite the higher concentration of mamaku, the results are still inconclusive as to whether the methodology was successful at encapsulating mamaku.

5.3.3 Removing the oil

One of the challenges of the emulsion templating method to encapsulate the mamaku is that the oil needs to be removed in order to transfer the encapsulated mamaku into an aqueous food system.

5.3.3.1 Preliminary trials

A similar study also involving encapsulating via emulsion templating, managed to successfully remove the oil and disperse their gelled beads in an aqueous form using ethanol to wash the oil then a centrifugation step to separate the oil out (Cayre, Noble & Paunov, 2004).

This method was adapted in this work, and involved a centrifuge process where about 50mL of 8% v/v PGPR emulsion was washed with 95% ethanol at a 1:1 ratio then centrifuged to separate the liquids. Then the samples were loaded into the centrifuge (Thermo scientific Heraeus Multifuge IS-R Centrifuge) and it was rotated at 4700 rpm for 10 minutes.

Each centrifuge cycle produced a system where the ethanol had accumulated at the top of the tube. The free oil was the next layer, followed by the gelatin/mamaku at the bottom. The oil and ethanol was easily removed each time by simply pouring out the transparent layers. Leaving behind the liquid that was not transparent and the clump of gelatin + mamaku at the bottom. These layers are shown clearly in Figure 5.10. The ethanol was then added again for the next cycle and these steps were repeated a total of four times.

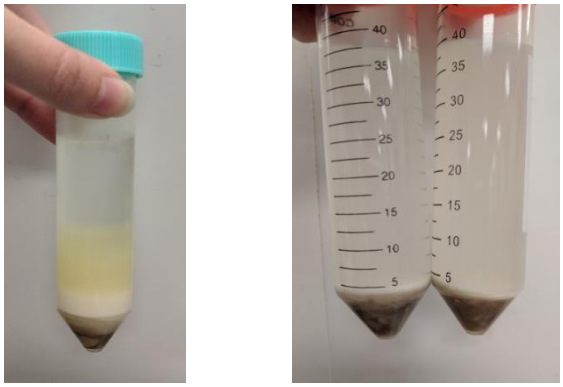

Figure 5.10: Image showing the layers created by centrifuging in the first cycle (left). Image showing the layers created by centrifuging in the last cycle (right).

The result produced about 10mL of gelatin/mamaku; this was subsequently diluted with RO water to 25mL. However, the mamaku/gelatin beads did clump together in the centrifuge, probably because of centrifuging at too high speeds for too long.

This meant that the beads had to be broken back up into small beads with an Ultra Turrax (T25 basic IKA LABORTECHNIK). This involved adding more RO water to give enough volume and (about 25mL) and then mixing. The Ultra Turrax was run at 13.00 1/min (speed 2) for two minutes until no more clumps were visible. The total volume was around 50mLs. This gave an effective concentration of mamaku of 0.45%wt/v.

After the first trial removing the oil, it was clear there was some issues with clumping of the encapsulated mamaku. The details of the second attempt can be found in Appendix L. Overall, this trial still had the same issues with clumping as the first trial.

5.3.3.2 Rheological characterisation

Flow behaviour properties were examined to determine whether the washed emulsion solution displayed any shear-thickening behaviour. If the mamaku was encapsulated successfully, the sample should not show shear-thickening behaviour. The rheometer, geometries and peltier plate used to measure the

viscosity profile are outlined in section 4.2.1, as are the settings used to programme the rheometer.

Figure 5.11, shows the viscosity profile of the diluted solution after using the Ultra Turrax to break up the clumps.

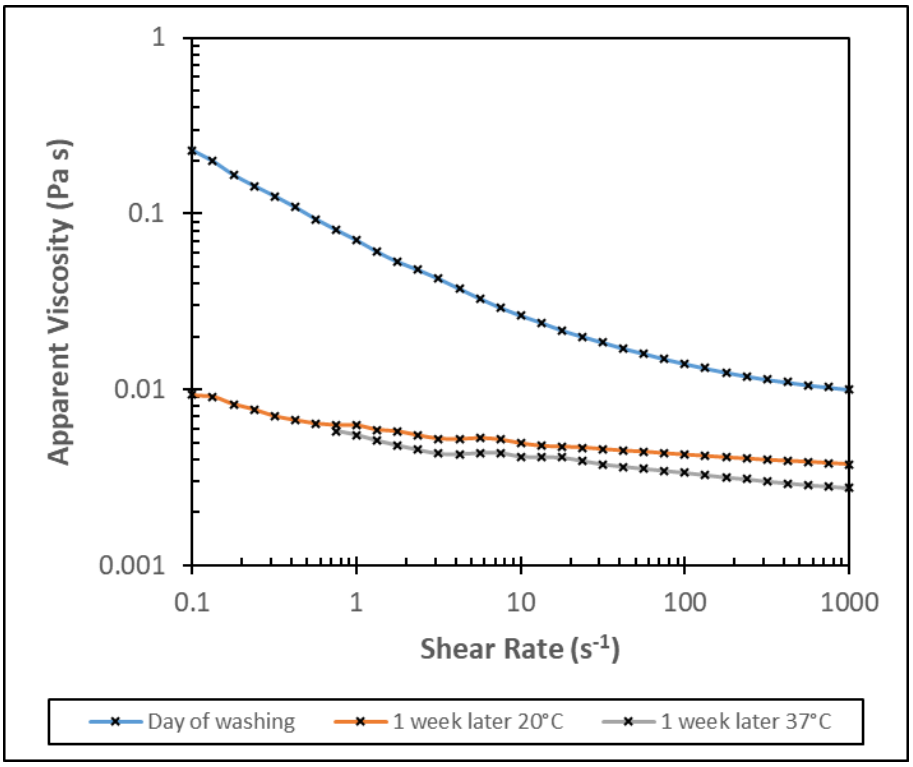

Figure 5.11: Viscosity profile for the washed encapsulated mamaku at 20°C and 37°C looking at the effect of storage on viscosity profile

This graph showed that the solutions do not show any shear-thickening behaviour, with the initial solution showing shear thinning behaviour. However, the reduced viscosity occurring when the sample was left in the fridge for one week showed that the emulsion changed over time, which could explain the different microstructures found in aged versus fresh samples (section 5.3.2.1). Again, at 37°C no shear-thickening peak was observed. There is a high chance that no thickening was detected in the solution due to the concentration of mamaku being too low to show any effect at 37°C, as previously mentioned above. Therefore, no conclusions can be made about whether the methodology was successful at encapsulating mamaku after washing to remove the oil.

5.3.3.3 Remaining issues with removing the oil

Removing the oil is a time consuming process, which does not appear to be fully suitable. This was most likely because of mamaku's unique elasticity and stickiness (Goh et al., 2007).

Scalability is an issue, as this is a batch process, so the complications around temperature control to limit damage to the mamaku and to ensure that the gelatin is successfully entrapping the mamaku, need to be considered. A further issue is the further dilution of the beads via the addition of RO water, as this reduces even more the concentration of the mamaku within the solution. Additionally, the use of solvents is not ideal for commercial use due to the quantity required.

Overall, having to remove such a large amount of oil from the system in order to obtain the encapsulated mamaku is not ideal for full-scale production. The 'double processing' required due to the difficulties with removing the oil leading to having to mix the final product thoroughly to break up clumps is also not ideal.

Furthermore, the risks associated with this second round of mixing, include the potential to release some mamaku from the gelatin structure allowing some shear-thickening properties to reform if the concentration gets high enough.

5.3.4 Remaining issues with emulsion templating

The mamaku concentration is a limiting factor due to the excessive dilution occurring both with the oil and when the oil is removed and RO water is added. The starting concentration of 4.5%wt/v was selected during the extraction when looking at the flow properties at 20^{o}C, before the combination of pH and temperature was investigated (section 4.3.6). At the concentrations used in these trials, it was not conclusive as to whether the mamaku was encapsulated successfully, or whether the concentration was simply too low for shear-thickening properties to be observed. This issue was compounded by the concentration issues found in Chapter 6 regarding the stomach in-vitro trials,

where the concentration of mamaku was found to need to be doubled or tripled to show the shear-thickening effect in the stomach's warm acidic conditions.

The lack of stability in an aqueous environment is a challenge for a food product. The intention was to put these encapsulated beads in a drink or other beverage and create a functional food product. However, the results obtained suggest there was a lack of stability of the system when placed in an aqueous environment, so further work on stabilisation would be required. There is a limiting factor on the coating or gelling agent added to stabilise the encapsulated mamaku, because this coating or gelling agent has the same constraints as the encapsulating agent did – it must be digested in the stomach in order to release the mamaku successfully. An alternative to a second coating, would be thickening the food matrix, e.g. with a polysaccharide, to reduce the proportion of free water which can interact with the encapsulated mamaku + gelatin beads – for example, placing the encapsulated mamaku in a yoghurt rather than a drink.

The removal of the oil is a major limitation of this encapsulation method for commercial viability. Not only does require several washing steps with solvents but mamaku's unique stickiness and elasticity makes the removal of oil step even more challenging as it requires a second mixing step to remove the clumps formed.

Overall, these challenges require more experiments involving the use of more concentrated mamaku and significant process development, before it could be considered for use on a commercial scale. Additional, work would be needed to establish that the encapsulation was successful.

5.4 Nozzle systems

5.4.1 Introduction

Seiffert (2011) explained that a disadvantage of successful emulsion templating system is the lack of control over the size of each individual encapsulated bead formed. The challenges faced with the emulsion templating experiments and removing the oil, led to looking at other systems, which might successfully encapsulate the mamaku with less difficulty.

Nozzle techniques aim to give this precise control over the size of the encapsulated product on an individual droplet basis, as explained in the literature review (section 2.6.6). Thus, these methods aimed to give consistent sized encapsulated beads, reducing any variation in the release of the active ingredient.

Experiments were conducted involving encapsulation using a micro injector, paint gun and spinning disk. The technologies all involved a similar process, where droplets are formed from an extrusion process, which aimed to encapsulate the mamaku upon gelation of the gelatin within the droplets. The experiment completed using a paint gun can be found in Appendix M. The experiment completed using a spinning disc can be found in Appendix N.

5.4.2 Micro injector

This technique involves encapsulation using a nozzle system. In such a system, beads are formed by extruding the solution through the vibrating nozzle, and then dropping the beads into an oil bath to set. Later after gelation is complete, the oil is removed. This process thus creates encapsulated ‘beads’.

Riddet Institute had a Micro Injector on site, which was offered as an alternative to ordering or making a nozzle/spinning disk system. The machine is an Inotech ENCAPSULATOR RESEARCH IE-50 R, and is shown in Figure 5.12.

Figure 5.12: Picture showing the micro injector

To aid the ability of the micro injector to spray the mamaku + gelatin solution, the machine was pressurised with compressed air controlled by the machine to be one bar. This aimed to increase the force applied to the syringe to help with the spraying of the mamaku + gelatin solution.

The formulation used is detailed in Table 5.11.

Table 5.11: Ingredient formulation

Ingredient	Quantity (mL/g)
Water (mL)	50
Gelatin (g)	7.5
mamaku (mL)	50
Total	100

The details and specifications for each ingredient are outlined below:

- Gelatin was sourced from Gelita Ltd. Its specification was Beef skin edible gelatine 250-bloom 14 mesh.
- Extracted mamaku solution was defrosted in the water bath at 52°C.
- Oil used was bulk Soya bean oil from Gilmours.
- PGPR used was manufactured by Danisco Grindsted PGPR 90 (polyglycerol polyricinoleate).

The methodology followed is shown in Figure 5.13.

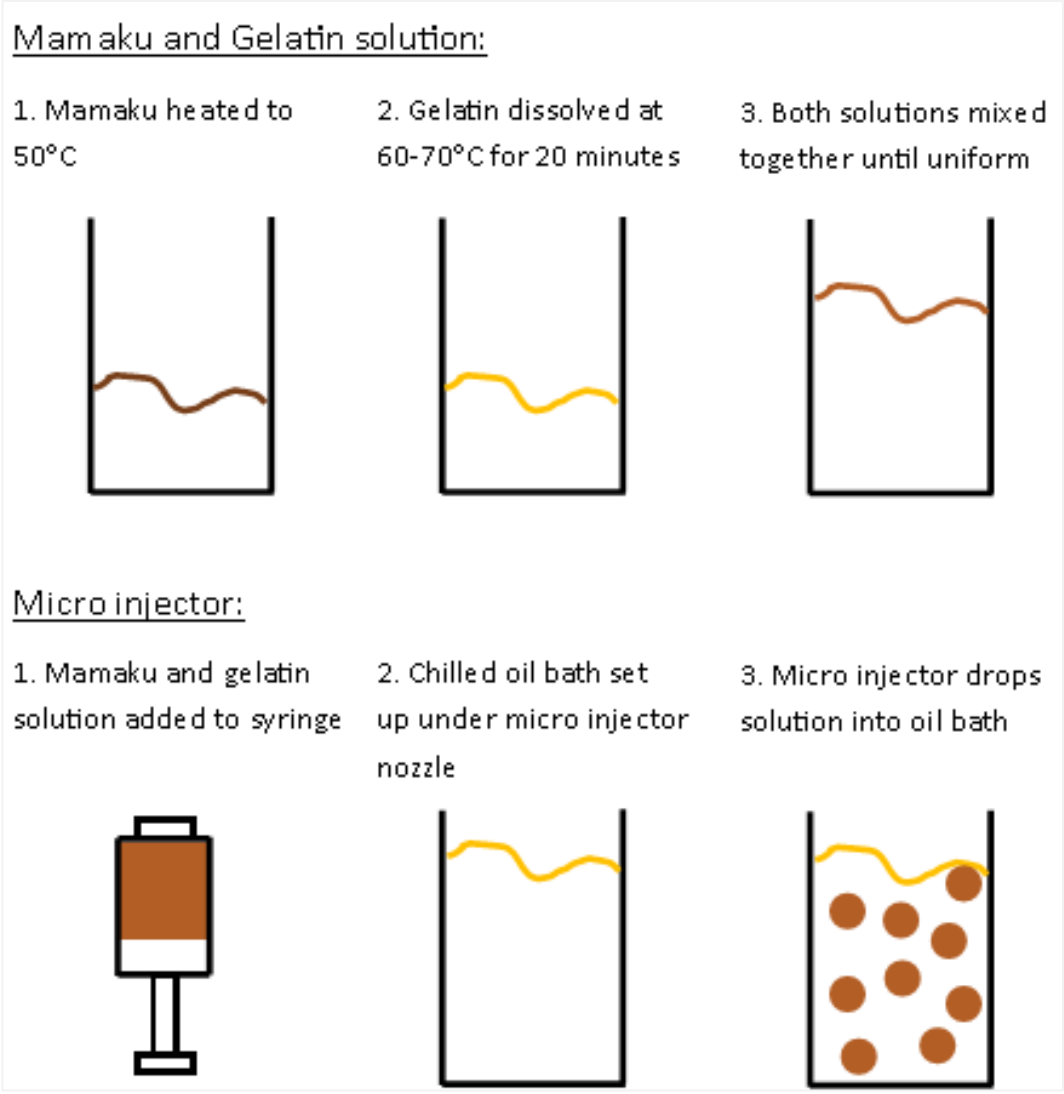

Figure 5.13: Flow diagram for micro injector methodology

The methodology followed is outlined below:

1. The 2.25%wt/v mamaku + 7.5%wt/v gelatin solution was prepared as outlined in section 5.2.2.
2. This solution, shown in Figure 5.14, was loaded into the micro injector syringe and extruded into a chilled oil bath. The solution was kept as warm as possible in a water bath at 55°C, until it was loaded into the syringe.

Figure 5.14: Image showing the mamaku + gelatin solution which was loaded into the syringe

Unfortunately, despite the added pressure, the machine could not overcome the elasticity/viscosity of the solution to form a spray. This meant only large drops were extruded not a continuous stream of small beads. The same result was found with both nozzle sizes available (200µm and 300µm). This lowered the production of beads to at most a few beads per minute, not the 50-1000 it was supposed to produce and instead of being in the µm size scale, they were around 5mm in diameter.

Figure 5.15: The final encapsulated mamaku from the micro injector

Figure 5.15 shows the final beads obtained in this trial. Each bead had a gelatin concentration of 7.5%wt/v and a mamaku concentration of 2.25%wt/v. The size of the beads shown in the picture was obtained with the highest speed, the highest vibration frequency settings and the lowest vibration amplitude. The larger nozzle produced slightly larger beads, but they were produced faster. The machine was not able to form a spray of droplets due to the high viscosity of the solution (and therefore, low capillary number) meaning that jetting regime was not achieved.

Therefore, it produced large droplets in the dripping regime. A comparison was completed with water in the syringe and the machine formed the fine spray of droplets without any issues. This led to the conclusion that the viscosity of the mamaku + gelatin solution was too high and was above the parameters the machine was designed to work with. In addition, the unique elasticity and stickiness of the mamaku (Goh et al., 2007) was likely to be further limiting the machine's ability to form a spray.

5.4.3 Remaining challenges

Although this micro injector method works to encapsulate the mamaku, it is far too slow to be commercially viable. Additionally the large size of the beads may be impractical for use in a food product. However, a bubble tea like product may be suitable if consumers did not chew the beads and melt the gelatin, re-forming the choking hazard. The speed issue was compounded by the concentration issues found in Chapter 6 regarding the stomach in-vitro trials, where the concentration of mamaku had to be doubled or tripled to show the shear-thickening effect in the stomach's warm acidic conditions. This would increase the viscosity of the mamaku + gelatin solution and would increase the problems forming droplets, due to the increased elasticity and stickiness of a higher concentration of mamaku.

The beads appear to be very stable while stored in the oil environment. However, the broken gel (section 5.5) and emulsion templating (section 5.3) experiments show stability issues when placed in an aqueous environment, and this was expected to be an issue with the micro injector based beads also. Therefore, the challenges around stabilising the beads might apply to this system as well and the same limiting factors would apply, as previously outlined in section 5.3.

5.5 Broken gel

The broken gel technique was tested as an option, due to the clumping occurring with the oil removal step of the emulsion templating system. The basis for the idea was to limit the inherent 'double processing' required by the emulsion templating

system. This aimed to avoid emulsion formation and instead form a large container of jelly, then once set break up the large lump of gel by forcing it through a syringe with mesh attached and adding some water to form a paste.

One key change to the formulation involved decreasing the amount of water used to dissolve the gelatin from 50% to 10% and increasing the mamaku volume. Overall, the gelatin concentration remained the same – 7.5%wt/v but the mamaku concentration was increased from 2.25%wt/v to 4.05%wt/v. This aimed to ensure the mamaku concentration was high enough to establish whether the encapsulation was successful.

5.5.1 Methodology

The methodology followed is outlined below:

1. 37.5g of gelatin was hydrated in 50 mL of water at 65-70^{o}C under continuous stirring at 400 rpm for 20 minutes.
2. Then 450mL of mamaku was added and mixed at 600 rpm for about 1 minute until the solution appeared uniform.
3. The gel was then allowed to set in the fridge overnight.
4. In order to break the gel, 36.656g of gel was placed in the syringe with a mesh attached with a diameter of 500µm and forced through the mesh.
5. Then 10mL of RO water was added and the paste was then pushed through a second pass and a third time until uniform. This is shown in Figure 5.16.

Figure 5.16: Before (left), during (left middle) and after (right middle and right) forcing the mamaku + gelatin gel through the syringe

The methodology followed is shown in Figure 5.17.

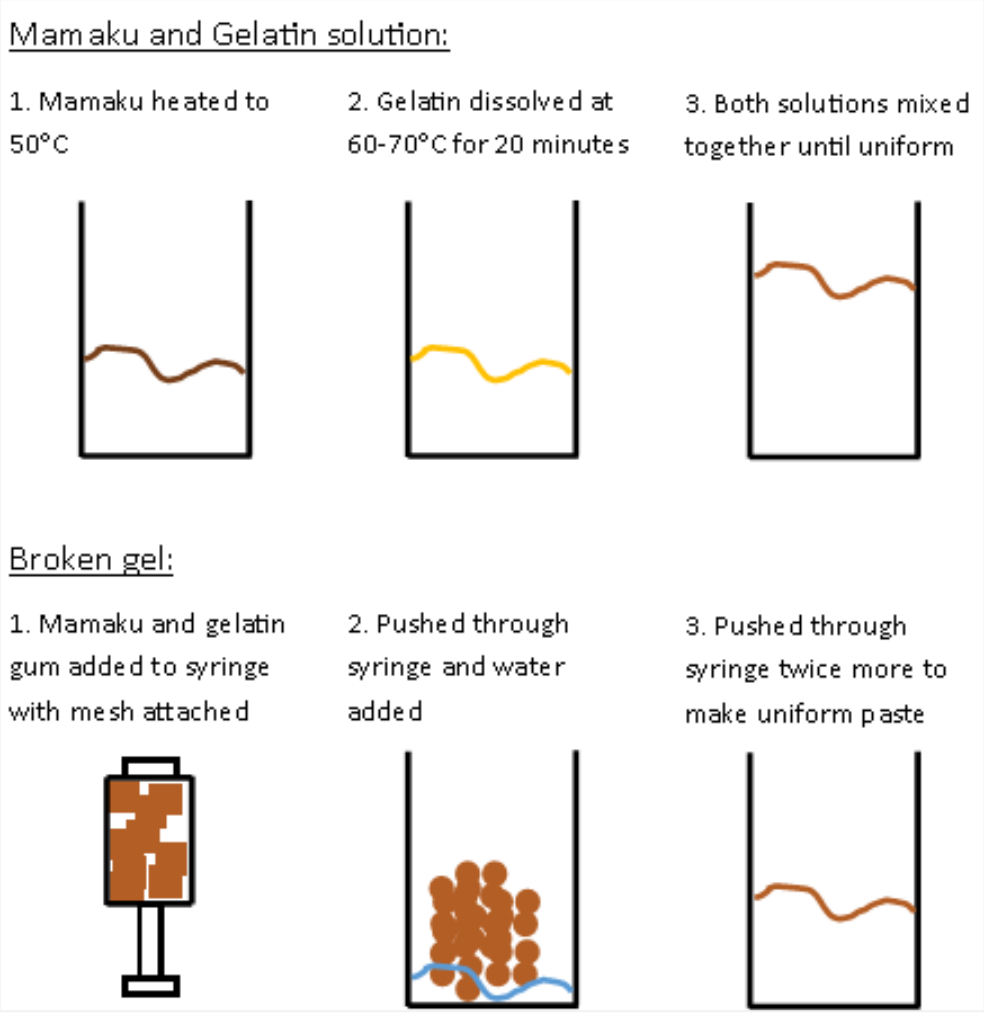

Figure 5.17: Flow diagram for broken gel methodology

The rheometer, geometries and peltier plate used to measure the viscosity profile are outlined in section 4.2.1, as are the settings used to programme the rheometer.

5.5.2 Results

The paste had a final gelatin concentration of ~5.9%wt/v and a mamaku concentration of ~3.2%wt/v. A viscosity profile was measured to identify whether the paste showed any shear-thickening behaviour. The results are shown in Figure 5.18.

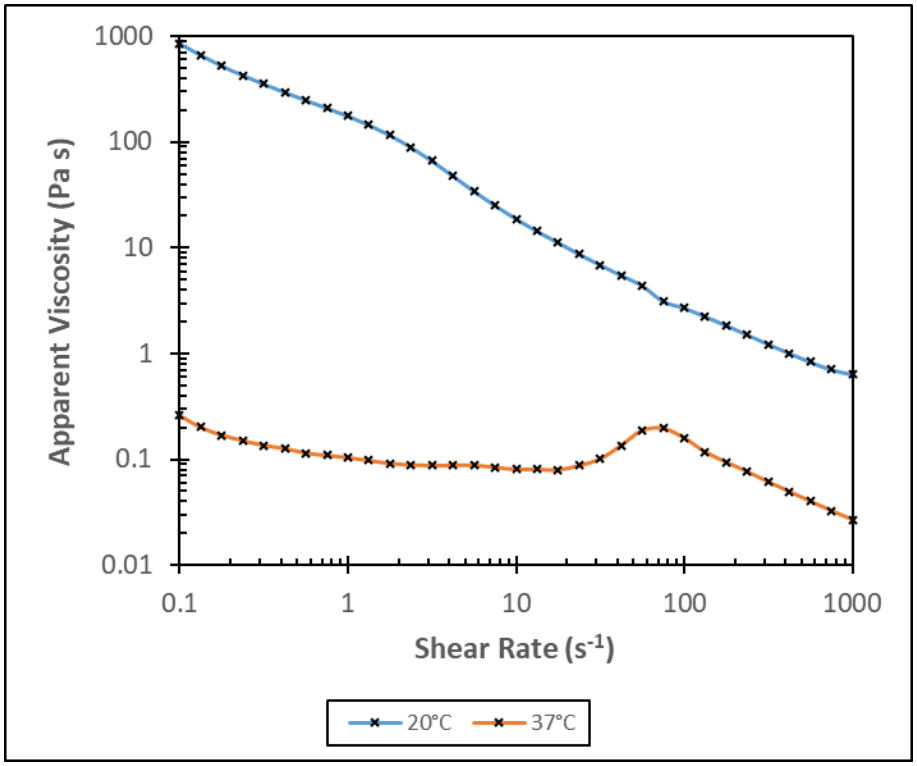

Figure 5.18: Viscosity profile for the broken gel at 20°C measured with concentric cylinder geometry, and at 37°C

These results show that no shear-thickening behaviour was observed at 20°C, meaning the mamaku was successfully encapsulated by the gelatin. Additionally when heated to 37°C, the gelatin released the mamaku leading to the recovery of the shear-thickening properties.

5.5.3 Remaining challenges

This method was easy and effective in producing small particles of ~500µm in diameter. It did successfully encapsulate the mamaku originally; however, there appears to be syneresis occurring after a few days chilled storage. This might make it unsuitable for use in a food product. Due to time constraints the percentage of mamaku released within the liquid formed have not been measured, nor have further trials measuring syneresis occurring with different storage conditions.

These stability issues suggest that the gelatin gel might be too porous to stop the mamaku from travelling out of the gelatin network when placed in an aqueous

environment. It was proposed that this was because the gelatin absorbs the free water in the solution as gelation occurs. Then when the encapsulated beads are transferred back into an aqueous solution, the mamaku not fully encapsulated was free to move out of the network. Additionally, the gelatin would absorb more water and swell further allowing more mamaku molecules to become free. Gelatin hydrogels (usually cross-linked with another polymer) are commonly being used in the medical research field due to its porosity when placed in an aqueous environment, e.g. for bone tissue regeneration (Georgopoulou et al., 2018; Shahrezaie et al., 2017) and nerve regeneration (Wang et al., 2017). Therefore, there are remaining challenges around stabilising the final product as discussed already in section 5.3.4.

5.6 Fluid gel

The fluid gel technique was tested as an option, due to the instability occurring with the broken gel technique. A fluid gel is made by continuously breaking the gel network as it forms. It was thought this different procedure might limit the syneresis occurring. Research done by Gladkowska-Balewicz, Norton and Hamilton (2014) served as the basis for the temperature sweep parameters chosen and the shear rate chosen for these experiments. The experiments aimed to give an understanding as to whether the process of making a fluid gel would encapsulate the mamaku successfully.

5.6.1 Methodology

The methodology followed is shown in Figure 5.19.

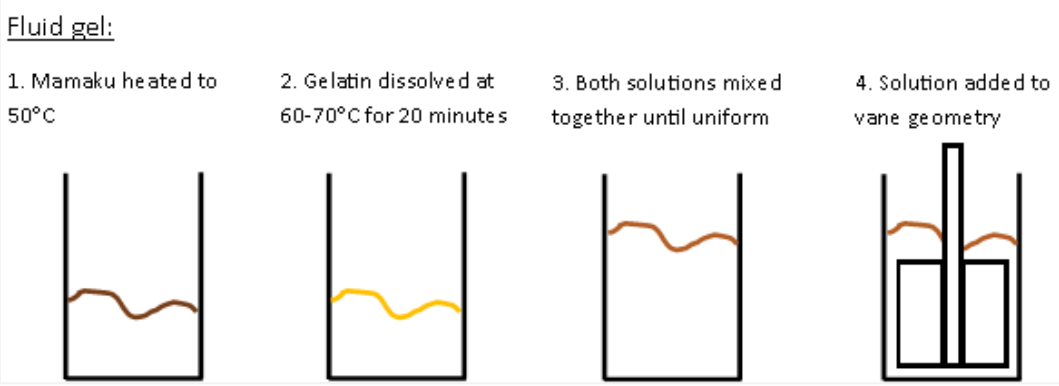

Figure 5.19: Flow diagram for fluid gel methodology

The methodology followed is outlined below:

1. 37.5g of gelatin was hydrated in 50 mL of water at 65-70°C under continuous stirring at 400 rpm for 20 minutes.
2. Then 450mL of mamaku was added and mixed at 600 rpm for about 1 minute until the solution appeared uniform.
3. This was equilibrated to 55°C before the required amount, approximately 15mL, was added to the rheometer to make the fluid gel.

The vane geometry (ST22-4V-40, part number 21015) was used to make the fluid gel in the rheometer. The settings used to programme the rheometer are detailed in Table 5.12.

Table 5.12: Interval settings for the fluid gel

Parameter	Interval	Temperature	Shear Rate
Profile chosen	Fixed measurement point duration	Heating rate – 1°C/minute	Constant
Value	2	/	600 s^{-1}
Initial	30s	55°C	/
Final	2s	18°C	/
Meas. Points	1111		

The rheometer, geometries and peltier plate used to measure the viscosity profile are outlined in section 4.2.1, as are the settings used to programme the rheometer.

5.6.2 Results

It was possible to form a fluid gel with the mamaku + gelatin solution, but with some difficulties due to mamaku's rod climbing properties. Figure 5.20 shows how most of the mamaku + gelatin solution climbed the rod during the production of the fluid gel.

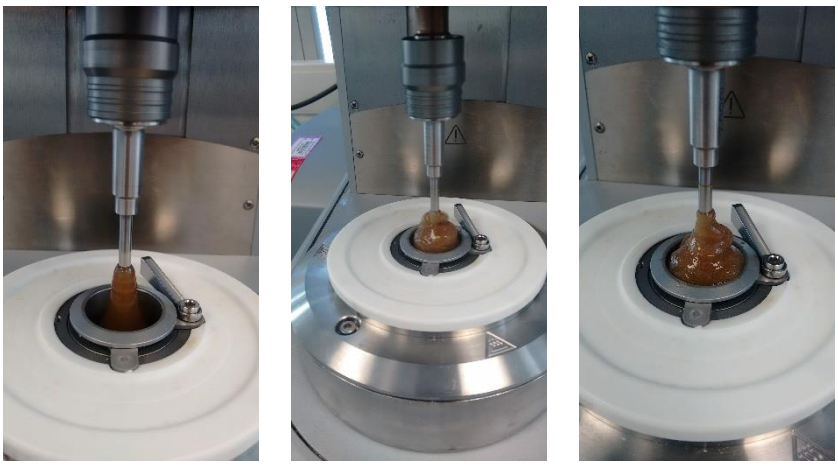

Figure 5.20: Pictures showing the mamaku + gelatin solution climbing the rod at different stages of producing the fluid gel

However, as gelation began to occur the solution did stop climbing the rod. The fluid gel produced is shown in Figure 5.21. The fluid gel had a gelatin concentration of ~7.5%wt/v and a mamaku concentration of ~4.1%wt/v.

Figure 5.21: Pictures showing the fluid gel produced

These images show that in order to disperse in a food product, the fluid gel would have to be dispersed in an aqueous medium and further broken up into discrete beads. The best technique for this is likely to be the broken gel methodology,

outlined in section 5.5. Alternatively, the Silverson mixer could be used to break up the fluid gel, similar to the methodology used breaking up the mamaku + gelatin clumps during the emulsion templating experiments, detailed section 5.3.

The fluid gel was produced twice to see if the method produced similar results each time. The viscosity profile for the fluid gel is shown in Figure 5.22.

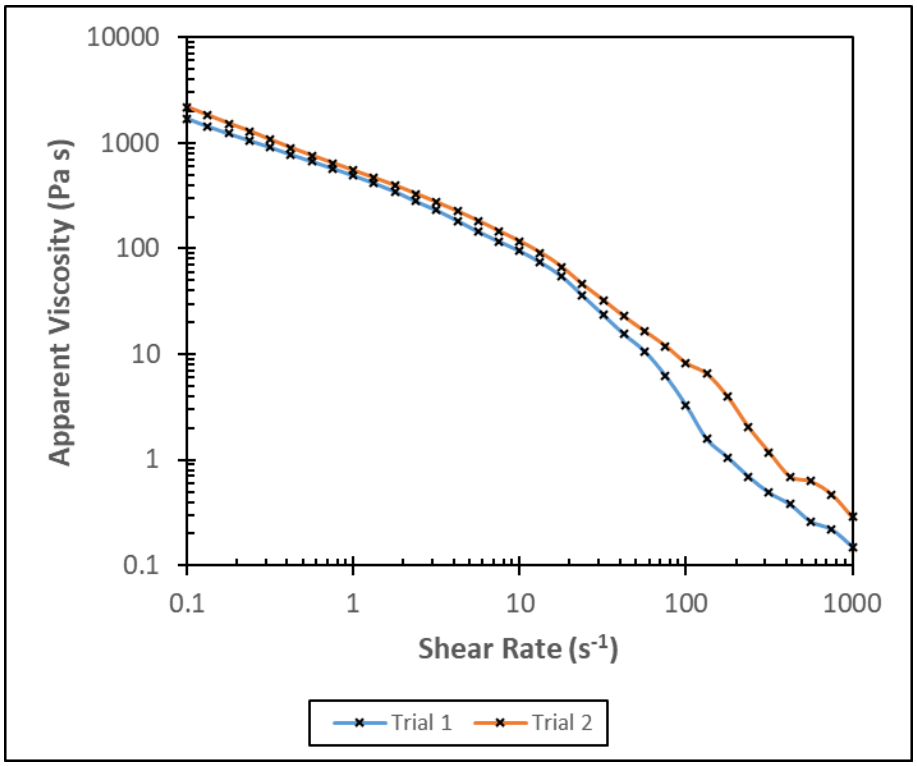

Figure 5.22: Viscosity profile for the two fluid gel samples measured at 20°C

This graph showed that both trials produced similar results and no shear-thickening behaviour was observed, indicating that the mamaku was encapsulated successfully.

5.6.3 Remaining challenges

The first challenge is designing a stirring mechanism that can make a fluid gel on a large scale. Additionally, the system needs to account for the ability of mamaku to climb any rod. The problem with this at a large scale is that the mamaku climbing the rod might result in product being lost as it can be spun completely off the rod. Additionally, process control is reduced, as any product climbing the rod will not

be subjected to the exact shear rates programmed. Furthermore, these issues are compounded by the concentration issues found in Chapter 6 regarding the stomach in-vitro trials, where the concentration of mamaku was found to need to be doubled or tripled to show the shear-thickening effect in the stomach's warm acidic conditions. This would change the viscosity of the mamaku + gelatin solution and would increase the rod climbing problems due to the increased shear-thickening properties of a higher concentration of mamaku (Goh et al., 2007).

The next challenge is breaking up the fluid gel into a paste of small uniform jellies. As discussed earlier this would need to be done either as per the broken gel method (section 5.5) or with the Silverson/Ultra Turrax, similar to how the clumps were broken up in the removing oil step of the emulsion templating method (section 5.3). Again, based on the other results obtained in the broken gel (section 5.5) and emulsion templating (section 5.3) experiments show stability issues when placed in an aqueous environment and this was expected to be an issue with the fluid gel based beads also. Therefore, the challenges around stabilising the beads might apply to this system, as will the same limiting factors previously outlined in section 5.3.

5.7 Discussion and conclusions

All the encapsulation techniques tried have remaining unsolved challenges associated with the intended final use of the encapsulated mamaku. The main contributor to the difficulties faced, was the unique elasticity and stickiness of the mamaku itself (Goh et al., 2007). In addition, the limitations in the intended use of the mamaku include that the mamaku needs to be delivered in a hydrated form (not dried) to the stomach, where the encapsulating material needs to break down and release the mamaku.

The biggest inadequacy of the results obtained, was that all the work was completed with a starting mamaku concentration of 4.5%wt/v. This was selected during the extraction when looking at the flow properties at 20^{o}C, before the

combination of pH and temperature was looked at (section 4.3.6). Work done in the in-vitro digestion chapter (Chapter 6), has shown that the mamaku concentration delivered to the stomach really needs to be at least 10%wt/v. However, increasing the concentration to this extent had a number of effects on encapsulation. Firstly, complicating the entrapment of mamaku within the gelatin gel, due to the larger quantity of polysaccharide in the solution. Secondly, increasing the viscosity, elasticity and stickiness of the solution making it that much harder to measure, pour and/or extrude into droplets.

All the encapsulation techniques tried involved gelatin being gelled to entrap the mamaku. This was because gelatin was thought to be the best encapsulating agent, due to its ability to form a thermo-reversible gel and since it is a protein, it is digested in the stomach. The initial gelatin experiments showed that 7.5%wt/v Type B 250-bloom strength gelatin was able to trap the 2.25%wt/v mamaku within its gelled structure. Additionally, this concentration of gelatin showed a melting point in the low-30s, low enough to promote melting in the stomach but likely to be high enough to be safe to consume while in the mouth. This gelatin concentration was used for all experiments involving the encapsulation of mamaku.

The lack of stability long term in an aqueous environment is a challenge for a food product. The intention was to put these encapsulated beads in a drink or other beverage and create a functional food product. However, there appears to be a lack of stability of the system when placed in an aqueous environment, so further work on stabilisation is required. There is a limiting factor on the coating or gelling agent added to stabilise the encapsulated mamaku, in that this coating or gelling agent has the same constraints as the encapsulating agent did – it must be digested in the stomach in order to release the mamaku successfully. An alternative to a second coating, would be thickening the food matrix, e.g. with a polysaccharide, to reduce the proportion of free water which can interact with the

encapsulated mamaku + gelatin beads – for example, placing the encapsulated mamaku in a yoghurt rather than a drink.

It was proposed that this instability was because the gelatin absorbs the free water in the solution as gelation occurs. Then when the encapsulated beads are transferred back into an aqueous solution, the mamaku not fully encapsulated was free to move out of the network. Additionally, the gelatin would absorb more water and swell further allowing more mamaku molecules to become free. Gelatin hydrogels (usually cross-linked with another polymer) are commonly being used in the medical research field, due to its porosity when placed in an aqueous environment. The research has potential uses for sustained drug delivery (Afzal et al., 2018; Lai, Cheng, Yang & Yen, 2018; Salerno et al., 2018), bone tissue regeneration (Georgopoulou et al., 2018; Shahrezaie et al., 2017), nerve regeneration (Wang et al., 2017) and cancer treatment (Zhang, Li, Kawazoe & Chen, 2017).

Emulsion templating is a successful encapsulating technique for some situations, but likely not this situation. The mamaku concentration was a limiting factor due to the excessive dilution occurring with both the oil, and when the oil was removed and RO water was added. At the concentrations used, it appears that the mamaku concentration was simply too low for shear-thickening properties to be observed, so it cannot be concluded whether encapsulation was successful or not. Additionally, the removal of the oil was a major limitation because it requires several washing steps with solvents and the clumping requires a second mixing step.

Of all the nozzle systems tried, only the micro injector successfully encapsulated the mamaku. However, it also presents several limitations, which would need to be overcome to use the encapsulated product in a food and prove it is safe to consume. Firstly, that the process may be too slow to be commercially viable and secondly, that the large size (3-5mm) of the beads may be impractical for use in a food product. Solving these issues would revolve around proving that if these

beads were chewed in the mouth, not enough mamaku could be released to instigate the thickening, which is expected to lead to choking. Additionally, investigation into a dropper system might speed up the process rather than using a micro injector system. However, more issues are created by the need to increase the concentration of mamaku, because the viscosity of the mamaku + gelatin solution would increase and the problems forming droplets would increase.

The broken gel method was easy and effective in producing small particles of ~500µm in diameter and it did successfully encapsulate the mamaku originally. However, the instability of the system due to syneresis occurring during storage remains unsolved.

The fluid gel method also presented challenges although it did successfully encapsulate the mamaku. The first challenge is designing a stirring mechanism that can make a fluid gel on a large scale. Additionally, this system needs to account for the ability of mamaku to climb any rod, so no product is wasted, and the parameters in the system are consistent. Lastly, the methodology to break up the fluid gel formed into smaller, consistently sized jellies dispersed in water is needed and this method needs to ensure the final jellies formed are stable.

Overall, abundant work on the encapsulation technology is needed to get a commercially viable method producing a stable final product, which is able to be stored in an aqueous environment for use in a food product. Additionally, evaluation into whether the constraints of the system are too limited should be completed to identify other techniques that might show more promise. There are several potential methods to solving the challenges, including reducing the free water content of the food matrix to keep the encapsulated product stable or continuing to use gelatin, but aiming for use in a non-aqueous food, e.g. a jelly or pill. Alternatively, an investigation into other encapsulating agents could be completed aiming either to remove gelatin completely or to use in combination with gelatin to provide a further barrier for stability.

6 Stomach in-vitro digestion

6.1 Introduction

The INFOGEST static in-vitro gastric digestion model was simplified for a quick determination as to whether the gelatin broke down in the stomach's conditions to release the mamaku (Minekus et al., 2014).

The aim of these trials was to provide a yes or no answer as to whether digestion in the stomach's conditions would enable the shear-thickening properties of the mamaku to reform. The intention was not to be certain of the kinetics of the digestion, because a static in-vitro model is simplified compared to the more complicated way food is digested in the human body, so it is not accurate to try to estimate kinetics from a static in-vitro digestion trial (Minekus et al., 2014).

In order to predict if, and how, the encapsulated mamaku break down in the stomach a benchtop system was developed. The most important considerations in replicating the stomach's conditions were as follows:

- A low but consistent shear rate as close to biological shear rates as possible (1-10s^{-1}) (Lentle et al., 2007). However, the lowest stirrer speed available was 40 rpm and therefore this was used.
- The presence of pepsin enzyme to digest proteins.
- The temperature of the stomach before food is added would be 37^{o}C. Food would quickly reach this temperature when ingested (Note that the likelihood of the final food product containing mamaku being chilled could change this assumption).
- The pH level of the stomach when food is introduced initially rises and there is a delay before it returns to ~3 (McClements & Decker, 2009).

6.2 Methodology

6.2.1 Development of the in-vitro methodology

In order to test the digestion of the encapsulated mamaku a stirrer system had to be created, aiming to provide more controllable shear to the whole sample than that provided with a magnetic stirrer. The beaker would be submerged in a water bath and held at 37°C. A wide flat stirrer blade was made, which would ensure all of the mixture was mixed evenly. A picture of the set-up is shown (without the water bath) in Figure 6.1.

Figure 6.1: Set up of the stirrer for testing digestion in the stomach

In addition, a beaker was chosen rather than a petri dish, because it was more likely a clamp could be added to hold the beaker in place in the water bath (to prevent the stirrer scraping the sides as the beaker moves slightly with the movement of the water in the water bath). The methodology is as follows:

- Encapsulated mamaku was added to RO water and heated to 37°C
- The pH was lowered with 0.1M HCl, to pH 3.0
- Porcine pepsin was added at 1%wt/v aiming to ensure it was in excess in the solution. Product specification is in Appendix O.
- A sample was taken after 30 minutes (and at 60 and 90 minutes depending on the amount of sample available) for rheological measurement.

6.2.2 Rheology

Depending on the concentration of mamaku, either a pipette or syringe was used to load the sample into the geometry with the appropriate amount (~5mL for double gap and ~15mL for concentric cylinder), eliminating any excess. As Wee (2015) explained, the unique rheological properties of mamaku leads to sample climbing the rod particularly when excessive quantity is added. The rheometer, geometries and peltier plate used to measure the viscosity profile are outlined in section 4.2.1, as are the settings used to programme the rheometer.

6.3 Factors affecting the in-vitro digestion

The results of the initial trials can be found in Appendix P. These trials showed unfavourable results since minimal shear-thickening properties were recovered during digestion. As a result of this, experimental work was designed to identify whether the minimal recovery of shear-thickening was solely caused by dilution of mamaku, or if other changes was occurring which were limiting the recovery of shear-thickening properties. This was done by looking at the factors affecting the in-vitro digestion and looking at potential interactions between the components.

6.3.1 Temperature and pH changes

In order to show the effect of temperature (37^{o}C) versus ambient (20^{o}C) and the effect of concentration on the rheological properties of mamaku solution (only mamaku solution), the viscosity profile was measured. These results have already been discussed in Chapter 4 but the results are reproduced in Figure 6.2.

The results demonstrate that the mamaku concentration where the shear-thickening effect was lost increased from 0.56%wt/v to 1.13%wt/v, with the increase in temperature from 20^{o}C to 37^{o}C, meaning that more than that concentration (1.13%wt/v) must be delivered to the stomach to see any shear-thickening effect. The mechanism for the reduction in viscosity observed was discussed in detail in section 4.3.5.

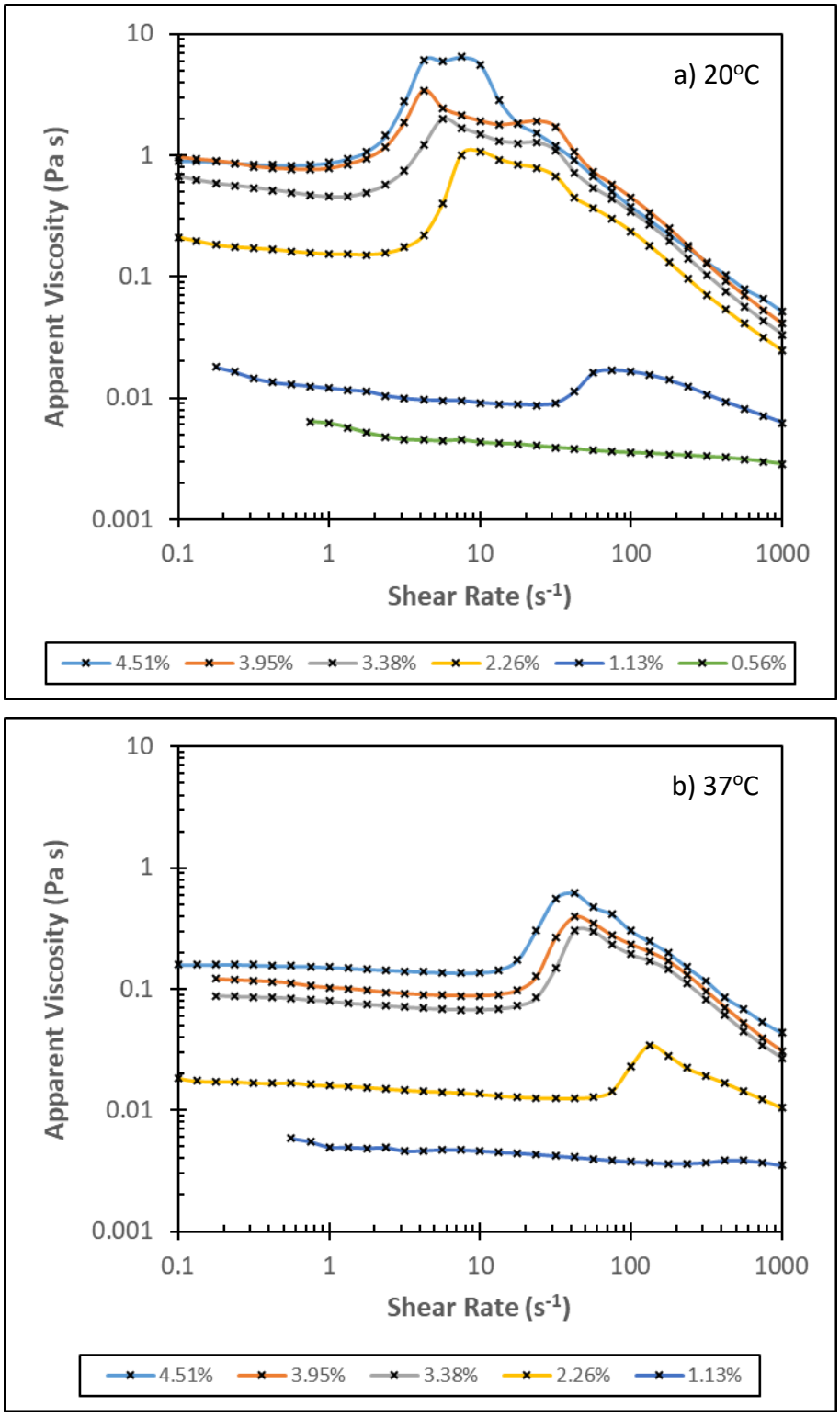

Figure 6.2: Viscosity profile showing the effect of mamaku concentration on the shear-thickening peak of mamaku at: (a) 20°C and (b) 37°C (reproduced from Chapter 4)

In order to show the effect of temperature (37°C) versus ambient (20°C) and the effect of pH on the rheological properties of 4.5%wt/v mamaku solution (only mamaku solution), the viscosity profile was measured. These results have already been discussed in Chapter 4 but the results are reproduced in Figure 6.3.

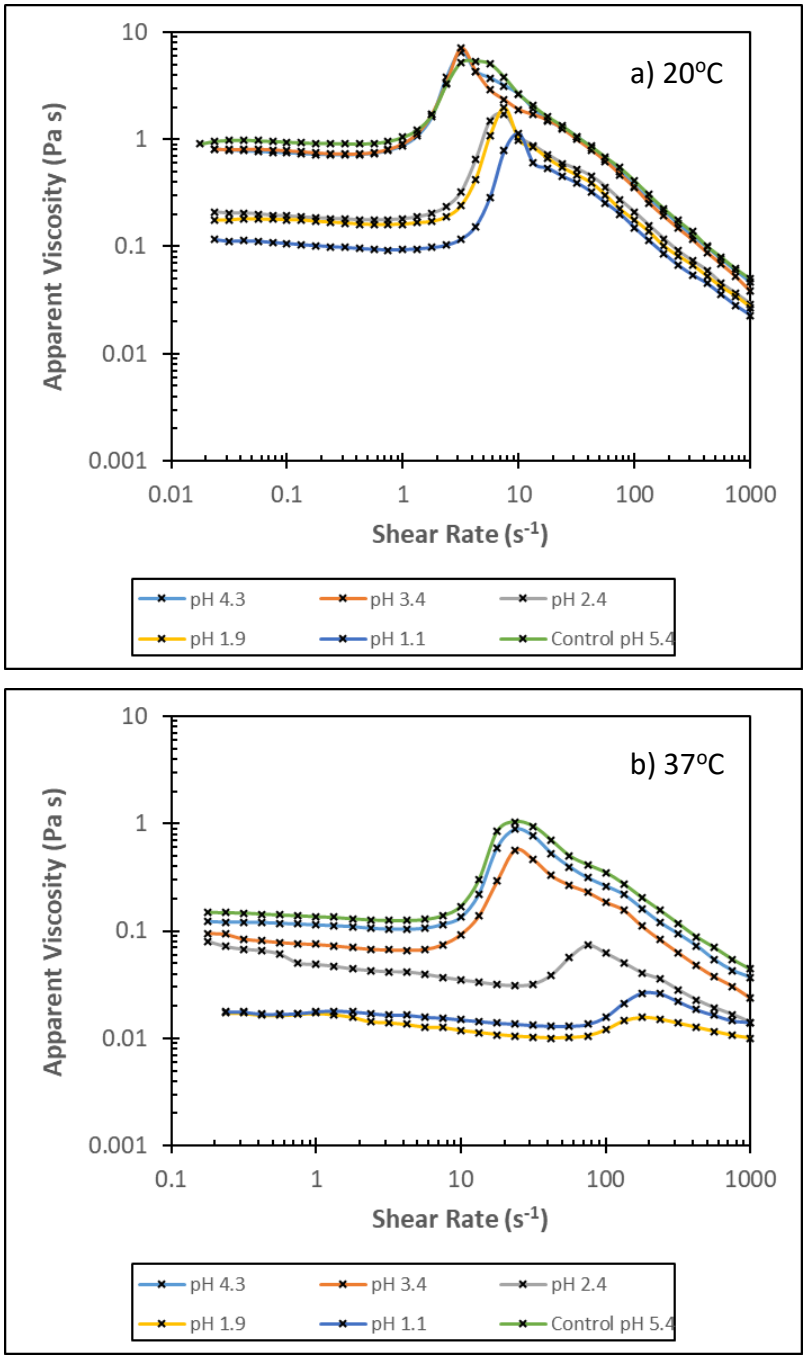

Figure 6.3: Viscosity profile showing the effect of pH on the shear-thickening peak of 4.5%wt/v mamaku at: (a) 20°C and (b) 37°C (reproduced from Chapter 4)

Figure 6.3 showed that when the temperature was increased from 20°C to 37°C, the pH, where the loss of shear-thickening peak viscosity became apparent for 4.5%wt/v mamaku, was increased from pH 2.4 to pH 3.4. The mechanism for the reduction in viscosity observed has already been discussed in detail in the mamaku analysis Chapter 4 in section 4.3.6. Decreasing the pH reduces the negative charges of the polysaccharide (Matia-Merino et al., 2012) because the pK_a of mamaku is ~2.0 (May, 2015). This means that there is less inter-molecular repulsion due to charge screening when the pH is decreased resulting in shrinkage of the molecular conformation (Wee et al., 2015a). Therefore, when the pH is reduced, higher shear rates are required to get the molecules to unfold because of the stronger intramolecular bonds. This delays the shear rate at onset of shear-thickening as shown in the results.

These findings led to the decision to increase the in-vitro digestion pH from 3.0 to 4.0, as detailed in section 6.3.3, to provide a higher chance of observing the shear-thickening peak. This was because the encapsulated mamaku already had a lower concentration of mamaku than that tested in Figure 6.3 because of dilution with gelatin. This meant that the shear-thickening peak was already considerably smaller than what was shown for 4.5%wt/v mamaku at all pH levels.

6.3.2 Potential interactions with components

The aim of this experiment was to compare the rheology of each individual component in the system to understand whether interactions were occurring, or if dilution was the culprit for the minimal shear-thickening properties regained in the initial trials in Appendix P. This work was completed at 37°C to mimic the conditions of the stomach. This was done by adjusting the total volume of each solution to give the same overall concentration of mamaku + gelation. The following solutions were prepared:

- 2.1%wt/v mamaku + 6.5%wt/v gelatin at pH 5.27 at 32.9°C
- 2.1%wt/v Mamaku at pH 5.52 at 31.6°C

- 2.1%wt/v mamaku + 6.5%wt/v gelatin reduced to pH 3.33 at 35.0°C

These solutions were then individually analysed to obtain viscosity profiles at 37°C to see what patterns emerged. The results of this are shown in Figure 6.4.

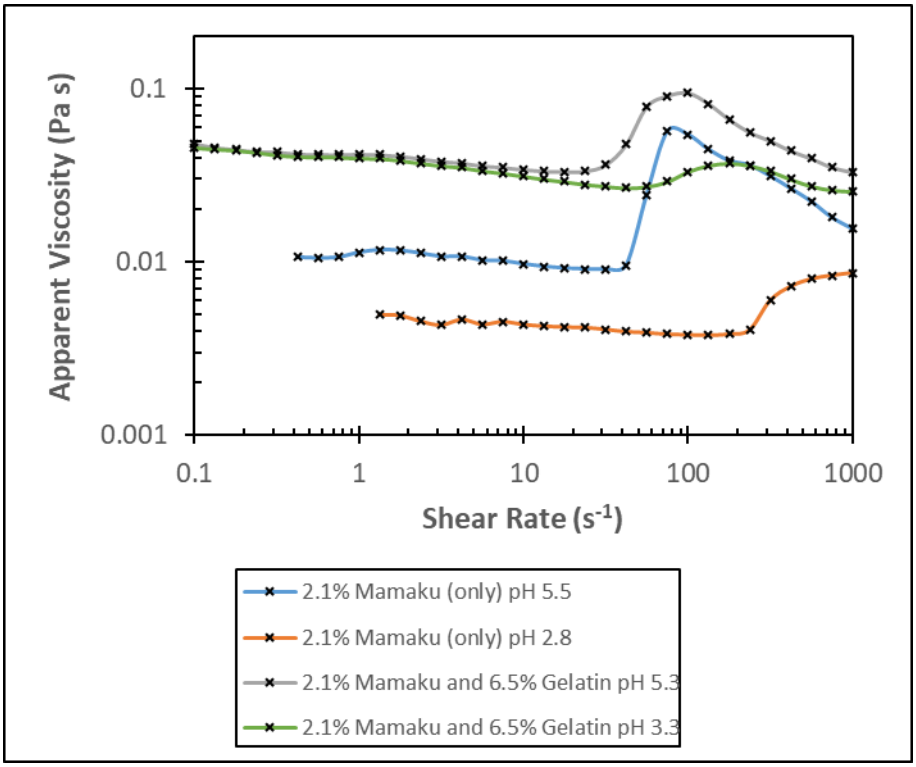

Figure 6.4: Viscosity profiles obtained at 37°C showing the difference in viscosity of 2.1%wt/v mamaku at pH 5.5 and at pH 2.8, 2.1%wt/v mamaku + 6.5%wt/v gelatin solution at pH 5.3 and at pH 3.3

Figure 6.4, showed that the addition of gelatin (at pH 5.3) increased the viscosity at all shear rates, when compared to the solution with only mamaku (at pH 5.5). The increased Newtonian viscosity, before the onset of thickening, provides an illusion that the shear-thickening peak viscosity had been suppressed. However, in reality, the peak viscosity was higher than that of mamaku solution alone. Additionally, the shear rates at onset of thickening have not shifted, nor have the shear rate at the peak viscosity. This provides confidence that at the mamaku's native pH ~5.2-5.3 there are no negative interactions affecting the shear-thickening peak viscosity, between mamaku + gelatin at 37°C. The extent of shear-thickening (the difference between peak viscosity and initial Newtonian viscosity),

does appear to reduce, however, this was also seen with increasing mamaku concentration and can be explained by more molecules being present in the solution, not necessarily being the result of an interaction between mamaku + gelatin.

Figure 6.4 showed a drastic reduction in the shear-thickening peak viscosity upon the reduction of pH to the mamaku at pH 2.8 (without gelatin present), when compared with mamaku at pH 5.5 (without gelatin present). The initial Newtonian viscosity decreased and the shear rates at the onset of thickening and at the peak viscosity, was increased upon the addition of acid. The mamaku (only) curve at pH 2.8 appears to show an increase in viscosity after the initial shear-thickening effect, meaning the viscosity curve does not show a typical shear-thickening then shear-thinning profile. This could be the onset of Taylor Vortex Flow where the viscosity rises because of a transition to one of the turbulent states (Mohammadigoushki & Muller, 2017). The low viscosity of the solution combined with the high shear rates can lead to Taylor Vortex Flow within the rheometer geometry above a critical shear rate (Mohammadigoushki & Muller, 2017).

Figure 6.4 also showed a drastic reduction in the shear-thickening peak viscosity upon the reduction of pH to the mamaku + gelatin solution (at pH 3.3), when compared with mamaku + gelatin solution at pH 5.3. The initial Newtonian viscosity showed no change, however, the shear rates at the onset of thickening and at the peak viscosity were increased upon the addition of acid. Additionally, the suppression in shear thickening seen for the mamaku + gelatin solution at pH 3.3 was greater than that seen with mamaku only at pH 2.8.

One potential reason for this reduction in shear-thickening peak viscosity was simply the effect of pH and temperature on mamaku, already discussed in section 6.3.1, where a large reduction in shear-thickening properties occurs and the shear rates at onset on thickening and the peak viscosity are increased. Lowering the pH reduces the negative charge of the polysaccharide (Matia-Merino et al., 2012). Since the pK_a of mamaku is ~2.0 (May, 2015), at pH 3.3, there are less inter-

molecular repulsion (compared to at pH 5.3), due to charge screening resulting in shrinkage of the molecular conformation, resulting in higher shear rates being required to force the molecules to unfold due to the stronger intramolecular bonds (Wee et al., 2015a).

However, another possible reason is an interaction between mamaku and gelatin at pH 3.3. Gelatin solutions are known to follow a Newtonian viscosity profile (Wulansari, Mitchell, Blanshard & Paterson, 1998). Type B gelatin has an isoelectric point between 4.7 and 5.3 (Gelatin Manufacturers Institute of America, 2012). This is the point at which gelatin will have a neutral charge. Above this point, it will be negatively charged. Below this point, it will be positively charged. This means that the gelatin within the native mamaku + gelatin solution was essentially neutrally charged or perhaps a slight negative charge. However, when exposed to the acid for digestion, the gelatin will become positively charged.

As previously discussed in Chapter 4, in order for shear-thickening to occur, the mamaku molecules must unfold and orientate in such a way that hydrogen bonds can form between mamaku molecules (Wee et al., 2015a). Additionally, positively charged cations must be present to screen the negatively charged groups within the mamaku for this to happen.

In this situation, these positively charged gelatin molecules might be interacting with the negatively charged mamaku molecules in the same way cations do. In particular, the extra positive charges in solution because of the gelatin would cause an overall reduction in the negative charge of the mamaku molecules. This means that there is less inter-molecular repulsion within the mamaku and results in shrinkage of the molecular conformation leading to a lower viscosity (Wee et al., 2015a). The stronger intramolecular bonds require higher shear rates to get the mamaku molecules to unfold. This could explain both phenomena shown in Figure 6.4, firstly the delayed onset of shear-thickening and secondly the reduced shear-thickening peak viscosity.

Digestion of the gelatin into peptides by the pepsin should resolve some of these issues because the molecules would be smaller, meaning the mamaku molecules can approach closer together, resulting in a higher shear-thickening peak viscosity.

6.3.3 Changes to the in-vitro methodology

After the initial trials outlined in Appendix P and the resulting investigation into the factors affecting the in-vitro digestion results, showed that the mamaku was far too diluted to show any shear-thickening peak, modifications were made to the system, including:

- Firstly, the dilution of mamaku to stomach juices was eliminated. In real life, normally the stomach dilutes the food or drink consumed by 50%.
- Secondly, the HCl acid used was increased from 0.1M to 1.0M to limit the total volume needed to lower the pH (although 0.1M HCl was recommended in the Pepsin specifications).
- Thirdly, the target pH was increased from 3.0 to 4.0 to limit the suppression in shear-thickening effect observed at 37^{o}C and at acidic pH and to reduce the positive charge on the gelatin molecules. It is evident that in the real human stomach the pH raises when food is first ingested then it slowly drops back to acidic over time. This means that in real life the shear-thickening peak suppression is likely to be less than what the results of these in-vitro trials are suggesting. Additionally, there is the possibility of formulating the mamaku + gelatin solution to contain a buffering agent, which would further help to increase the pH in the stomach to increase the shear-thickening peak size.

6.4 In-vitro digestion results

After modifying the in-vitro methodology to provide more optimal conditions for the shear-thickening peak to be observed, the remaining limiting factor was concentration of mamaku. The following experiments involve in-vitro digestion of various solutions of mamaku + gelatin at various concentrations. Some solutions

involved encapsulated mamaku and others just 'mamaku + gelatin' mixed together at various concentrations. The experiments are presented in chronological order of increasing mamaku concentration and involved the following solutions and concentrations (established after the acid was added):

- Washed emulsion gelled droplets with a concentration of 0.80%wt/v mamaku + 1.48%wt/v gelatin;
- 2.2%wt/v mamaku mixed with 7.2%wt/v gelatin (no encapsulation technology was used);
- Broken gel paste with a concentration of 3.0%wt/v mamaku + 5.6%wt/v gelatin;
- Fluid gel with a concentration of 4.0%wt/v mamaku + 7.3%wt/v gelatin;
- 8.6%wt/v mamaku mixed with 7.1%wt/v gelatin (no encapsulation technology was used), and
- 12.9%wt/v mamaku mixed with 7.1%wt/v gelatin (no encapsulation technology was used).

This experimental work aimed to establish the concentration of mamaku required in the stomach to get shear-thickening properties to occur at the biological shear rates of the stomach, 1-10s^{-1}. Past work was done with 16.4%wt/wt rehydrated freeze-dried mamaku without any encapsulation, when the solution was shown to delay gastric emptying (Lentle et al., 2010). However, this concentration was chosen to match the apparent viscosity of 1.5% guar gum at the biological shear rates. Therefore, it was thought that lower concentrations might show some shear-thickening effect at biological shear rates and consequently less mamaku would be required for a similar effect.

The experiments also aimed to confirm whether the encapsulation techniques present any challenges breaking down to release the mamaku.

6.4.1 0.80%wt/v mamaku + 1.48%wt/v gelatin (gelled droplets)

This trial was completed using the mamaku encapsulated by emulsion templating after washing to remove the oil, as outlined in section 5.3, with final concentration within the emulsion of 0.81%wt/v mamaku + 1.5%wt/v gelatin. The flow diagram for the methodology followed is shown in Figure 6.5.

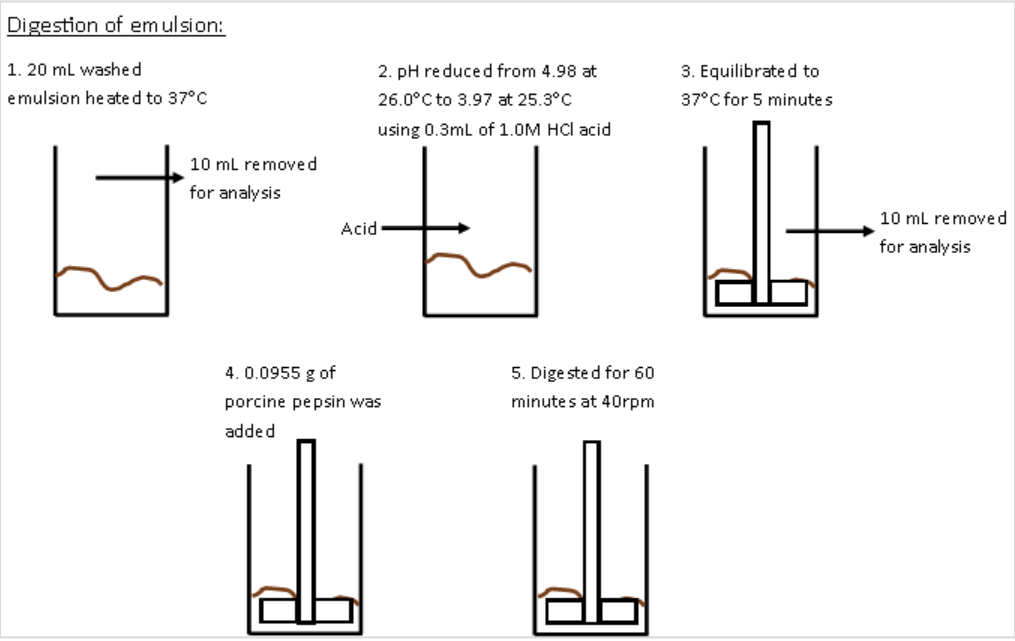

Figure 6.5: Flow diagram for the in-vitro digestion of the emulsion with oil removed

After adding the acid, the concentration of mamaku was 0.80%wt/v and the concentration of gelatin was 1.48%wt/v. Images of the emulsion mixing at 40 rpm in the water bath are shown in Figure 6.6.

Figure 6.6: In-vitro digestion of the emulsion based encapsulated mamaku

Samples were periodically taken at various intervals: before acid was added, after acid was added (but no pepsin) and after 60 minutes of digestion. The viscosity profiles are shown in Figure 6.7.

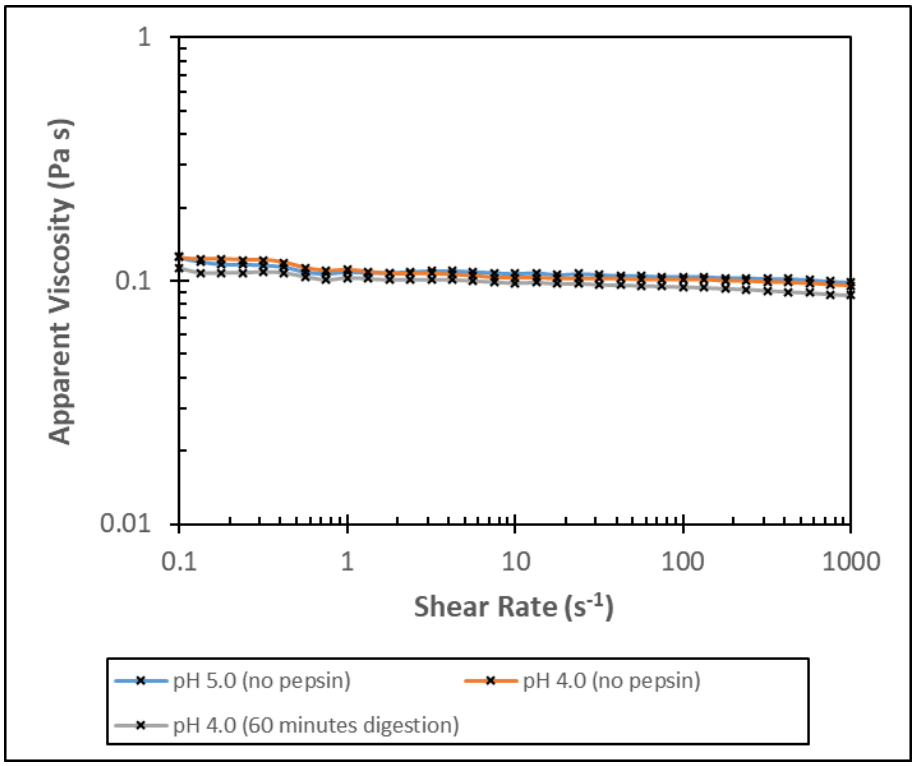

Figure 6.7: Viscosity profile at 37°C for the emulsion with the oil removed, measured at pH 5.0 (before digestion with pepsin), at pH 4.0 (before digestion with pepsin), and after 60 minutes digestion with concentration of 0.80%wt/v mamaku + 1.48%wt/v gelatin

Figure 6.7 showed that no shear-thickening behaviour was regained, very likely due to the concentration of mamaku being too low to show any thickening behaviour. This led to the next trial, mamaku + gelatin solution with no encapsulation method, to identify the mamaku concentration required to produce the desired shear-thickening effect.

6.4.2 2.2%wt/v mamaku + 7.2%wt/v gelatin solution

This trial was completed using a 2.3%wt/v mamaku + 7.5%wt/v gelatin solution freshly made up, as follows:

1. The 250 mL of mamaku was defrosted and equilibrated to 50°C in a water bath.
2. The 37.5 g of gelatin was hydrated in 250 mL of water at 60-70°C for 20 minutes at about 400 rpm.
3. The mamaku was added and mixed at 600 rpm for about 1 minute until the solution appeared uniform.

The flow diagram for the methodology followed is shown in Figure 6.8.

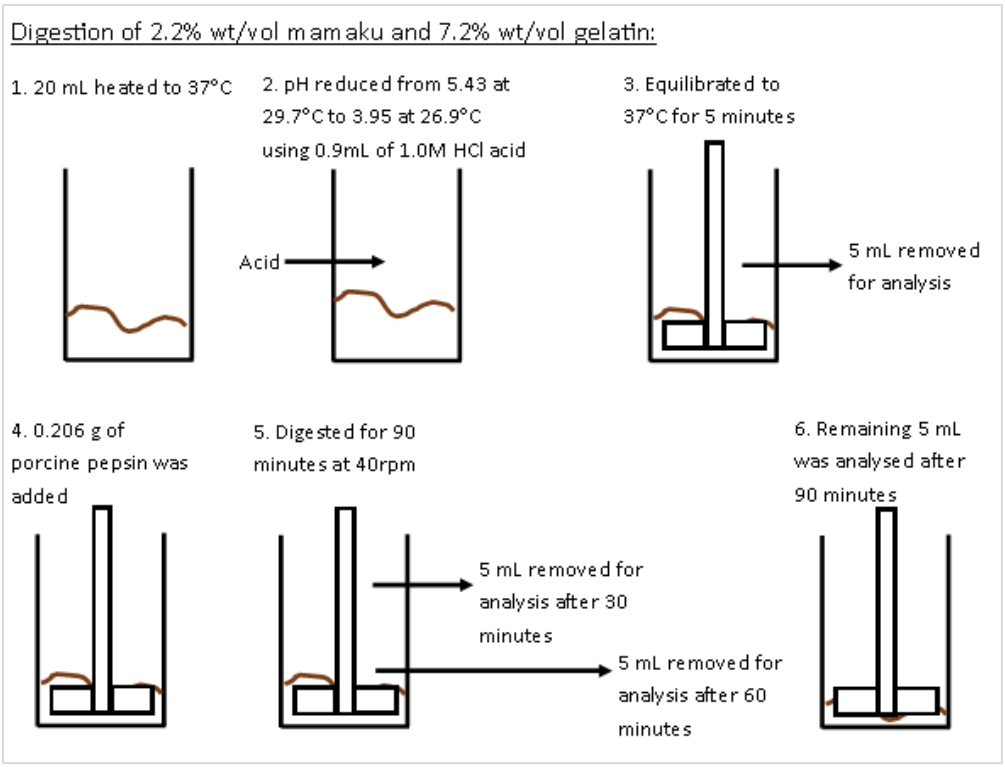

Figure 6.8: Flow diagram for the in-vitro digestion of the 2.2%wt/v mamaku + 7.2%wt/v gelatin solution

After adding the acid, the concentration of mamaku was 2.2%wt/v and the concentration of gelatin was 7.2%wt/v. A picture of this solution mixing at 40 rpm in the water bath is shown in Figure 6.9.

Figure 6.9: Picture showing the in-vitro digestion occurring in the water bath

Samples were periodically taken at various intervals: before acid was added, after acid was added (but no pepsin), after 30 minutes of digestion, after 60 minutes of digestion and after 90 minutes of digestion. The viscosity profiles are shown in Figure 6.10.

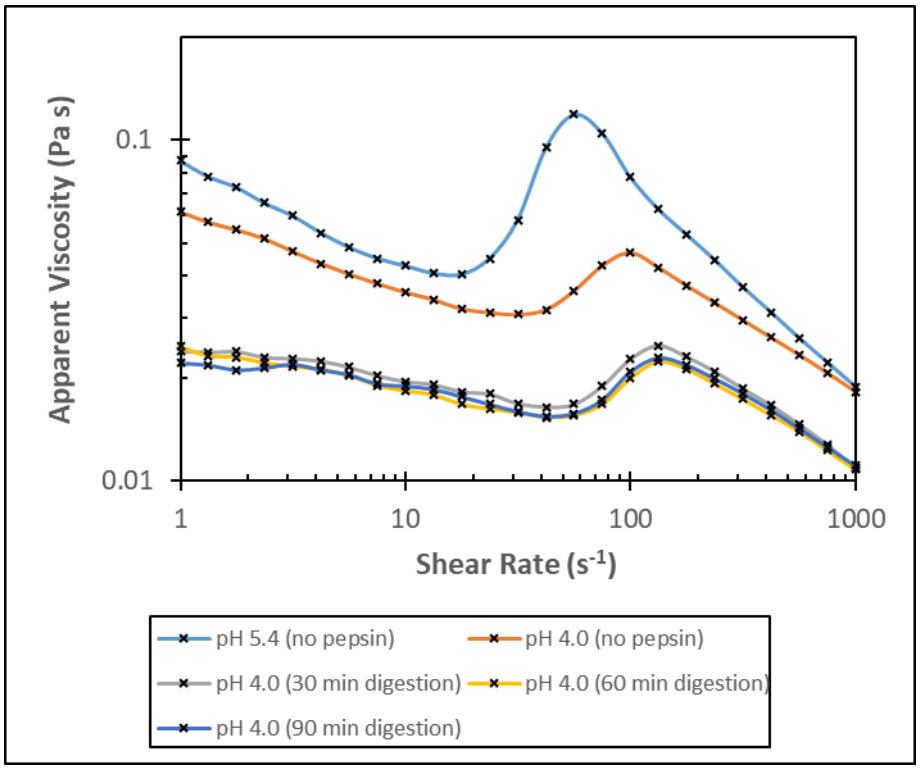

Figure 6.10: Viscosity profile at 37°C for the mamaku + gelatin solution, measured at pH 5.4 (before digestion with pepsin), at pH 4.0 (before digestion with pepsin), and after 30, 60 and 90 minutes digestion with concentration of 2.2%wt/v mamaku + 7.2%wt/v gelatin

Figure 6.10 showed that the shear-thickening peak becomes visibly supressed as soon as the acid was added, with both a reduction in peak viscosity and an increase in the shear rate at onset of shear-thickening. However, the digestion showed that the viscosity was reduced further by digestion of the gelatin resulting in a shift of the curve down to lower viscosities. Furthermore, most of the digestion occurs during the first 30 minutes shown by the minimal change in the viscosity profile after 60 and 90 minutes.

At this mamaku concentration, 2.25%wt/v, the digestion results showed that the extent of shear-thickening occurring after digestion is reduced, and occurred at shear rates higher than the target of $1s^{-1}$ to $10s^{-1}$. Thus, higher mamaku concentrations were targeted in the next experiments.

6.4.3 3.0%wt/v mamaku + 5.6%wt/v gelatin (broken gel)

The next system investigated was the formation of a gel broken into a paste allowing a greater concentration of mamaku to be encapsulated, as per encapsulation via broken gel outlined in section 5.5. This gave an overall concentration of 3.15%wt/v mamaku + 5.89%wt/v gelatin. A flow diagram for the methodology is shown in Figure 6.11.

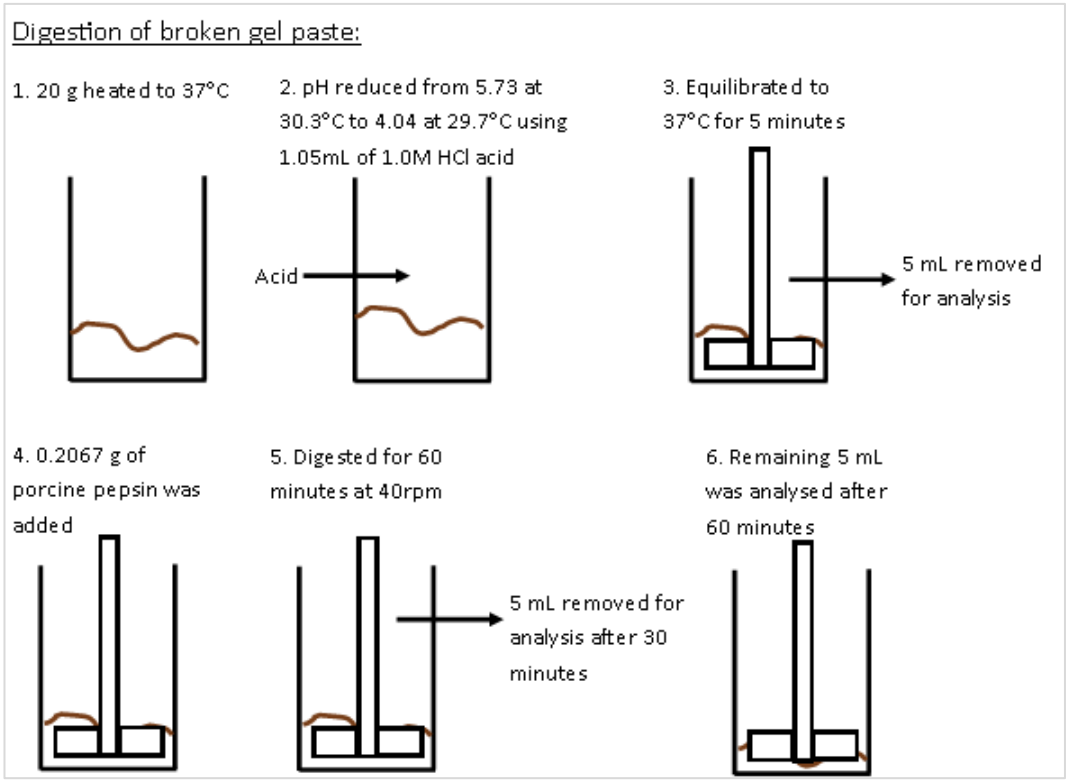

Figure 6.11: Flow diagram for the in-vitro digestion of the 3.0%wt/v mamaku + 5.6%wt/v gelatin broken gel paste

After adding the acid, the concentration of mamaku was 3.0%wt/v and the concentration of gelatin was 5.6%wt/v. Images of the melted broken gel paste mixing at 40 rpm in the water bath are shown in Figure 6.12.

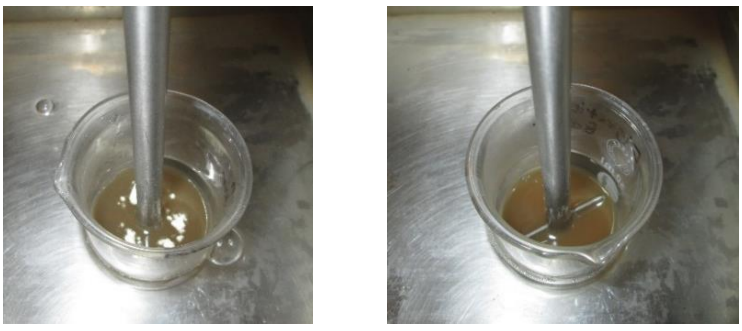

Figure 6.12: Pictures showing the in-vitro digestion occurring in the water bath

Samples were periodically taken at various intervals: before acid was added, after acid was added (but no pepsin), after 30 minutes of digestion and after 60 minutes of digestion. The viscosity profiles are shown in Figure 6.13.

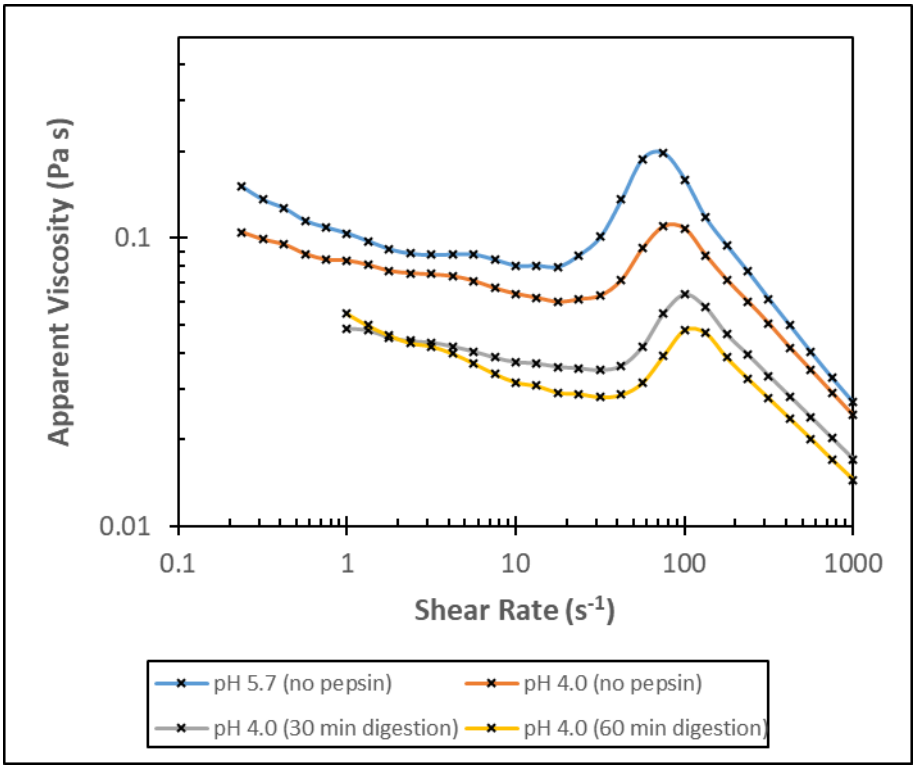

Figure 6.13: Viscosity profile at 37°C for the broken gel paste, measured at pH 5.7 (before digestion with pepsin), at pH 4.0 (before digestion with pepsin), and after 30 and 60 minutes digestion with concentration of 3.0%wt/v mamaku + 5.6%wt/v gelatin

Figure 6.13 showed that very similar trends to the previous trial was observed. Again, the viscosity and the shear-thickening peak becomes visibly supressed as soon as the acid was added with both a reduction in peak viscosity, and an increased shear rate at the onset of shear-thickening. Additionally, the viscosity becomes further reduced by the digestion of the gelatin resulting in a shift of the curve down to lower viscosities. Furthermore, a slight decrease in viscosity was shown after 60 minutes digestion time, compared to 30 minutes.

The results show there is a possible interaction occurring with the gelatin and mamaku upon the addition of acid, as first discussed in the component study in section 6.3.2. It was proposed that the lower pH, changes the charge on the gelatin and allows an interaction to occur which both disrupts and delays the shear-thickening mechanism due to the reduction of intramolecular repulsion.

Overall, at this concentration of mamaku, 3.15%wt/v, the peak was still occurring at shear rates higher than the target of 1-10s^{-1} and therefore not suitable for the functional food to cause the effect. Thus, higher mamaku concentrations again were targeted in the subsequent experiments.

6.4.4 4.0%wt/v mamaku + 7.3%wt/v gelatin (fluid gel)

The next system investigated was completed using mamaku encapsulated through the production of a fluid gel as outlined in section 5.6, with final concentration of 4.1%wt/v mamaku + 7.5%wt/v gelatin. The fluid gel methodology only produced a small sample ~15 mL, reducing the number of test carried out. After adding the acid, the concentration of mamaku was 4.0%wt/v and the concentration of gelatin was 7.3%wt/v. A flow diagram for the methodology is shown in Figure 6.11.

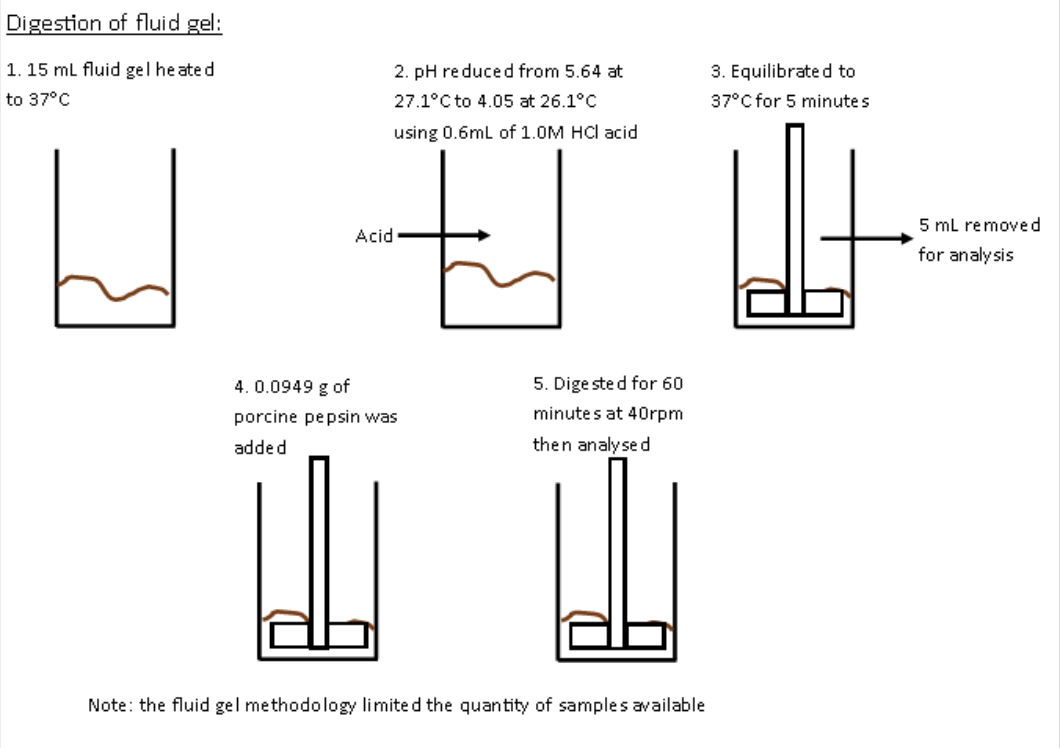

Figure 6.14: Flow diagram for the in-vitro digestion of the 4.0%wt/v mamaku + 7.3%wt/v gelatin fluid gel

Samples were periodically taken at various intervals: after the acid addition (before pepsin) and after 60 minutes of digestion. The viscosity profiles are shown in Figure 6.15.

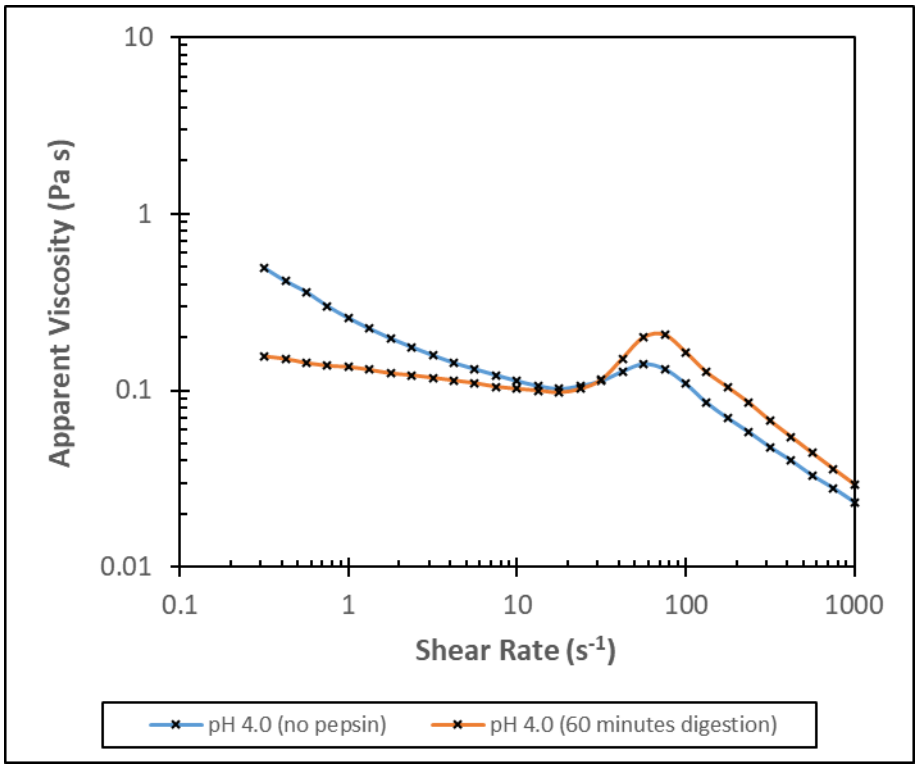

Figure 6.15: Viscosity profile at 37°C for the fluid gel, measured at pH 4.0 (before digestion with pepsin), and after 60 minutes digestion with concentration of 4.0%wt/v mamaku + 7.3%wt/v gelatin

Figure 6.15 showed that the digested solution had a lower initial Newtonian viscosity; however, it had a higher shear-thickening peak viscosity, showing similar shear rates at the onset of shear-thickening and at the peak viscosity.

These findings show that letting the solution digest actually increases the shear-thickening peak viscosity from that observed after the acid was added. This was only observed when using the fluid gel technique, but it also coincided with the highest concentration of mamaku so far.

The peak still occurred at shear rates higher than the target of 1-10s^{-1}. Thus, higher mamaku concentrations again were targeted in the subsequent experiments.

6.4.5 8.6%wt/v mamaku + 7.1%wt/v gelatin solution

10%wt/v mamaku solution was made up from freeze-dried mamaku and allowed to hydrate overnight. Work done in mamaku analysis, Chapter 4, has shown that the rehydration of freeze-dried mamaku negatively affects the shear-thickening properties of mamaku and reduces the viscosity at all shear rates. Therefore, although this solution had a concentration of 10%wt/v, the native viscosity profile would not match what 10%wt/v would look like if the solution had only been concentrated and frozen rather than freeze-dried.

Starting concentrations of mamaku (9.0%wt/v) + gelatin (7.5%wt/v) were used resulting in final concentrations of 8.6%wt/v mamaku + 7.1%wt/v gelatin after acid addition. A flow diagram for the methodology is shown in Figure 6.16.

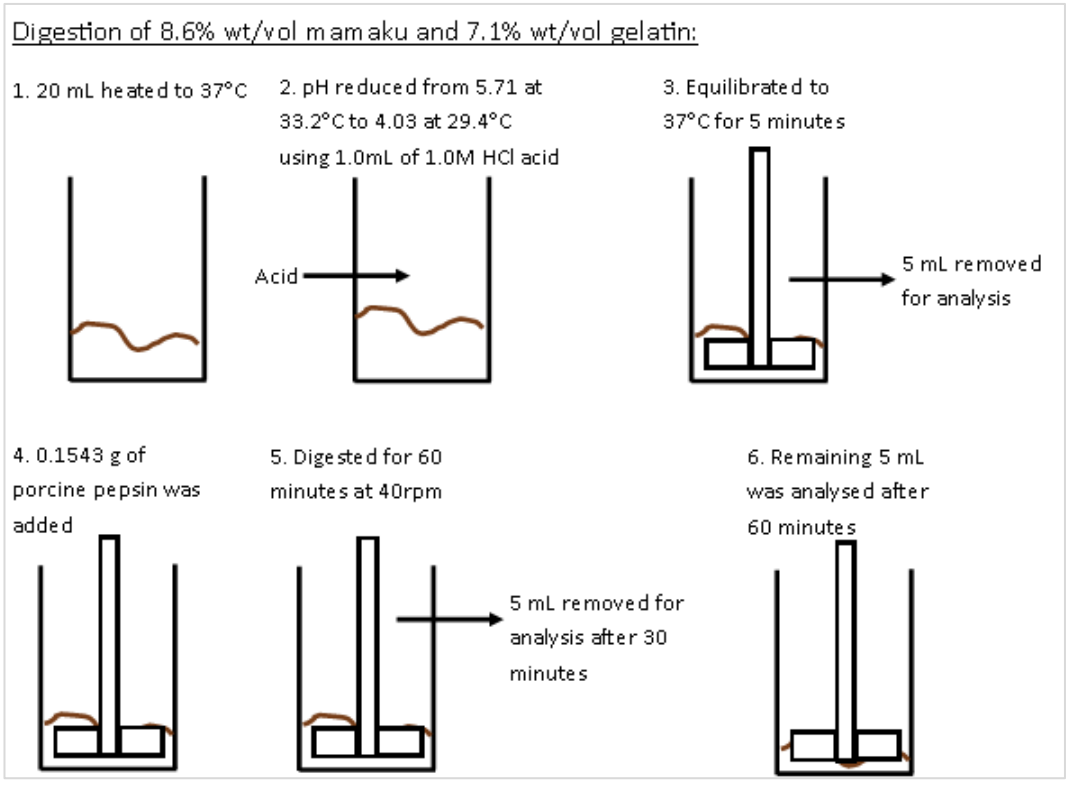

Figure 6.16: Flow diagram for the in-vitro digestion of the 8.6%wt/v mamaku + 7.1%wt/v gelatin solution

Samples were periodically taken at various intervals: including a comparison of mamaku with no gelatin present reduced to pH 4.0, mamaku + gelatin solution

before the addition of acid, mamaku + gelatin solution after the addition of acid (but no pepsin), after 30 minutes of digestion and after 60 minutes of digestion. The viscosity profiles are shown in Figure 6.17.

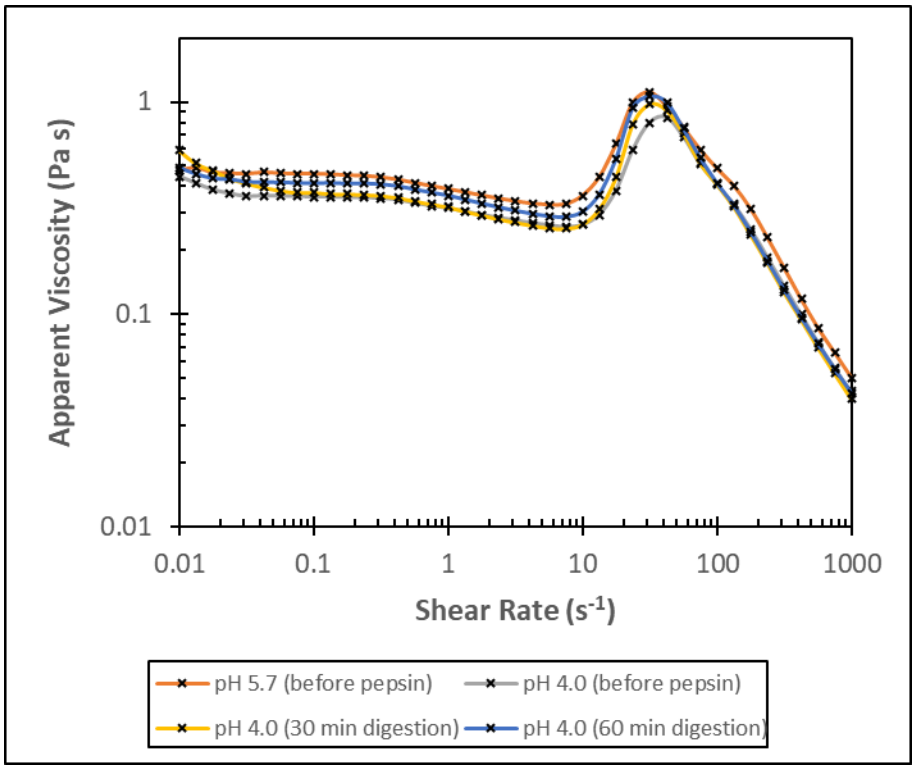

Figure 6.17: Viscosity profile at 37°C for the 8.6%wt/v mamaku + 7.1%wt/v gelatin solution, measured at pH 5.7 (before digestion with pepsin), at pH 4.0 (before digestion with pepsin), and after 30 and 60 minutes digestion

Figure 6.17 showed that the most suppression to shear-thickening properties occurs after acid addition (without pepsin). Digesting the solution for 30 minutes increased the shear-thickening peak viscosity with minimal change to the initial Newtonian viscosity. Digesting further, increased the initial Newtonian viscosity of the solution almost back to the same as the mamaku + gelatin solution before the acid was added. At this point, the peak viscosity had also recovered to the equivalent viscosity of mamaku + gelatin solution without acid present. Throughout all these changes, the shear rates at onset of thickening and peak viscosity did not change.

The thickening occurred at shear rates slightly higher than the target ~40s^{-1}; therefore, further testing was completed at a higher mamaku concentration to check if the onset of thickening would be shifted into the target range (1-10s^{-1}).

6.4.6 12.9%wt/v mamaku + 7.1%wt/v gelatin solution

15%wt/v mamaku solution was made up using freeze-dried mamaku and allowed to hydrate overnight. As explained in section 6.4.5 the rehydration of freeze-dried mamaku negatively affects the shear-thickening properties of mamaku and reduces the viscosity at all shear rates. Starting concentrations of mamaku (13.5%wt/v) + gelatin (7.5%wt/v) were used. After adding the acid, the concentration of mamaku was 12.9%wt/v and gelatin was 7.1%wt/v. A flow diagram for the methodology is shown in Figure 6.18.

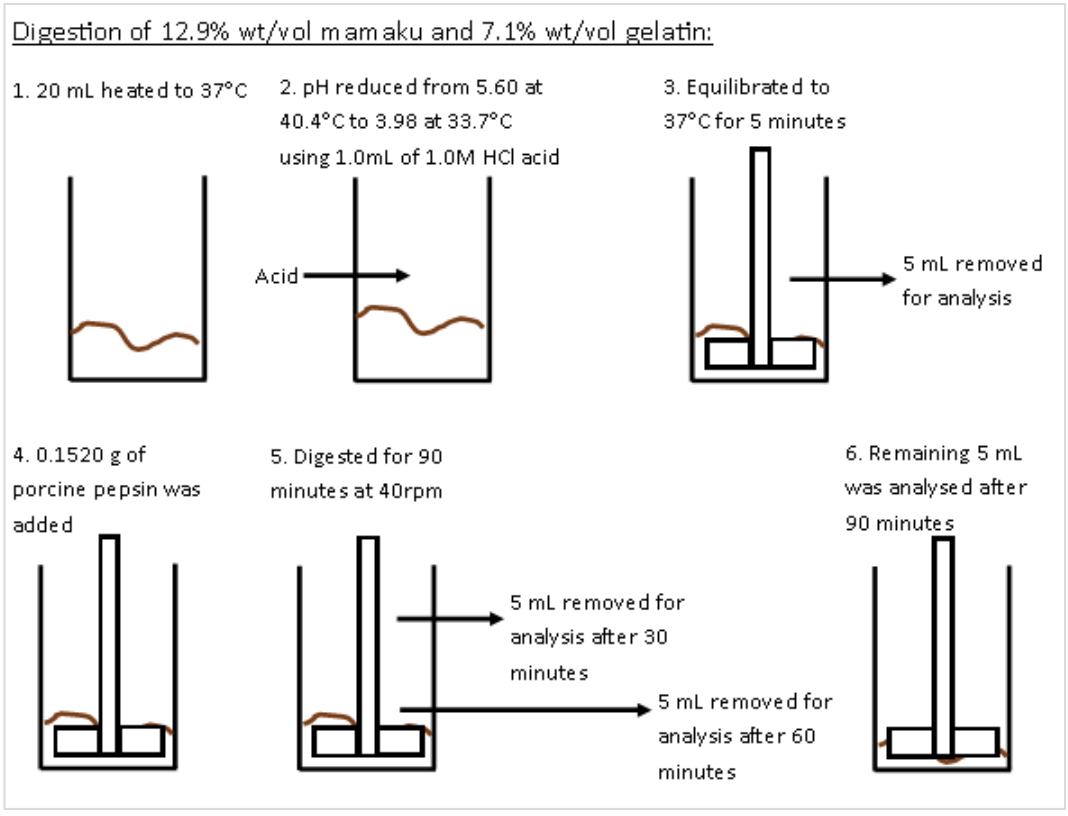

Figure 6.18: Flow diagram for the in-vitro digestion of the 12.9%wt/v mamaku + 7.1%wt/v gelatin solution

Samples were periodically taken at various intervals: including a comparison of 15%wt/v mamaku (with no gelatin) at pH 5.6, mamaku + gelatin solution before the addition of acid, mamaku + gelatin solution after the addition of acid (but no pepsin), after 30 minutes of digestion, after 60 minutes of digestion and after 90 minutes of digestion. The viscosity profiles are shown in Figure 6.19.

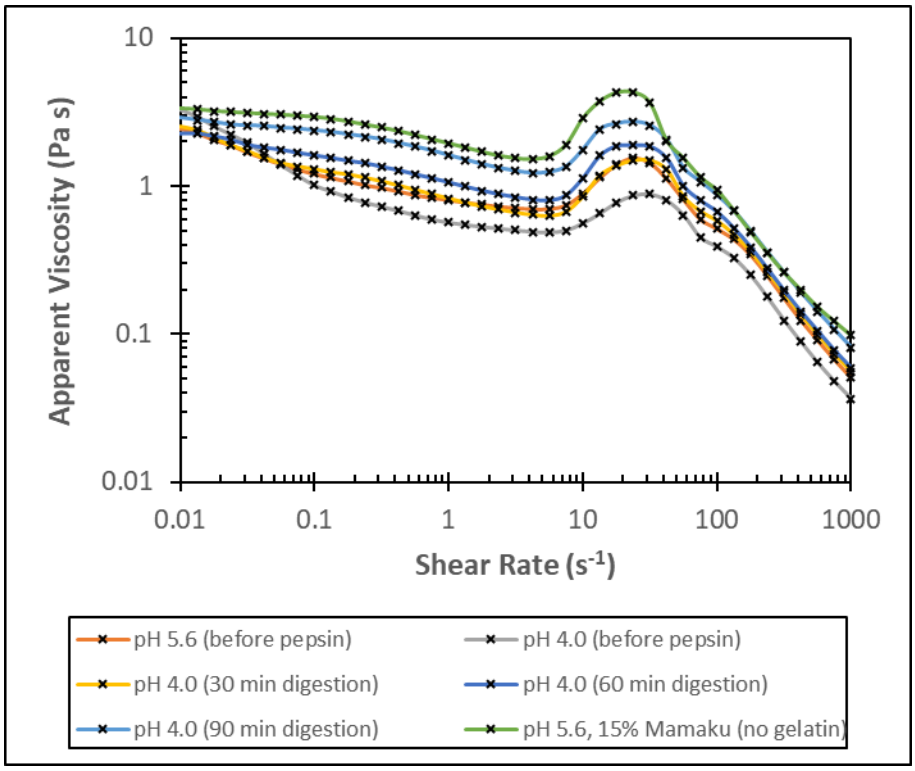

Figure 6.19: Viscosity profile at 37°C for the 12.9%wt/v mamaku + 7.1%wt/v gelatin solution, measured at pH 5.6 (before digestion with pepsin), at pH 4.0 (before digestion with pepsin), and after 30, 60 and 90 minutes digestion. A comparison of 15%wt/v mamaku (no gelatin) at pH 5.6 was included.

Figure 6.19 showed that the greatest reduction to shear-thickening behaviour occurred after the addition of acid (without pepsin). Digesting the solution for 30 minutes increased the shear-thickening peak viscosity and increased the initial Newtonian viscosity. This shifted the viscosity profile to one very similar to the native mamaku + gelatin solution. Interestingly, digesting further continued to shift the curve upwards showing further increases to the initial Newtonian viscosity and shear-thickening peak viscosity. After 90 minutes digestion the curve

had almost recovered shear-thickening properties to the same extent as the mamaku solution with no gelatin present.

In all cases, the shear rates at onset of thickening and peak viscosity did not change. The thickening occurred at shear rates just inside the target of 1-10s^{-1}. This leads to the belief that if the concentration of mamaku was high enough the mamaku truly can show shear-thickening ability at the shear rates of the stomach at acidic pH.

6.5 Discussion and conclusions

This work on in-vitro digestion of mamaku + gelatin firstly showed the importance of factoring in dilution in the body into the food product and within the food/drink matrix. This means that the encapsulated mamaku needs to be at a very high concentration to offset the dilution occurring.

The in-vitro results showed that the gelatin within the encapsulated mamaku can melt at body temperature and pepsin can break down the gelatin. This successfully allowed the mamaku to be released in the in-vitro stomach conditions and the shear thickening properties to be successfully recovered. However, the shear-thickening properties were only recovered when the concentration of mamaku was high enough to overcome the reduction in shear-thickening observed at the temperature of the stomach (>1.13%wt/v mamaku to show any shear-thickening behaviour). Additionally, a visible reduction in shear-thickening was observed at the acidic pH of the stomach (observed at pH 3.2 or lower for 4.5%wt/v mamaku).

The concentration study showed that digestion of the gelatin into peptides by the pepsin appears to resolve some of the thickening reduction issues, however only when the concentration of mamaku was 4.0%wt/v or above.

There are two potential mechanisms for the recovery of shear-thickening properties, as first proposed in section 6.3; firstly, above 4%wt/v mamaku concentration reducing the pH to 4.0 appears to show less reduction in the shear-

thickening peak viscosity than that observed at lower concentrations of mamaku. Secondly, if the reduction in shear-thickening was caused by an interaction between mamaku and gelatin at acidic pH, upon digesting the gelatin molecules, these become smaller. Therefore even if mamaku molecules are interacting with digested gelatin peptides, the mamaku molecules can still approach closer together, resulting in more interactions leading to a higher shear-thickening peak viscosity.

Overall, this analysis and the results obtained in the in-vitro trials, provide confidence that the concentration can be optimised to deliver the highest amount of shear-thickening at the correct shear rates. In particular, the concentration delivered to the stomach really needs to be at least 10%wt/v. However, the higher concentration work (>5%wt/v mamaku) was completed with rehydrated freeze-dried mamaku. This means that viscosity results obtained are likely to be lower than the viscosities obtained when using mamaku from the alternative processing method – concentrating then freezing until use. This is because freeze-drying and subsequent rehydration has been shown to reduce the functionality of mamaku, compared to the concentrating and freezing step (Chapter 4), resulting in lower viscosity at all shear rates and a lower peak viscosity at similar concentrations.

The results obtained in the in-vitro trials provide confidence that the concentration can be optimised to deliver the highest amount of shear-thickening at the correct shear rates. In particular, the concentration of mamaku delivered to the stomach really needs to be at least 10%wt/v of rehydrated freeze-dried mamaku.

7 Overall Conclusions

7.1 Extraction

The extraction process development aimed to scale up the benchtop process for extraction of mamaku from 200kg of Black Tree Fern fronds. A mass and energy balance was completed to provide some insight into the yield obtained, finding that 56%wt/wt yield was obtained based on the frozen solution and 2.8%wt/wt yield was obtained based on an estimate of the final weight of material if it was freeze-dried.

Analysis of the rheological properties of mamaku indicated that there was minimal degradation of the mamaku via freeze-thaw cycling. However, rehydrating freeze-dried mamaku, as opposed to concentrating and freezing, reduced the viscosity profile of the mamaku solutions including a reduction in the peak viscosity as well as the shifting of shear rate at onset of thickening to higher shear rates. Furthermore, the critical temperature for processing was found to be 63^{o}C, whereby the mamaku can be held at that temperature for 60 minutes without degradation. Heating the mamaku to 110^{o}C resulted in the complete loss of all shear-thickening properties.

Additionally, the rheological analysis indicated that increasing the concentration of mamaku can considerably reduce the shear rates at which the onset of thickening occurs, as well as the rates at which the peak viscosity is reached. The mamaku extracted for this project appeared to have slightly better shear-thickening properties compared to mamaku extracted in the past within the research group – without controlling the age of the fern or the season of extraction. Lastly, the findings showed that there was a reduction in shear-thickening viscosity and shear rates at onset of thickening and peak viscosity, at the pH and temperature conditions of the stomach.

7.2 Encapsulation

The project aimed to encapsulate mamaku to allow mamaku to be swallowed safely, targeting release in the stomach in a hydrated form, and without incorporating calories if used as an ingredient in functional foods aiming to target weight loss.

Initial experiments showed that gelatin was a promising protein to use as an encapsulating agent, by entrapping the mamaku when gelling, also being potentially digested in the stomach by pepsin and melting at around body temperature (dependent on the gelatin type and concentration), therefore aiding the release of the mamaku in the stomach. The gelatin experiments showed that 7.5%wt/v gelatin was able to entrap successfully 2.25%wt/v mamaku within its gelled structure. Additionally, this concentration of gelatin showed a melting point ~31^{o}C, low enough to promote melting in the stomach but likely to be high enough to be safe to consume while in the mouth.

A number of different encapsulation techniques were trialled, showing various degrees of success. The most promising technique was the fluid gel system. The nozzle techniques proved not be suitable for the properties of mamaku. The emulsion templating system showed challenges around removing the oil. The micro-injector based system produced beads likely to be too large for practical use in a food product. The biggest inadequacy of the results obtained was that all the work was done with a starting mamaku concentration of 4.5%wt/v, which proved to be too low in the in-vitro testing. Additionally, the gelatin gel appeared to be unstable when placed in an aqueous environment, so further stabilisation would be required.

Overall, abundant work on the encapsulation technology is needed to get a commercially viable method producing a stable final ingredient, which can be used in food products containing an aqueous phase.

7.3 In-vitro digestion

This work highlighted the changes in mamaku's shear-thickening behaviour when exposed to both temperature and pH (37^{o}C and pH 3.0-4.0) with the digestive enzymes. The in-vitro digestion of mamaku + gelatin showed the importance of factoring in the dilution effects occurring in the stomach and also when formulating the food/drink matrix of the final product. This means that the encapsulated mamaku needs to be at a very high concentration to offset the dilution. The in-vitro results showed that the gelatin within the encapsulated mamaku can melt at body temperature and pepsin can break down the gelatin. This successfully allowed the mamaku to be released in the in-vitro stomach conditions and the shear thickening properties to be successfully recovered. However, mamaku's shear-thickening properties were only observed when the concentration of mamaku was high enough to overcome the suppression from the acidity and temperature of the stomach, above 2.2%wt/v mamaku concentration. The individual component study showed there are two reasons why a suppression in shear thickening is observed upon addition of acid. First, a reduction in the pH reduces the shear thickening effect of mamaku due to reduced charges on the mamaku molecules. Secondly, this reduction in the pH also creates a possible interaction between mamaku and gelatin due to the reversal of charges on the gelatin molecules.

The in-vitro digestion study at different mamaku + gelatin concentrations showed that increasing the mamaku concentration above 4%wt/v, increased the shear-thickening peak viscosity observed after digestion (as opposed to the decrease overserved at mamaku concentration of <4%wt/v).

The results obtained in the in-vitro trials provide confidence that the concentration can be optimised to deliver the highest amount of shear-thickening at the correct shear rates. In particular, the concentration of mamaku delivered to the stomach really needs to be at least 10%wt/v of rehydrated freeze-dried mamaku, to obtain thickening at the desired shear rates 1-10s^{-1}.

Overall, further research would enable a conclusion as to the viability of encapsulating Mamaku using gelatin, as well as optimizing the encapsulation process based on fluid gel formation, for use in a functional food product providing satiety effect to the consumer to aid with weight loss.

8 Recommendations

A number of recommendations can be made from the results of this work, including the following:

Extraction

1. More research on the extraction process is needed to optimise the extraction including – the quantity of water required for extraction, whether the age and season the fronds were harvested in affects the yield and the shear-thickening functionality obtained.
2. More research is needed from an agriculture point of view, to identify the best soil types or other parameters, which affect the growth of the black fern tree to optimise the quantity of mamaku within the fronds.
3. While extracting mamaku use a concentration + freezing process (rather than rehydrating freeze-dried mamaku at the concentration needed) to get the highest shear-thickening functionality possible.

Encapsulation

1. Establish whether 7.5%wt/v gelatin is high enough concentration to entrap the higher concentrations of mamaku within the gelled network.
2. Try dialysis with dilute mamaku to remove thickening effect before concentrating it to see if this improves the encapsulation process (ability to measure, pour and/or extrude into droplets of the concentrated solution) and stability issues of the encapsulated product.
3. Investigate whether the simpler concept of consuming dialysed mamaku in a food or drink, followed by a shot of electrolyte to regain the thickening properties, would be safe for consumers, or would the residual salt in the mouth post a health risk through potential choking.
4. Repeat encapsulation experiments with higher concentrations of mamaku before ruling out potential techniques.

5. Investigate whether a dropper system would be faster at producing droplets than the micro injector.
6. Identify whether the larger 'bubble tea' sized beads would post a health risk to consumers (e.g. do people swallow them or chew them and if they are chewed will the thickening effect be re-gained before they reach the stomach).
7. Investigate whether the mamaku + gelatin solution could be eaten as a jelly without regaining the thickening effect before the mamaku reaches the stomach, resulting in no need for stability in an aqueous environment.
8. Investigate the porosity of gelatin further to establish how much mamaku is leaching out and whether this poses a safety issue in the final food product. Also establish ways to solve this issue whether by further stabilisation of the encapsulated product or through thickening of the food matrix (e.g. with polysaccharides) to reduce the free water which can interact with the gelatin.
9. Identify if a different encapsulating agent than gelatin would be more optimal for the situation, for example proteins such as pea protein, casein or whey protein isolate which, after heat induced denaturation, can form networks through calcium induced crosslinking.
10. Identify whether there would be more value in placing the encapsulated mamaku in a jelly/gummy pill for ingestion, followed by a glass of water to overcome the stability issues in an aqueous environment.

In-vitro digestion

1. In-vitro experiments with 10-15%wt/v mamaku obtained via concentration (rather than freeze-drying) need to be carried out to establish the concentration needed to show the desired rheology in the stomach.
2. Establish whether there is indeed an interaction between mamaku and gelatin at acidic pH or if the reduction in shear-thickening is solely because of the acid present and conduct trials to establish whether there is an interaction between mamaku and pepsin, by investigating the components further individually during in-vitro digestion trials.

3. Establish the effect of pH at 37^{o}C for 10-15%wt/v mamaku, on the shear-thickening properties of these more concentrated solutions, to understand if it remains a limitation to the recovery of shear-thickening properties in the stomach.
4. Conduct trials to establish if a buffering agent does need to be added to offset the acidity in the stomach, or alternatively, if the food matrix itself will provide enough buffering capacity for the high acid content. If so, establish which buffering agent and the quantity to add to the mamaku + gelatin solution.

9 References

Afzal, S., Khan, S., Ranjha, N., Jalil, A., Riaz, A., & Haider, M. et al. (2018). The Structural, Crystallinity and Thermal Properties of pH responsive Interpenetrating Gelatin/Sodium Alginate Based Polymeric Composites for the Controlled Delivery of Cetirizine HCl. *The Turkish Journal Of Pharmaceutical Sciences*, 15(1), 63-76. https://doi.org/10.4274/tjps.64326

BeMiller, J., & Kumari, G. (1972). beta-elimination in uronic acids: evidence for an ElcB mechanism. *Carbohydrate Research*, 25(2), 419-428. https://doi.org/0.1016/s0008-6215(00)81653-5

Bengtsson, H., Wikberg, J., & Tornberg, E. (2011). Physicochemical characterization of fruit and vegetable fiber suspensions. II: effect of variations in heat treatment. *Journal Of Texture Studies*, 42(4), 281-290. https://doi.org/10.1111/j.1745-4603.2010.00276.x

Bleiel, S., Kent, R., & Brodkorb, A. (2017). Encapsulation Efficiency and Capacity of Bioactive Delivery Systems. In M. Augustin & L. Sanguansri (Eds.), *Engineering Foods for Bioactives Stability and Delivery* (1st ed., pp. 171-198). New York: Springer New York. Retrieved from https://ebookcentral.proquest.com/lib/massey/reader.action?docID=4756752

Brooker, S., Cambie, R., & Cooper, R. (1987). *New Zealand medicinal plants* (2nd ed., p. 72). Auckland, New Zealand: Reed Publishing (NZ) Ltd.

Cayre, O., Noble, P., & Paunov, V. (2004). Fabrication of novel colloidosome microcapsules with gelled aqueous cores. *Journal Of Materials Chemistry*, 14(22), 3351-3355. https://doi.org/10.1039/b411359d

Femenia, A., García-Pascual, P., Simal, S., & Rosselló, C. (2003). Effects of heat treatment and dehydration on bioactive polysaccharide acemannan and cell wall polymers from Aloe barbadensis Miller. *Carbohydrate Polymers*, 51(4), 397-405. https://doi.org/10.1016/s0144-8617(02)00209-6

Femenia, A., Selvendran, R., Ring, S., & Robertson, J. (1999). Effects of Heat Treatment and Dehydration on Properties of Cauliflower Fiber. *Journal Of Agricultural And Food Chemistry*, 47(2), 728-732. https://doi.org/10.1021/jf980462k

Foster, T. (2008). *Plant Heritage New Zealand: Te Whakapapa O Nga Rakau Interpreting the Special Features of Native Plants*. North Shore, New Zealand: Raupo.

García-Segovia, P., Andrés-Bello, A., & Martínez-Monzó, J. (2011). Rehydration of air-dried Shiitake mushroom (Lentinus edodes) caps: Comparison of conventional and vacuum water immersion processes. *LWT - Food*

Science And Technology, 44(2), 480-488. https://doi.org/10.1016/j.lwt.2010.08.010

Gelatin Manufacturers Institute of America. (2012). *Gelatin Handbook*. New York: Gelatin Manufacturers Institute of America, 12.

Georgopoulou, A., Papadogiannis, F., Batsali, A., Marakis, J., Alpantaki, K., & Eliopoulos, A. et al. (2018). Chitosan/gelatin scaffolds support bone regeneration. *Journal Of Materials Science: Materials In Medicine*, 29(5). https://doi.org/10.1007/s10856-018-6064-2

Gladkowska-Balewicz, I., Norton, I., & Hamilton, I. (2014). Effect of process conditions, and component concentrations on the viscosity of κ-carrageenan and pregelatinised cross-linked waxy maize starch mixed fluid gels. *Food Hydrocolloids*, 42, 355-361. https://doi.org/10.1016/j.foodhyd.2014.03.003

Goff, H. (1995). The use of thermal analysis in the development of a better understanding of frozen food stability. *Pure And Applied Chemistry*, 67(11), 1801-1808. https://doi.org/10.1351/pac199567111801

Goh, K., Matia-Merino, L., Hall, C., Moughan, P., & Singh, H. (2007). Complex Rheological Properties of a Water-Soluble Extract from the Fronds of the Black Tree Fern,Cyathea medullaris. *Biomacromolecules*, 8(11), 3414-3421. https://doi.org/10.1021/bm7005328

Goh, K., Matia-Merino, L., Pinder, D., Saavedra, C., & Singh, H. (2011). Molecular characteristics of a novel water-soluble polysaccharide from the New Zealand black tree fern (Cyathea medullaris). *Food Hydrocolloids*, 25(3), 286-292. https://doi.org/10.1016/j.foodhyd.2010.06.005

Jafari, S. (2017). An overview of nanoencapsulation techniques and their classification. In S. Jafari (Eds.), *Nanoencapsulation Technologies for the Food and Nutraceutical Industries* (1st ed., pp. 1-27). London: Academic Press. Retrieved from https://ebookcentral.proquest.com/lib/massey/reader.action?docID=4838970

Kocherbitov, V. (2016). The nature of nonfreezing water in carbohydrate polymers. *Carbohydrate Polymers*, 150, 353-358. https://doi.org/10.1016/j.carbpol.2016.04.119

Krokida, M., & Marinos-Kouris, D. (2003). Rehydration kinetics of dehydrated products. *Journal Of Food Engineering*, 57(1), 1-7. https://doi.org/10.1016/s0260-8774(02)00214-5

Lai, Y., Cheng, P., Yang, C., & Yen, S. (2018). Electrolytic deposition of hydroxyapatite/calcium phosphate-heparin/gelatin-heparin tri-layer composites on NiTi alloy to enhance drug loading and prolong releasing for biomedical applications. *Thin Solid Films*, 649, 192-201. https://doi.org/10.1016/j.tsf.2018.01.051

Lairon, D. (2009). Digestion and Absorption of Lipids. In D. McClements & E. Decker (Eds.), *Designing Functional Foods - Measuring and controlling food structure breakdown and nutrient absorption* (1st ed., pp. 66-89). Cambridge: Woodhead Publishing.

Lakkis, J. (2007). Introduction. In J. Lakkis (Ed.), *Encapsulation and Controlled Release Technologies in Food Systems* (1st ed., pp. 1-12). Oxford: Blackwell Publishing.

Lele, A., & Mashelkar, R. (1998). Energetically crosslinked transient network (ECTN) model: implications in transient shear and elongation flows. *Journal Of Non-Newtonian Fluid Mechanics*, 75(1), 99-115. https://doi.org/10.1016/s0377-0257(97)00070-0

Lentle, R., Janssen, P., Asvarujanon, P., Chambers, P., Stafford, K., & Hemar, Y. (2007). High definition mapping of circular and longitudinal motility in the terminal ileum of the brushtail possum Trichosurus vulpecula with watery and viscous perfusates. *Journal Of Comparative Physiology B*, 177(5), 543-556. https://doi.org/10.1007/s00360-007-0153-8

Lentle, R., Janssen, P., Goh, K., Chambers, P., & Hulls, C. (2010). Quantification of the Effects of the Volume and Viscosity of Gastric Contents on Antral and Fundic Activity in the Rat Stomach Maintained Ex Vivo. *Digestive Diseases And Sciences*, 55(12), 3349-3360. https://doi.org/10.1007/s10620-010-1164-y

Matia-Merino, L., Goh, K., & Singh, H. (2012). A natural shear-thickening water-soluble polymer from the fronds of the black tree fern, Cyathea medullaris: Influence of salt, pH and temperature. *Carbohydrate Polymers*, 87(1), 131-138. https://doi.org/10.1016/j.carbpol.2011.07.027

McClements, D. (2012). Requirements for food ingredient and nutraceutical delivery systems. In D. McClements & N. Garti (Eds.), *Encapsulation Technologies and Delivery Systems for Food Ingredients and Nutraceuticals* (1st ed., pp. 3-18). Philadelphia: Woodhead Publishing. https://doi.org/10.1533/9780857095909.1.3

McClements, D. (2014). *Nanoparticle- and microparticle-based delivery systems* (1st ed.). Boca Raton: CRC Press.

McClements, D., & Decker, E. (2009). Controlling lipid bioavailability using emulsion-based delivery systems. In D. McClements & E. Decker (Eds.), *Designing Functional Foods - Measuring and controlling food structure breakdown and nutrient absorption* (1st ed., pp. 481-498). Cambridge: Woodhead Publishing.

Minekus, M., Alminger, M., Alvito, P., Ballance, S., Bohn, T., & Bourlieu, C. et al. (2014). A standardised static in-vitro digestion method suitable for food – an international consensus. *Food & Function*, 5(6), 1113-1124. https://doi.org/10.1039/c3fo60702j

Mirsky, A., & Pauling, L. (1936). On the structure of native, denatured, and coagulated proteins. Proceedings of the National Academy of Sciences of the United Statesof America, 22, 439–447.

Mohammadigoushki, H., & Muller, S. (2017). Inertio-elastic instability in Taylor-Couette flow of a model wormlike micellar system. *Journal Of Rheology*, 61(4), 683-696. https://doi.org/10.1122/1.4983843

Moughan, P. (2009). Digestion and Absorption of Proteins and Peptides. In D. McClements & E. Decker (Eds.), *Designing Functional Foods - Measuring and controlling food structure breakdown and nutrient absorption* (1st ed., pp. 148-167). Cambridge: Woodhead Publishing.

Osorio, F., Bilbao, E., Bustos, R., & Alvarez, F. (2007). Effects of Concentration, Bloom Degree, and pH on Gelatin Melting and Gelling Temperatures Using Small Amplitude Oscillatory Rheology. *International Journal Of Food Properties*, 10(4), 841-851. https://doi.org/10.1080/10942910601128895

Oxley, J. (2012). Coextrusion for food ingredients and nutraceutical encapsulation: principles and technology. In D. McClements & N. Garti (Eds.), *Encapsulation Technologies and Delivery Systems for Food Ingredients and Nutraceuticals* (1st ed., pp. 131-150). Philadelphia: Woodhead Publishing. https://doi.org/10.1533/9780857095909.2.131

Pang, Z., Deeth, H., Sopade, P., Sharma, R., & Bansal, N. (2014). Rheology, texture and microstructure of gelatin gels with and without milk proteins. *Food Hydrocolloids*, 35, 484-493.

Roos, Y., & Livney, Y. (2017). Microencapsulation Technologies. In M. Augustin & L. Sanguansri (Eds.), *Engineering Foods for Bioactives Stability and Delivery* (1st ed., pp. 119-142). New York: Springer New York. Retrieved from https://ebookcentral.proquest.com/lib/massey/reader.action?docID=4756752

Salerno, A., Verdolotti, L., Raucci, M., Saurina, J., Domingo, C., & Lamanna, R. et al. (2018). Hybrid gelatin-based porous materials with a tunable multiscale morphology for tissue engineering and drug delivery. *European Polymer Journal*, 99, 230-239. https://doi.org/10.1016/j.eurpolymj.2017.12.024

Seiffert, S. (2011). Functional Microgels Tailored by Droplet-Based Microfluidics. *Macromolecular Rapid Communications*, 32(20), 1600-1609. https://doi.org/10.1002/marc.201100342

Shahrezaie, M., Moshiri, A., Shekarchi, B., Oryan, A., Maffulli, N., & Parvizi, J. (2017). Effectiveness of tissue engineered three-dimensional bioactive graft on bone healing and regeneration: an in vivo study with significant clinical value. *Journal Of Tissue Engineering And Regenerative Medicine*, 12(4), 936-960. https://doi.org/10.1002/term.2510

Tepsongkroh, B., Harnsilawat, T., Maisuthisakul, P., & Chantrapornchai, W. (2015). Influence of Polyglycerol Polyricinoleate and Biopolymers on Physical Properties and Encapsulation Efficiency of Water-in-Oil-in-Water Emulsions Containing Mango Seed Kernel Extract. J*ournal Of Dispersion Science And Technology*, 36(8), 1126-1133. https://doi.org/10.1080/01932691.2014.956116

Thies, C. (2001). Microencapsulation: What it is and purpose. In P. Vilstrup (Ed.), *Microencapsulation of Food Ingredients* (1st ed., pp. 1-26). Surrey: Leatherhead Publishing.

Thies, C. (2012). Microencapsulation methods based on biopolymer phase separation and gelation phenomena in aqueous media. In D. McClements & N. Garti (Eds.), *Encapsulation Technologies and Delivery Systems for Food Ingredients and Nutraceuticals* (1st ed., pp. 177-207). Philadelphia: Woodhead Publishing. https://doi.org/10.1533/9780857095909.2.177

Wang, S., Guan, S., Zhu, Z., Li, W., Liu, T., & Ma, X. (2017). Hyaluronic acid doped-poly(3,4-ethylenedioxythiophene)/chitosan/gelatin (PEDOT-HA/Cs/Gel) porous conductive scaffold for nerve regeneration. *Materials Science And Engineering: C-Materials For Biological Applications*, 71, 308-316. https://doi.org/10.1016/j.msec.2016.10.029

Wang, Y., Bamdad, F., Chen, L., & Song, Y. (2012). Hydrogel particles and other novel protein-based methods for food ingredient and nutraceutical delivery systems. In D. McClements & N. Garti (Eds.), *Encapsulation Technologies and Delivery Systems for Food Ingredients and Nutraceuticals* (1st ed., pp. 412–450). Philadelphia: Woodhead Publishing. https://doi.org/10.1533/9780857095909.3.412

Wee, M. (2015). *Physico-chemical characterisation and functionality of the polysaccharide extracted from the New Zealand black tree fern, Cyathea medullaris (mamaku)* (Doctoral dissertation, Massey University, Palmerston North, New Zealand). Retrieved from https://muir.massey.ac.nz/handle/10179/6941

Wee, M., Lentle, R., Goh, K., & Matia-Merino, L. (2017). The first of the viscoceuticals? A shear-thickening gum induces gastric satiety in rats. *Food & Function*, 8(1), 96-102. https://doi.org/10.1039/c6fo01464j

Wee, M., Matia-Merino, L., & Goh, K. (2015). The cation-controlled and hydrogen bond-mediated shear-thickening behaviour of a tree-fern isolated polysaccharide. *Carbohydrate Polymers*, 130, 57-68. https://doi.org/10.1016/j.carbpol.2015.03.086

Wee, M., Matia-Merino, L., & Goh, K. (2015). Time- and shear history-dependence of the rheological properties of a water-soluble extract from the fronds of the black tree fern, Cyathea medullaris. *Journal Of Rheology*, 59(2), 365-376. https://doi.org/10.1122/1.4905006

Wee, M., Matia-Merino, L., Carnachan, S., Sims, I., & Goh, K. (2014). Structure of a shear-thickening polysaccharide extracted from the New Zealand black tree fern, Cyathea medullaris. *International Journal Of Biological Macromolecules*, 70, 86-91. https://doi.org/10.1016/j.ijbiomac.2014.06.032

Wulansari, R., Mitchell, J., Blanshard, J., & Paterson, J. (1998). Why are gelatin solutions Newtonian?. *Food Hydrocolloids*, 12(2), 245-249. https://doi.org/10.1016/s0268-005x(98)00038-1

Zhang, J., Li, J., Kawazoe, N., & Chen, G. (2017). Composite scaffolds of gelatin and gold nanoparticles with tunable size and shape for photothermal cancer therapy. *Journal Of Materials Chemistry B*, 5(2), 245-253. https://doi.org/10.1039/c6tb02872a

Zuidam, N., & Shimoni, E. (2010). Overview of Microencapsulates for Use in Food Products or Processes and Methods to Make Them. In N. Zuidam & V. Nedovic (Eds.), *Encapsulation Technologies for Active Food Ingredients and Food Processing* (1st ed., pp. 3-30). New York: Springer-Verlag New York.

10 Appendix

Table of contents

Appendix A Microbiology report 1

Date/time received	28/08/2017
Date/time tested	28/08/2017
Tested by	Haoran Wang
Testing lab	Massey IFNHH/SEAT Micro suite
Sample type	Mamaku extract
Methods	Non selective pour plate for APC

Sample number	Sample name	APC (30°C)
1	Mamaku extract (Frozen for weekend)	4.0×10^{4}CFU/ml
2	Mamaku extract (Chilled for weekend)	4.5×10^{4}CFU/ml

Appendix B Microbiology report 2

Date/time received	15/09/2017
Date/time tested	15/09/2017
Tested by	Haoran Wang
Testing lab	Massey IFNHH/SEAT Micro suite
Sample type	Mamaku extract
Methods	Non selective pour plate for APC

Sample number	Sample name	APC (30°C)
1	Mamaku extract	2.1×10^{4}CFU/ml

Appendix C Microbiology report 3

Date/time received	19/10/2017
Date/time tested	19/10/2017
Tested by	Haoran Wang
Testing lab	Massey IFNHH/SEAT Micro suite
Sample type	Mamaku extract
Methods	Non selective pour plate for APC

Sample number	Sample name	APC (30°C)
1	Mamaku extract	6.0×10^{1}CFU/ml

Appendix D Nutrition report

MASSEY UNIVERSITY
COLLEGE OF HEALTH
TE KURA HAUORA TANGATA

Nutrition Laboratory
Riddet Innovation
T: +64 6 3505869
Email: F.S.Jackson@massey.ac.nz
http://nutritionlab.massey.ac.nz

TO:	Lara/Rebecca Tresidder	AT:	MIFST
SUBJECT:	Analysis Report	DATE:	15/11/17
TRIAL:	TN17-869	SAMPLES RECEIVED:	13/10/17

Number of pages in this report: 2

TN17-869 Results are on an as received basis

NutLab ID	Sample Name	Moisture %	Ash %	Protein %	Fat %	Carb %	Starch %	TDF %	Sugars g/100g
TN17-869-01	Concentrated	92.5	1.45	0.14	0.05	5.25	0.16	0.58	4.5
TN17-869-02	Batch 2 (gum) Mamaku	95.1	1.09	0.08	0.03	3.34	0.06	0.38	2.7

Methodology

Ash : Furnace 550°C AOAC 942.05 (Feed, meat)
Crude protein : AOAC 968.06 (Dumas method). N-P = 6.25
Fat : (Mojonnier) Acid, (Baked, extruded products) AOAC 922.06
Total Dietary fibre : Megazyme, AOAC 991.43
Avail Carbohydrate (Carb) : By difference
Starch : α-amylase Megazyme kit, AOAC 996.11
Sugars : Phenol sulphuric, Sub-contracted
Moisture : Vacuum oven, AOAC 990.19, 990.21

Samples will be discarded one month from date of this report unless otherwise requested by client.

Fliss Jackson
Manager, Nutrition Laboratory
Riddet Innovation
Massey Institute of Food Science and Technology
Massey University, Private Bag 11222
Palmerston North 4442, New Zealand
DDI 06 350 5869
Fax 06 350 5772
Email. F.S.Jackson@massey.ac.nz

Appendix E Equations used to calculate heat capacity of the mamaku extract

Heat capacity of the mamaku extract was estimated based on the nutritional content of the final mamaku extract.

The equation is below:

$$C_p = C_p(protein\ content) + C_p(fat\ contet) + C_p(carbohydrate\ content) + C_p(ash\ content) + C_p(water\ content)$$

Where:

$$C_p\ (protein\ content) = (2008.2 + 1208.9 * 10^{-3} * (Temperature) - 1312.9 * 10^{-6} * (Temperature^2)) * Protein\ content$$

$$C_p\ (fat\ content) = \left(1984.2 + 1473.3 * 10^{-3} * (Temperature) - 4800.8 * 10^{-6} * (Temperature^2)\right) * Fat\ content$$

$$C_p\ (carbohydrate\ content) = \left(1548.8 + 1962.5 * 10^{-3} * (Temperautre) - 5939.9 * 10^{-6} * (Temperature^2)\right) * Carbyhydrate\ content$$

$$C_p\ (ash\ content) = (1092.6 + 1889.6 * 10^{-3} * (Temperature) - 3681.7 * 10^{-6} * (Temperature^2)) * Ash\ content$$

$$C_p\ (water\ content) = \left(4176.2 - 9086.2 * 10^{-5} * (Temperature) + 5473.1 * 10^{-6} * (Temperature^2)\right) * Water\ content$$

Appendix F Calculations involved in the mass and energy balance

Enthalpy was calculated as follows:

$$Enthalpy\ \left(\frac{kJ}{kg}\right) = heat\ capacity \left(\frac{kJ}{kg * \ ^oC}\right) * temperature\ (\ ^oC)$$

Cooling energy required was calculated as follows:

$$Cooling\ energy\ \left(\frac{kJ}{batch}\right) = mass\ flow\ rate\ \left(\frac{kg}{batch}\right) * (initial\ temperature - final\ temperature)\ (\ ^oC) * specific\ heat\ \left(\frac{kJ}{kg * \ ^oC}\right)$$

Quantity of steam was calculated as follows:

$$steam\ \left(\frac{kg}{batch}\right) = \frac{heating\ energy\ required\ \left(\frac{kJ}{batch}\right)}{enthalpy\ of\ steam\ \left(\frac{kJ}{kg}\right)}$$

Enthalpy of steam was calculated as follows:

$$enthaply\ steam\ \left(\frac{kJ}{kg}\right) = vaporisation\ enthalpy\ \left(\frac{kJ}{kg}\right) + specific\ heat\ of\ water\ at\ 100^oC\ \left(\frac{kJ}{kg * \ ^oC}\right)$$

Heating energy for holding periods was calculated as follows:

$$Heating\ energy\ for\ holding\ periods\left(\frac{kJ}{batch}\right) = \%\ heat\ lost\ from\frac{mass}{volume} * \ mass\ flow\ rate\text{^}\ \left(\frac{kg}{batch}\right) * (temperature\ difference\ between\ solution\ and\ air)\ (\ ^oC) * specific\ heat\ of\ air\ \left(\frac{kJ}{kg *\ ^oC}\right) * number\ of\ minutes\ being\ held\ for\ (minutes)$$

^assuming the mass flow rate is actually in kg/batch minutes

Cooling energy for cooling and freezing was calculated as follows:

$$Cooling\ energy\ \left(\frac{kJ}{batch}\right) = mass\ flow\ rate\left(\frac{kg}{batch}\right) * specific\ heat\ \left(\frac{kJ}{kg *\ ^oC}\right) * (temperature\ difference\ between\ solution\ and\ 0^oC\ )\ (\ ^oC) + mass\ flow\ rate\ \ \left(\frac{kg}{batch}\right) * specific\ heat\ \left(\frac{kJ}{kg *\ ^oC}\right) * (temperature\ difference\ between\ 0^oC\ and\ the\ freezer\ temperature)\ (\ ^oC) + latent\ heat\ of\ fusion\ \left(\frac{kJ}{kg}\right) * mass\ flow\ rate\ \left(\frac{kg}{batch}\right)$$

Appendix G Frond weights before and after mulching, including the amount of water added

Table G.1: Raw weights of fronds before and after mulching

Before (kg)	After (kg)
5.87	12.01
7.03	11.37
8.94	10.05
11.17	13.91
23.76	10.92
16.31	7.96
19.71	9.98
22.91	11.51
13.95	9.71
	10.51
	10.32
	11.13
	12.23
	11.83
	11.31
	6.82

Table G.2: Calculation of total weight after mulching, dry weight of fronds and water added during mulching

Dry weight of fronds (kg)	Total weight (kg)	Water added (kg)
129.65	171.57	41.92

Appendix H Weights before and after extraction 1, including yield data of mamaku extract and pulp

Table H.1: Data collected on the weights before and after hot water extraction for extraction 1 batch 1

Component	Weight before extraction (kg)			Weight after extraction(kg)	Dry Weight of Pulp (kg)
	Mulched Fronds	Water	Total		
Bucket Weights	12.21	18.08		19.49	7.77
	11.52	16.60		16.60	7.73
	10.63	19.97		18.39	7.50
	9.71	19.84		16.69	7.63
	13.85	16.04		16.23	7.81
	11.32	15.78		18.53	8.01
	11.97	17.77		16.12	7.58
		17.76		20.30	11.78
		18.27		17.59	
				3.83	
Batch Total	**81.21**	**160.11**	**241.32**	**163.77**	**65.81**
Yield of pulp			0.8104		
Yield (wet)			0.6786		
Yield (dry)			2.0166		

Table H.2: Data collected on the weights before and after hot water extraction for extraction 1 batch 2

Component	Weight before extraction (kg)			Weight after extraction(kg)	Dry Weight of Pulp (kg)
	Mulched Fronds	Water	Total		
Bucket Weights	6.29	6.19		17.96	7.81
	7.29	7.13		15.36	7.58
	5.96	10.60		18.09	7.41
	5.44	11.30		19.00	7.29
	5.07	11.19		18.91	7.95
	5.79	8.20		16.85	8.21
	5.44	11.17		18.95	7.95
	8.41	7.10		16.76	7.45
	5.71	7.98		17.32	7.77
	4.67	8.31		19.22	7.77
	6.82	15.17			7.94
	7.78	15.30			3.30
	7.68	16.62			
	7.68	9.80			
		10.14			
		11.12			
		12.57			
Batch Total	**90.03**	**179.89**	**269.92**	**178.42**	**88.43**
Yield of pulp			0.9822		
Yield (wet)			0.6610		
Yield (dry)			1.9818		

Table H.3: Summary of data obtained from the weights before and after hot water extraction for extraction 1

Component	Weight before extraction (kg)			Weight after extraction(kg)	Dry Weight of Pulp (kg)
	Mulched Fronds	Water	Total		
Batch Total	171.24	340	511.24	342.19	154.24
Yield of pulp				0.9007	
Yield (wet)				0.6693	
Yield (dry)				1.9983	

Note: Temp set at 55^{o}C, allowed to reach temperature then left for 15 minutes

Appendix I Weights before and after extraction 2, including yield data of mamaku extract and pulp

Table I.1: Data collected on the weights before and after hot water extraction for extraction 2 batch 3 – extraction of pulp from batch 1

Component	Weight before extraction (kg)			Weight after extraction(kg)
	Mulched Fronds	Water	Total	
Bucket Weights	7.77	13.83		19.99
	7.73	11.55		20.36
	7.5	11.73		20.93
	7.63	11.91		17.21
	7.81	11.14		18.64
	8.01	11.05		18.16
	7.58	11.14		17.09
	11.78	6.51		
		17.04		
		15.58		
		12.32		
Batch Total	**65.81**	**133.8**	**199.61**	**132.38**
Yield (wet)				0.6632
Yield (dry)				2.0115

Table I.2: Data collected on the weights before and after hot water extraction for extraction 2 batch 4 – extraction of pump from batch 2

Component	Weight before extraction (kg)			Weight after extraction(kg)
	Mulched Fronds	Water	Total	
Bucket Weights	7.81	9.88		15.49
	7.58	12.64		18.84
	7.41	11.49		16.47
	7.29	12.37		17.59
	7.95	11.85		16.92
	8.21	10.98		17.61
	7.95	9.92		18.71
	7.45	13.09		20.48
	7.77	9.96		19.91
	7.77	11.26		16.89
	7.94	10.48		17.04
	3.3	14.15		15.2
		16.06		
		13.41		
		9.17		
Batch Total	**88.43**	**176.71**	**265.14**	**211.15**
Yield (wet)				0.7964
Yield (dry)				2.3878

Table I.3: Summary of data obtained from the weights before and after hot water extraction for extraction 2

Component	Weight before extraction (kg)			Weight after extraction(kg)
	Mulched Fronds	Water	Total	
Batch Total	154.24	310.51	464.75	343.53
Yield (wet)			0.7392	
Yield (dry)			2.2272	

Appendix J Weight at the end of evaporation

Parameters include:

- product side: -30 inches mercury gage = 0kPa abs = 100%vacuum
- steam side: -12 inches mercury gage to -15 inches mercury gage
- temp product 50^{o}C
- temp steam 70^{o}C

Overall, the mamaku was in the evaporator for between 2-3 hours of total.

Table J.1: Final results from the first round of evaporation

Final Weights (kg)
19.52
18.92
18.56
2.63
14.59
18.22
14.26
17.4
9.43
8.21
17.5
7.48
7.86
6.92
11.45
15.94
19.71
228.6

Table J.2: Final results from the second round of evaporation

Final Weights (kg)
19.81
18.12
18.97
19.3
76.2

Appendix K Gelatin Specifications

GELITA
Improving Quality of Life™

Product Specification

250 bloom 14 mesh
Edible Bovine Gelatine

Document: G005-0501-250-14
Revision: A
Date effective: 17/02/15

Product Specification
250 bloom 14 mesh Edible Gelatine

1.0 PRODUCT

250 Bloom 14 Mesh Grade edible Gelatine

2.0 DESCRIPTION

A light coloured edible Beef Skin (Type B) Gelatine powder, soluble in hot water to form a clear solution with a characteristic bouillon like taste and odour. Gelatine is a purified protein obtained from the partial hydrolysis of collagen extracted from selected beef skins.

This product can be supplied as Halal certified. Where Halal certified is applicable raw materials are selected entirely from cattle slaughtered under Islamic supervision.

3.0 INGREDIENTS

Gelatine from Beef Skin

4.0 SPECIFICATIONS

Specifications	UOM	Min	Max	Lab Method
Bloom	grams	240	260	LAB 003
pH	N/A	4.5	6.0	LAB 006
Sulphur Dioxide	ppm		100	LAB 008B
Ignition Residue	%		3.0	LAB 011
Moisture	%		12.0	LAB 012
Arsenic	ppm		1	LAB 014
Lead	ppm		1.5	LAB 014
Heavy Metals	ppm		40	LAB 014
Hydrogen Peroxide	ppm		5	LAB 009
Microbiological	**UOM**		**Limit**	**Lab Method**
Standard Plate Count	CFU/g		1000	LAB 021
Coliforms	Absent/g		Absent	LAB 022
Escherichia Coli	Absent/g		Absent	LAB 022
Salmonella sp.	Absent/25g		Absent	LAB 023

Product Specification
250 bloom 14 mesh Edible Gelatine

5.0 GENERAL

This product complies with the current Australian and New Zealand Food Standards Code

6.0 PRODUCT INFORMATION AND PACKAGING

Individual bags are labelled by product name and lot number. Bags are multiwall paper with an incorporated polythene liner containing 25kg net.

7.0 STORAGE

Bags should be stored in a cool, dry area. When so stored there should be no major changes in product properties for a period of five years.

8.0 MANUFACTURING SITE

GELITA NZ Ltd, 30 Barton St, Woolston, Christchurch, NZ, 8023.

9.0 GENETICALLY MODIFIED ORGANISM (GMO) STATUS

Gelatine manufactured by GELITA is not derived from any genetically modified material.

There is no commercially available GM raw material for gelatine production.

GELITA does not require labelling as a Genetically Modified Food, as defined under the current Australia New Zealand Food Standard Code.

10.0 AUTHORISED BY:

Darryn Gear
Quality & Compliance Coordinator

GELITA
Improving Quality of Life™

Product Specification

CNC
Pharmaceutical Bovine Gelatine

Document: 257-0501-200-18
Revision: A
Date effective: 17/02/15

Product Specification
CNC Pharmaceutical Gelatine

1.0 PRODUCT

200 Bloom 18 Mesh Grade Pharmaceutical Gelatine

2.0 DESCRIPTION

A light coloured pharmaceutical Beef Skin (Type B) Gelatine powder, soluble in hot water to form a clear solution with a characteristic bouillon like taste and odour. Gelatine is a purified protein obtained from the partial hydrolysis of collagen extracted from selected beef skins.

This product can be supplied as Halal certified. Where Halal certified is applicable raw materials are selected entirely from cattle slaughtered under Islamic supervision.

3.0 INGREDIENTS

Gelatine from Beef Skin

4.0 SPECIFICATIONS

Specifications	UOM	Min	Max	Lab Method
Bloom	grams	170	210	LAB 003
pH	N/A	4.5	6.0	LAB 006
Conductivity	$mScm^{-1}$		1.0	
Viscosity	mPa.s	2.6	3.5	LAB 008A
Sulphur Dioxide	ppm		50	EP
Ignition Residue	%		2.0	LAB 011
Moisture	%		12.0	LAB 012
Arsenic	ppm		1	LAB 014
Iron	ppm		30	LAB 014
Copper	ppm		10	LAB 014
Lead	ppm		1.5	LAB 014
Zinc	ppm		30	LAB 014
Chromium	ppm		10	LAB 014
Hydrogen Peroxide	ppm		5	LAB 009
Microbiological	**UOM**		**Limit**	**Lab Method**
Standard Plate Count	CFU/g		1000	LAB 021
Coliforms	Absent/g		Absent	LAB 022
Escherichia Coli	Absent/g		Absent	LAB 022
Salmonella sp.	Absent/25g		Absent	LAB 023

Product Specification
CNC Pharmaceutical Gelatine

5.0 GENERAL

This product complies with the current Australian and New Zealand Food Standards Code and current European Pharmacopeia

6.0 PRODUCT INFORMATION AND PACKAGING

Individual bags are labelled by product name and lot number. Bags are multiwall paper with an incorporated polythene liner containing 25kg net.

7.0 STORAGE

Bags should be stored in a cool, dry area. When so stored there should be no major changes in product properties for a period of five years.

8.0 MANUFACTURING SITE

GELITA NZ Ltd, 30 Barton St, Woolston, Christchurch, NZ, 8023.

9.0 GENETICALLY MODIFIED ORGANISM (GMO) STATUS

Gelatine manufactured by GELITA is not derived from any genetically modified material.

There is no commercially available GM raw material for gelatine production.

GELITA does not require labelling as a Genetically Modified Food, as defined under the current Australia New Zealand Food Standard Code.

10.0 AUTHORISED BY:

Darryn Gear
Quality & Compliance Coordinator

Appendix L Trial 2 removing the oil

The aim of this trial was to introduce water during the centrifuging steps to help distribute the encapsulated mamaku to stop clumping. Additionally, lower centrifuge speeds would be trialled to see if that helped limit clumping.

Each centrifuge tube was loaded up with 20mL of the 8%v/v PGPR emulsion (100mL total), 5 mL of RO water and 25 mL of 95% ethanol. The tubes were inverted and shaken to mix the different liquids for 15 seconds. Then they were loaded into the centrifuge and it was turned on for 10 minutes at 20^{o}C at 1500 rpm. This did create a clump of mamaku + gelatin at the bottom. Additionally there was a distinct oil layer and a water/ethanol layer as well as a bottom layer of unseparated oil/emulsion. The oil was removed, as was most of the clear water/ethanol layer.

Then 5mL of RO water was added and another 25mL of ethanol. The tubes were inverted and shaken to mix the different liquids for 15 seconds. Then they were loaded into the centrifuge and it was turned on for 5 minutes at 20^{o}C at 1200 rpm. Again, the distinct oil layer was removed, as was most of the water/ethanol layer. There was still a small amount of unseparated oil/emulsion layer. So this was repeated one more time.

What was obtained was ~50mL of mamaku gelatin clumps dispersed in water (obviously with some ethanol based on smell). A further 50mL of RO water was added before mixing to break up the clumps using the Ultra Turrax for one minute this gives the same effective concentration as the emulsion before washing – 0.45%wt/v. The final product is shown in the Figure L.1.

Figure L.1: Encapsulated mamaku with clumps broken up, dispersed in RO water

Overall, this trial showed improvement on the hardness of the clumps formed when centrifuging. Although clumping was still an issue, the clumps were much more easily broken up with the Ultra Turrax this time.

More work to remove the clumping completely would make this a more suitable technique, because then a more concentrated product could be created

Appendix M Paint spray gun

This trial was based on the idea that the hot solution of mamaku + gelatin could be sucked up and sprayed out of the paint gun into individual droplets. These droplets would land in a cold oil bath promoting the gelatin to gel and set the structure. The methodology for making the gelatin + mamaku solution is outlined below:

1. The 250 mL of water to hydrate the gelatin was added to a heated magnetic stir plate and allowed to heat to around 65^{o}C. The magnetic stirrer speed was set to about 400 rpm.
2. The 37.5g of gelatin was added to the water and allowed to mix for 20 minutes adjusting the temperature to stay above 60^{o}C and no higher than 70^{o}C.
3. Then the 250mL of mamaku was added and mixed at 600 rpm for about 1 minute until the solution appeared uniform.
4. The gel was then allowed to set in the fridge overnight.

The setup of the paint gun and cold oil bath is shown in Figure M.1.


Figure M.1: Images showing the paint gun and set up of the cold oil bath

The mamaku + gelatin solution was heated to 55^{o}C then added to the container of the paint gun. The paint gun was held aiming to spray the solution into the cold oil bath.

Disappointingly, this trial was a failure as with all the other nozzle-based techniques tried. Despite trying the full range of speeds and the two nozzles available (including one, which had the ability to change its size), the solution could not be sprayed into droplets.

This technique failed to break up the mamaku + gelatin solution into individual droplets. Either instead, it refused to spray any of the solution or it sprayed a continuous stream of solution depending on the speed and nozzle sizes chosen.

Appendix N Spinning disc trial

The spinning disc set up was designed and made by Allan Hardacre. It was based on the idea that the hot solution of mamaku + gelatin could be sucked up and spun out into individual droplets. These droplets would land in a cold oil bath promoting the gelatin to gel and set the structure.

Allan's setup used a die grinder with a custom attachment that sucked up the solution and spun it out along the bottom of the disc to the edge.

The oil bath was set up as shown in Figure N.1, with cold oil in the bottom of the bucket and syringed around the sides of the bucket to limit how much mamaku would stick to the sides.

Figure N.1: Images showing loading the chilled oil into the syringe (left) and then distributing this cold oil around the sides of the bucket (right)

The methodology for making the gelatin + mamaku solution is outlined below:

1. The 50 mL of water to hydrate the gelatin was added to a heated magnetic stir plate and allowed to heat to around 65^{o}C. The magnetic stirrer speed was set to about 400 rpm.
2. The 37.5g of gelatin was added to the water and allowed to mix for 20 minutes adjusting the temperature to stay above 60^{o}C and no higher than 70^{o}C.
3. Then the 450mL of mamaku was added and mixed at 600 rpm for about 1 minute until the solution appeared uniform.
4. The gel was then allowed to set in the fridge overnight.

As shown in Figure N.2, the mamaku + gelatin solution was heated to 55ºC then added to a smaller container and stuck to the bottom of the bucket. The die grinder was lowered so the tip of it touched the mamaku solution and could suck it up when turned on.

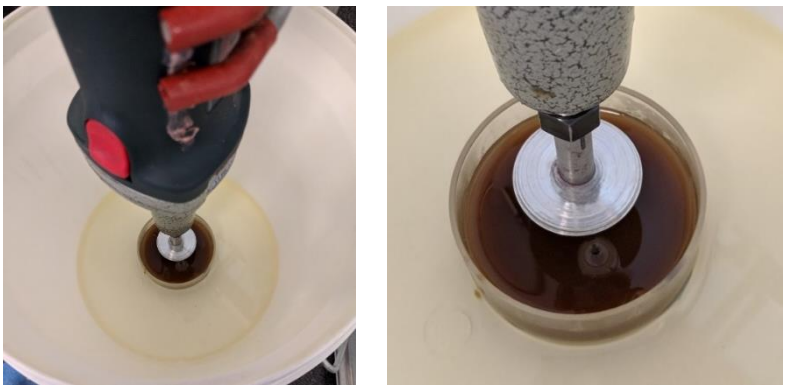

Figure N.2: Images showing the set-up of the die grinder inside the bucket including the container with the mamaku + gelatin solution in it and the oil spread on the sides and bottom of the bucket

Disappointingly, this trial was a failure as with all the other nozzle-based techniques tried. This technique failed to break up the mamaku + gelatin solution into individual droplets. Instead, it just sprayed a continuous stream of mamaku + gelatin out away from the die grinder.

It appears that the sliminess of the mamaku is the limiting factor to these techniques. For example, a water solution does not resists the shear forces applied and this technique results the water stream breaking up into individual droplets (atomisation).

Appendix O Pepsin specifications

SIGMA-ALDRICH® sigma-aldrich.com

3050 Spruce Street, Saint Louis, MO 63103, USA
Website: www.sigmaaldrich.com
Email USA: techserv@sial.com
Outside USA: eurtechserv@sial.com

Product Specification

Product Name:
Pepsin from porcine gastric mucosa – powder, ≥250 units/mg solid

Product Number:	**P7000**
CAS Number:	9001-75-6
MDL:	MFCD00081840
Storage Temperature:	2 - 8 °C

TEST	Specification
Appearance (Color)	Off White to Yellow to Beige
Appearance (Form)	Powder
Solubility (Color)	Colorless
Solubility (Turbidity)	Clear to Slightly Hazy
1 mg/mL, 0.01N HCl	
units/mg solid	≥ 250
One unit will produce a change in A280 of 0.001 per min at pH 2.0 at 37 Deg C, measured as TCA-soluble products using hemoglobin as substrate. (final volume= 16 mL. Light path= 1 cm)	
Recommended Retest Period	----------
2 years	
Loss on Drying	≤ 4 %

Specification: PRD.3.ZQ5.10000009124

Appendix P Initial in-vitro digestion trials

Micro injector beads at pH 3.0

This trial was completed using the encapsulated mamaku beads from the second trial involving the micro injector. The pH of 9.977g of mamaku beads was reduced to 2.97 (from 6.02) using 30 drops of 0.1N HCl acid.

This was placed in the water bath at 37°C with the stirrer turned on for 5 minutes until equilibrated. The mamaku beads fully melted within 3 minutes of being added to the water bath. This is shown in Figure P.1.

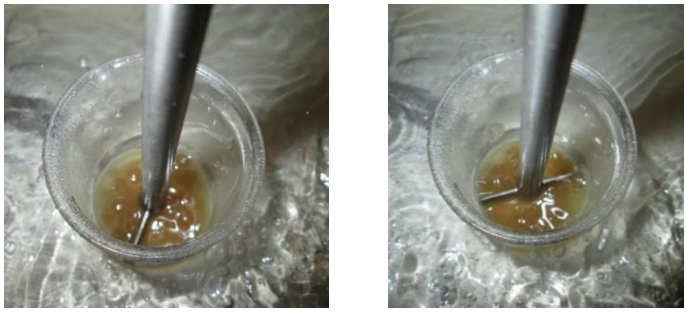

Figure P.1: Images taken before melting (left) and as the beads began to melt (right) as the sample was heated in the water bath

0.114g of porcine pepsin was added (1%wt/v solution) and was left mixing at 40rpm for 30 minutes in the water bath. This is shown in Figure P.2.

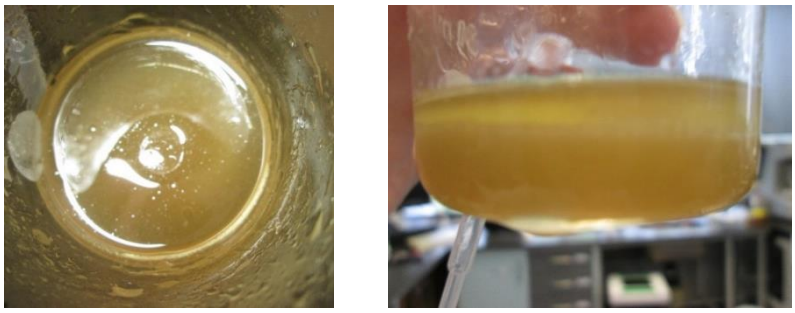

Figure P.2: Images showing the sample at the end of the 30 minutes digestion

Dilute shear-thickening behaviour could be seen visually during this time with the solution slightly climbing the stirrer. At the end of the 30 minutes, the sample was placed in the rheometer to observe if any shear-thickening behaviour could be

observed. A comparison viscosity profile was measure using melted encapsulated mamaku beads at 37°C with no pepsin or acid added. The results are shown in Figure P.3.

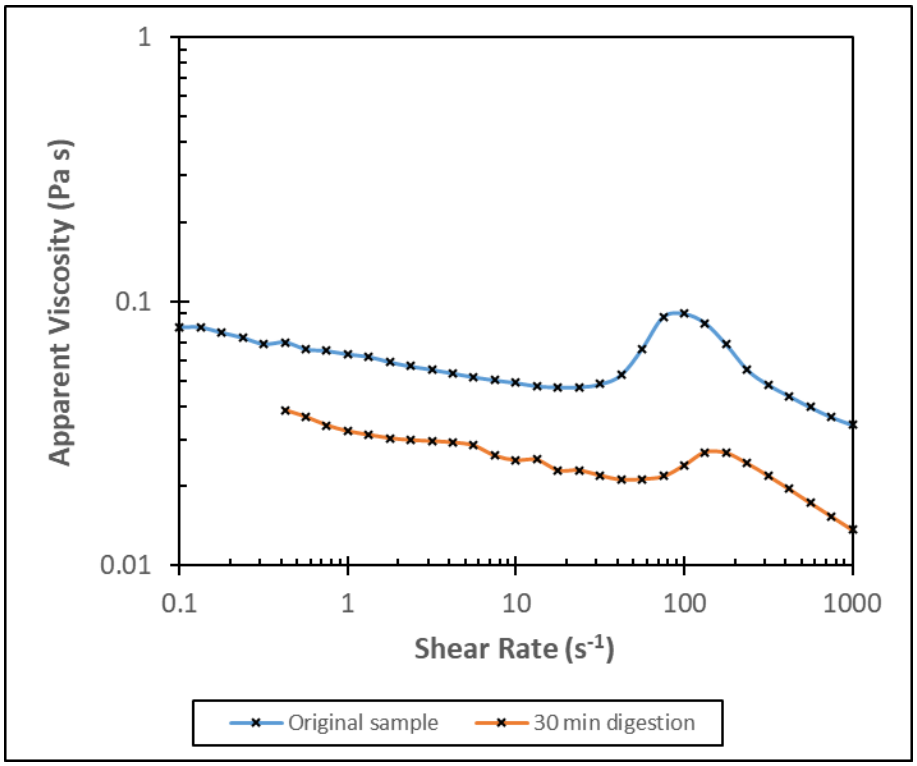

Figure P.3: Viscosity profile obtained before and after digestion

The graph showed that there is some shear-thickening regained but it is very small and at shear rate higher than the ideal 1-10s^{-1}.

Mamaku + Gelatin pH 3.1

The pH of the 10mL of mamaku + gelatin solution after addition of 0.75mL of 1M acid was 3.16 at 32.3°C. 10mLs of this was placed in the water bath at 37°C. 0.102g of porcine pepsin was added (1%wt/v solution) and was left mixing at 40rpm for 120 minutes in the water bath.

At the end of the 120 minutes, the pH was measured to see if there was a change, 3.31 30.3°C. Then the sample was placed in the rheometer to observe if any shear-thickening behaviour could be observed. The results are shown in Figure P.4.

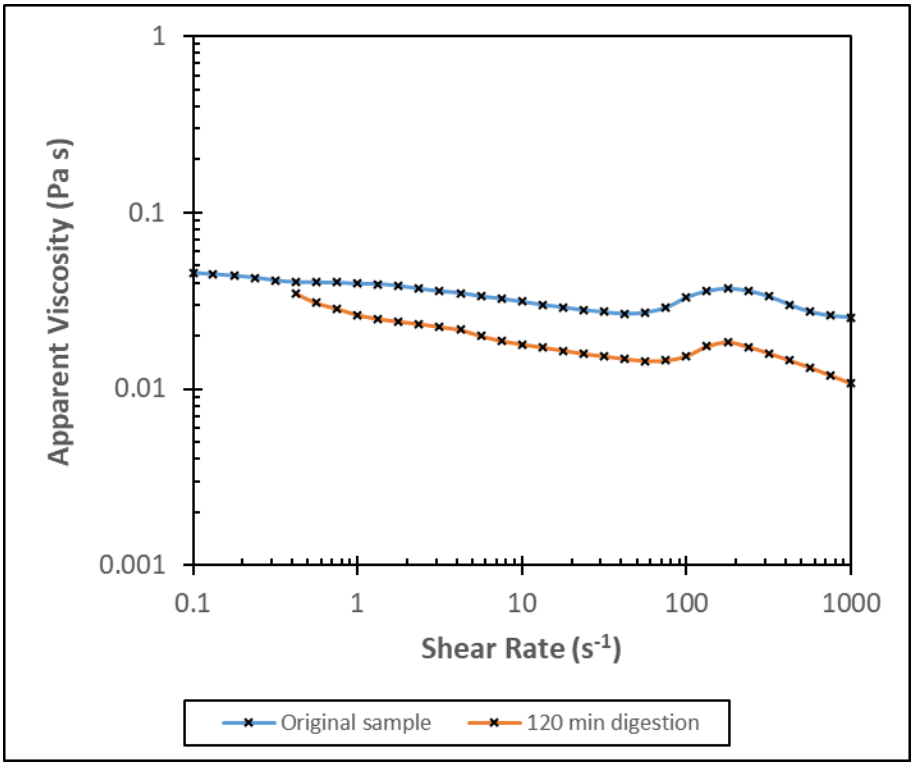

Figure P.4: Viscosity profile obtained before and after digestion

The graph showed that there is some shear-thickening regained, but again it is very small and at shear rate higher than the ideal 1-10s^{-1}. A comparison was done using a control sample of mamaku + gelatin with the pH reduced but before pepsin was added, and after 120 minutes of digestion as shown in the graph.

The mamaku concentration is 2.1%wt/v after addition of the acid. The gelatin concentration is 6.5%wt/v.